2024

Evaluating the microstructure, mechanical and optical properties of novel multi-layered zirconia materials subjected to repeated firing

BOSTON UNIVERSITY

HENRY M. GOLDMAN SCHOOL OF DENTAL MEDICINE

THESIS

EVALUATING THE MICROSTRUCTURE, MECHANICAL AND OPTICAL PROPERTIES OF NOVEL MULTI-LAYERED ZIRCONIA MATERIALS SUBJECTED TO REPEATED FIRING

by

HOMOUD A. KAKOOLI

MChD/BChD Dental Surgery, BSc Oral Science
University of Leeds, 2016

CAGS in Prosthodontics
Boston University, 2024

Submitted in partial fulfillment of the requirements for the degree of

Master of Science in Dentistry
In the Department of Restorative Sciences and Biomaterials

2024

Approved by:

First Reader ______________________________

Russell A. Giordano II, D.M.D., C.A.G.S., D.M.Sc.

Professor and Director, Division of Biomaterials

Department of Restorative Sciences & Biomaterials

Assistant Dean for Biomaterials & Biomaterials Research

Second Reader ______________________________

Yuwei Fan, M.Sc., Ph.D.

Research Associate Professor of Biomaterials

Third Reader ______________________________

Hideo Yamamoto, D.D.S., D.M.D., C.A.G.S.

Clinical Professor of Restorative Sciences and Biomaterials

ACKNOWLEDGMENTS

First and foremost, I would like to thank my family and friends for their constant support throughout my life, for which without I would not be here. I would like to thank Dr. Russell Giordano for his constant guidance and leadership throughout this research project. He has supplied me with a great amount of knowledge required to conduct this research project, for which I am thankful. Next, I would like to thank Dr. Yuwei Fan for his ongoing advice and supervision, for his depth of knowledge in carrying out tests was essential in helping me carry on with this experiment to the upmost levels. I would like to thank my colleagues in the research lab, whose delightful conversations and considerations provided a temporary relief during increased workloads. I would like to thank Dr. Minglei Zhao (Frank) for his never-ending hard work, support and assistance provided throughout this project. He has been a major asset in the research lab, and has provided copious amounts of skills to tackle the many different problems we have faced while conducting this research. He has been a mentor and a friend throughout this journey, and for that I am indebted. I would like to thank Boston University Henry M. Goldman School of Dentistry that allowed me to conduct this research under their support and supervision. Last but not least, I would like to thank the Kuwaiti government for supplying me with a scholarship, for which I am eternally thankful and grateful for.

EVALUATING THE MICROSTRUCTURE, MECHANICAL AND OPTICAL PROPERTIES OF NOVEL MULTI-LAYERED ZIRCONIA MATERIALS SUBJECTED TO REPEATED FIRING

HOMOUD A. KAKOOLI

Boston University, Henry M. Goldman School of Dental Medicine, 2024

Primary Advisor: Russell A. Giordano II, D.M.D., C.A.G.S., D.M.Sc.

Professor and Director, Division of Biomaterials, Department of Restorative Sciences and Biomaterials, Assistant Dean for Biomaterials and Biomaterials Research

ABSTRACT

OBJECTIVES: This study aims to fill these voids in the literature regarding the microstructure, mechanical and optical properties of multilayered zirconia subjected to repeated firing. It will aim to increase knowledge and understanding of this type of novel material, whether multilayered by chroma or composition.

MATERIALS AND METHODOLOGY: The three materials examined are ZirCAD Prime by Ivoclar Vivadent, Origin Beyond+ Hybrid by B and D Dental Technologies, and Katana HTML by Kuraray Noritake. Beam-shaped specimens were sectioned to the correct size from discs of the three zirconia materials and subsequently cleaned, polished, and annealed. Ten specimens taken from each group were subjected to one, three, and five repeated firings, which were then used for the destructive flexural strength test using a universal testing machine. Another set of smaller specimens were produced and used for the non-destructive tests, prepared in the same manner as the other specimens, with 2 samples present in each group. These small specimens were examined for the following properties: contrast ratio and CIELAB measurements on a white and black background using a spectrophotometer, crystallographic phase changes using x-ray diffraction (XRD), and elemental analysis using energy dispersive spectroscopy (EDS).

RESULTS: Repeated firings did not have any significant effects across all brands of materials for all tests conducted. However, significant differences existed between the different materials, and within their different layers for all tests conducted unrelated to repeated firing. Significant differences only existed in flexural strength depending on annealing, polishing status, type of polishing, and size independent of repeated firing. Annealing yielded weaker specimens than non-annealed, polished specimens were stronger than non-polished ones, automated polishing resulted in stronger specimens than manually polished ones, and smaller specimens were stronger than larger ones in terms of flexural strength.

CONCLUSIONS: Within the limitations of this study, repeated firing has no significant effects on the various multilayered zirconia tested in this study. There is a significant difference in flexural strength between the materials studied. Significant differences in flexural strength also existed between specimens that were annealed versus ones that were not; and between specimens that were polished versus ones that were not. This study has increased knowledge regarding this novel material.

TABLE OF CONTENTS

LIST OF TABLES

LIST OF FIGURES

LIST OF ABBREVIATIONS

A / -A	Annealed / Not Annealed
Al_2O_3	Alumina
BU	Boston University
CAD/CAM	Computer Aided Design / Computer Aided Manufacture
c	Cubic
°C	Degrees Celsius
COV	Covariance
EDS	Energy Dispersive X-Ray Spectroscopy
et al.	Et Alia
e.g.	Exempli Gratia
FLS	Fit of Least Squares
ISO	International Standards Organization
i.e.	that is
Kα	K-alpha
KT	Katana HTML
KT2	Katana HTML 2 (automated polishing)
kV	Kilo Volt
LSM	Least Squares Mean
LTD	Low Temperature Degradation
m	Monoclinic
mA	Milliampere

min	Minute(s)
µm	Micrometer
mm	Millimeter
mol %	Molar Percentage
MPa	Mega Pascal
MPa $m^{1/2}$	Mega Pascal per Square Root of a Meter
N	Newtons
N (tables and figures)	Number
OB	Origin Beyond+ Hybrid
p	P-value
P / A	Polished / Annealed
P / -A	Polished / Not Annealed
P / -P	Polished / Not Polished
PFM	Porcelain Fused to Metal
PJC	Porcelain Jacket Crown
PTT	Phase Transformation Toughening
RPM	Revolutions Per Minute
SD/Std Dev	Standard Deviation
SEM	Scanning Electron Microscope
t	Tetragonal
t->m	Tetragonal to Monoclinic transformation
TZI	inCoris TZI

Y_2O_3	Yttria
Y-TZP	Yttria Stabilized Tetragonal Zirconia Polycrystal
3Y or 3Y-TZP	3 Percent by Mole Yttria Stabilized Tetragonal Zirconia Polycrystal
4Y or 4Y-ZP	4 Percent by Mole Yttria Stabilized Zirconia Polycrystal
5Y or 5Y-ZP	5 Percent by Mole Yttria Stabilized Zirconia Polycrystal
wt.	by Weight
XRD	X-Ray Diffraction
ZrO_2	Zirconia Dioxide / Zirconia
ZP	ZirCAD Prime
1R	One Repeated Firing
3R	Three Repeated Firings
5R	Five Repeated Firings

CHAPTER 1. INTRODUCTION

1.1 HISTORY OF DENTAL CERAMICS

Dentistry is an ever-changing field that is constantly looking to improve on its current procedures and materials, in particular, biocompatible dental restorations that mimic tooth-like properties. Of the many materials used in dentistry, ceramics are one of the most preferred and sought-after choices. Ceramic is defined as any inorganic, non-metallic solid that is made up of compounds that are shaped and then heated at high temperatures to form a solid. They contain a glass and crystalline structure, and are generally hard, heat and corrosion resistant, and brittle materials. Ceramics have many uses in our world that range from pottery to their use in kitchen appliances, and finally in the dental field mainly for dental restorative work. In the field of prosthetic and restorative dentistry, the main goal is the introduction of highly aesthetic restorations that show long-term durability. As such, dental ceramics proved to be the material of choice over the years.

Ceramics were first introduced into the dental field by Charles H. Land when he first patented his porcelain jacket crown (PJC) back in 1889 (Helvey, 2010). Its use was widespread across the field up until the 1950's, until it was superseded with the porcelain fused to metal (PFM) crown made by Abraham Weinstein (Helvey, 2010). PJC's weakness due to internal microcracking was solved with the PFM as the metal bonded to the ceramic helped diminish and prevent propagation of cracks from the ceramic. While stronger, it was less aesthetic due to the inclusion of an opaquer that was used to block out the metal (Helvey, 2010). Although stronger, the PFM was certainly not aesthetic and not ideal to be used anteriorly (Helvey, 2010).

A movement back to ceramics was made when W. McLean and T. H. Hughes decided to add aluminous porcelain to the feldspathic ceramics, in 1965. These crowns contained 40-50% alumina crystals, which effectively doubled the strength of the original PJC (Helvey, 2010). However, the increase in strength was not enough as their use posteriorly resulted in fractures and failures (Helvey, 2010). Their use anteriorly was also limited as the aluminous porcelain had a significantly higher opacity.

In the 1980's, IPS Ivoclar introduced Empress ® 1 to the market, a high leucite-containing all-ceramic. Leucite helps match the coefficient of thermal expansion of the feldspathic porcelain to the metal it is bonded to, as well as limiting the crack propagations of the feldspathic porcelain (Helvey, 2010). However, although it has good translucency and optics, its strength is still a limiting factor as it is not able to withstand the mastication forces loaded on molars.

During the same period, Vita introduced a glass-infused ceramic core material named In-Ceram ®. It consisted of an 85% by volume alumina, which resulted in a strong material with diminished translucency. As such, Vita replaced the sintered alumina with spinel, which improved translucency but decreased strength. Vita later modified the core to include a mixture of both alumina and zirconium dioxide (ZrO_2) crystals, which resulted in a flexural strength of 700 MPa. This was intended for use in the posterior region in multi-unit restorations and single crowns. In the mid 1990's, Nobel Biocare introduced the Procera All-Ceram ® core, which was made from a 99.9% alumina, which would be layered with a feldspathic porcelain. This was the first material introduced to the market that was produced using Computer Aided Design / Computer Aided Manufacturing (CAD/CAM) (Helvey, 2010).

The introduction of CAD/CAM into the dental field triggered a whole new notion of manufacturing ceramic substructures, mainly consisting of alumina (Al_2O_3) or zirconium dioxide (ZrO_2) for its superior physical properties. Multi-unit frameworks with ZrO_2 substructures report flexural strengths of 900-1300 MPa with very accurate marginal fits. These frameworks can either be milled oversized to compensate for the shrinkage that occurs in zirconia after sintering, or were milled after sintering to avoid the shrinkage factor (Burgess, 2018). Nevertheless, both techniques yielded very high flexural strength results, making it suitable to be used in large multi-unit restorations in the posterior region.

1.2 ZIRCONIA

Initially discovered back in the 18th century, zirconium is a naturally occurring metal. It had limited uses back in the day where it was involved in the making of heavy-duty bricks and glass with a high refractive index (Carver, 2018). When combined with oxygen, the silver color metal transforms into a white, polymorphic, crystalline solid known as zirconium dioxide, or zirconia. Helmer and Driskell (1969) published the first study relating to the biomedical properties of zirconia. A few years later, Garvie and

Nicholson (1972) discovered that doped zirconia with oxides like yttria (Y_2O_3), calcia, or magnesia to avoid an unfavorable phase transformation, which will be explained more in detail in the next subsections. The most used in dentistry is 3Y-TZP, this correlates to 3% by mol yttria tetragonal-stabilized zirconia, which reports flexural strengths of 900-1100 MPa, and a fracture toughness of 8 – 10 MPa $m^{1/2}$ (Giordano and McLaren, 2014). However, the use of 4Y-ZP and 5Y-ZP has also been on the rise due to their favorable optical properties. It has since been used in the medical field where it is used in orthopedics to produce hip and knee joints. It made its first appearance into the dental field in the early 80's briefly, but flourished heavily in the 2000's with the introduction and mainstream usage of CAD/CAM technology in dental labs. It is mostly used for restorations such as crowns, multi-unit frameworks, posts, and implants.

Once extracted from zircon, the zirconia powder is produced in the required particle size and composition. Several oxides which act as dopants are added to the mixture: yttria to stabilize the tetragonal phase transformation, hafnium oxide to reduce pore development, alumina to reduce water corrosion and stabilize grain boundaries, and a number of colorants, usually rare earth minerals, to adjust the shade and add color (Burgess, 2018). The powder, which contains binder and additives, is placed into flexible molds and is pressed using an isostatic method. This method, which compresses the submerged mold from all directions, allows for a pressed material that is uniform in density with reduced porosity (Burgess, 2018). Heat is then carefully applied to the material, which causes removal of the binder and other additives. The partially sintered zirconia hardens enough to maintain its shape, but is soft enough to be easily machined (Denry and Kelly, 2008).

Dental restorations made from zirconia are usually fabricated via one of two different methods: soft-machining and hard-machining, which usually relate to the disc's sintered state. With soft-machining, the zirconia disc is still in its 'green state', as such the machining is more cost-effective and less time consuming (Denry and Kelly, 2008). Moreover, it prevents unwanted phase transformation as studies have shown that this technique provides a surface virtually-free of the monoclinic phase of zirconia (Denry and Kelly, 2008). The milled shape or restoration is then fully sintered, which results in 20-25% volumetric shrinkage of the material. This will be discussed in the subsequent subsections. On the other hand, hard machining is done with the zirconia disc fully sintered, thus eliminating the shrinkage factor before milling the restoration. This process, however, is extremely time consuming, and has the possibility of inducing microcracks in the zirconia, thereby increasing its susceptibility to low-temperature degradation and lowering its long-term reliability (Denry and Kelly, 2008).

1.2.1 CRYSTALLINE PHASES

As previously mentioned, zirconia is a polymorphic, crystalline solid. Although it has many phases, zirconia usually exists in three major solid phases at room temperature: monoclinic (*m*), tetragonal (*t*), and cubic (*c*) phase. These phases relate to the temperature applied to the powder. The first phase, monoclinic, exists between room temperature up to 1170 °C. Adding more heat, the tetragonal phase exists between 1170 °C to 2370 °C, with it being stable at 1170 °C. The tetragonal phase is the most mechanically advantageous phase. The cubic, exists between 2370 °C up to the melting point (Zhang, 2018). The cubic phase is the most stable phase of the three, with it having the most desirable optical properties that come at the expense of strength (Kim, 2020; Zhang, 2014). Figure 1 shows the arrangement of particles in the different phases and Figure 2 shows a phase diagram of zirconia.

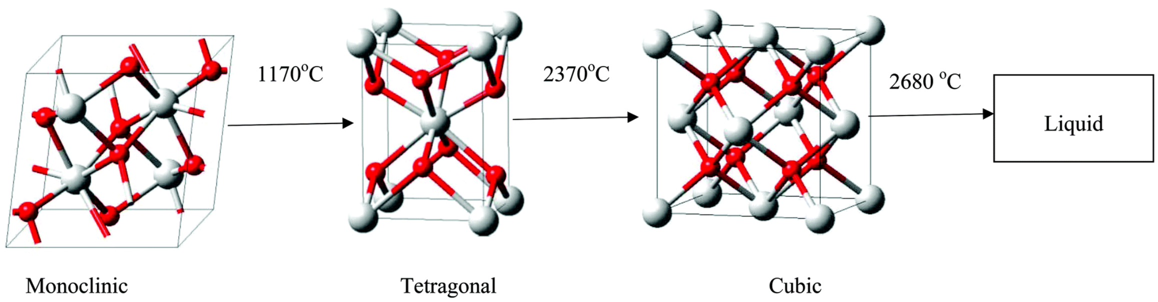

Figure 1: Three major crystal phases of zirconia (Gautam et. al, 2016)

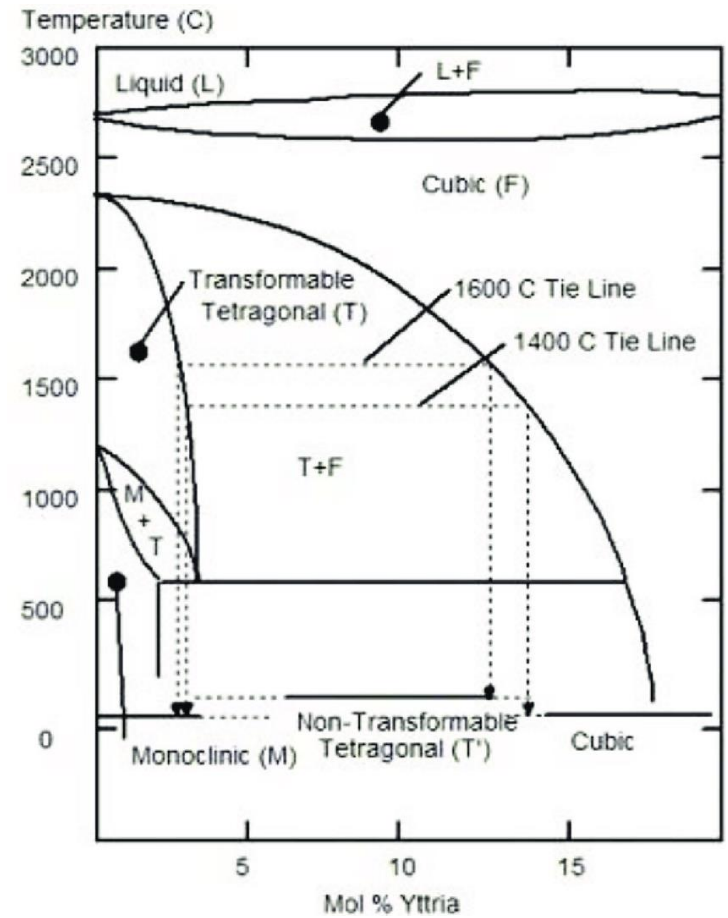

Figure 2: Phase diagram of zirconia showing where each phase exists in accordance with mol % yttria and temperature (Prakasam et al., 2018)

1.2.2 PHASE TRANSFORMATION TOUGHENING (PTT) AND YTTRIA CONTENT

Phase transformation toughening (PTT) is a phenomenon that occurs during the cooling process from *t* -> *m*. It usually results in volumetric expansion of about 3 - 4.5% in 3Y-TZP, which can lead to catastrophic failure if occurring in an uncontrolled manner due to cracks and flaws developing (Denry and Kelly, 2008). This transformation can result in increased compressive forces within the zirconia, as the particles expand creating compressive stress to resist crack propagation, leading to an increase in flexural strength and fracture toughness, which can be seen in Figure 3 (Žmak et al., 2020). To control this transformation favorably, dopants are added to stabilize the material, with the most commonly used being yttria (Y_2O_3). Phase transformation can also occur when zirconia is subjected to stress during polishing or grinding, leading to an increase in monoclinic content (Denry and Kelly, 2008). PTT effects can be reduced or reversed through an annealing process, also termed as regeneration firing, where the material is annealed at 1000 ^{o}C for 15 minutes (Denry and Kelly, 2008). Though this would reduce the strength of the material as the compressive stresses at the surface are relaxed, it would not heal or repair any microcracks or flaws that may have occurred during the process (Denry and Kelly, 2008).

For pure zirconia without any dopants, the unwanted phase transformation from tetragonal to monoclinic phase occurs, resulting in volumetric expansion. Since there are no dopants in pure zirconia, this expansion could become catastrophic, resulting in fracture of the zirconia. Garvie and Nicholson (1972) discovered that yttria (Y_2O_3) can prevent this uncontrolled phase transformation of zirconia and cause it to be more stable, changing the yttria content of zirconia has a wide range of effects on the material. They observed that Yttria can control this volumetric expansion to favorable amounts, preventing the zirconia from fracturing. The most commonly used mol% of yttria are 3Y, 4Y, and 5Y which correspond to 5.2 - 5.5, 7.0, and 8.8 - 9.4 % content by weight, respectively. As the yttria content increases, the zirconia becomes more stable since as there is a shift from a tetragonal to more a cubic phase. This results in a more translucent zirconia, but at the expense of strength. With 3Y zirconia, flexural strength ranges between 900-1200MPa, with a fracture toughness of 3.5 to 4.5 MPa·$m^{1/2}$; 4Y zirconia has a flexural strength of about 700-900 MPa and fracture toughness of 2.5 - 3.5 MPa·$m^{1/2}$; and 5Y zirconia has a range of 600-800 MPa with a fracture toughness of 2.2 - 4 MPa·$m^{1/2}$ (Burgess, 2018). Though 5Y-ZP has is considered weaker compared to 3Y-TZP, it remains stronger than most ceramics available on the market such as lithium disilicate. Chevalier et al. (2004) reported that 3Y-TZP is unfavorable to exist together with 4Y-ZP or 5Y-ZP as there would be less yttria ions available to enrich the tetragonal grains in the 3Y, making it unstable and thus risking a tetragonal to monoclinic phase transformation to occur. As reported by Hayashi et al (2004), the coefficient of thermal expansion also seems to be affected where an increase in yttria content results in a decrease of the thermal expansion coefficient, with the authors reporting values for 3% mol YZP and 8% mol YZP as 10.8 x 10^{-6} K^{-1} and 10.1 x 10^{-6} K^{-1}, respectively, measured at 873 K. A mismatch in the coefficient of thermal expansion during sintering would most likely cause warping in the sintered zirconia, especially multilayered zirconia by composition, leading to inaccuracies in fit in the final restoration (Hayashi et al., 2004).

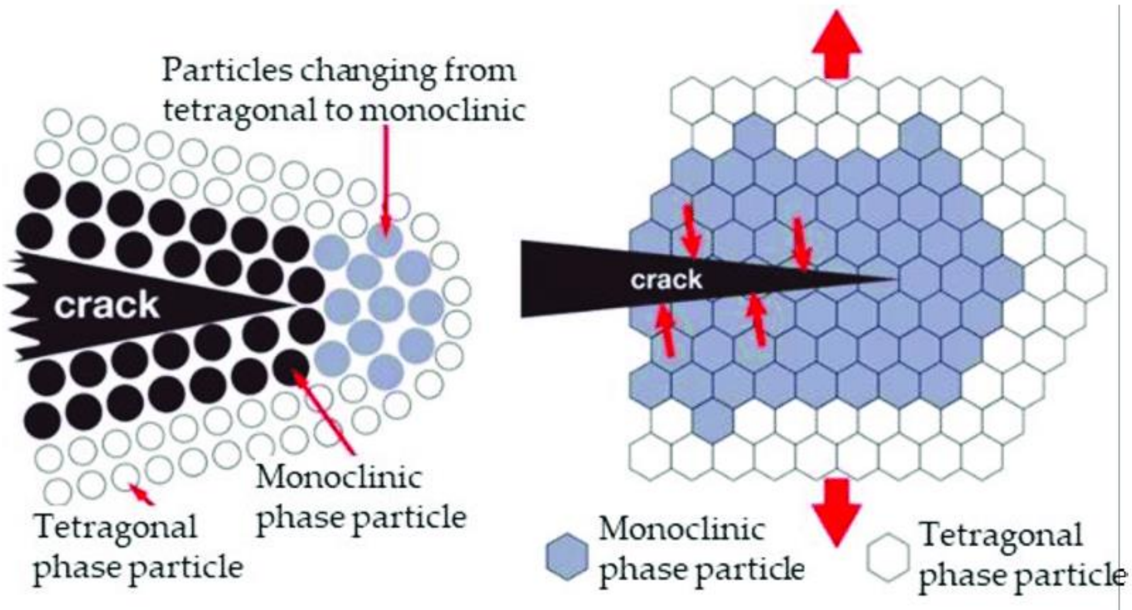

Figure 3: Phase transformation toughening of zirconia (Žmak et al., 2020).

1.2.3 SINTERING

Dental zirconia is sintered at temperatures between 1350 - 1550 °C with holding times between 2-4 hours (Ahmed et al., 2014). Zirconia sintered in these parameters usually results in the highest flexural strength. Sintering times vary from material to material mostly due to the zirconia powder's formulation, whether it contains sintering aids like alumina or other oxides or additives. A number of studies have reported that increasing sintering temperatures, above 1300 °C, and decreasing sintering times would result in better translucency, increasing the contrast ratio, grain size, and density in the zirconia ceramic (Ahmed et al., 2014; Ebeid et al., 2014; Hallman et al., 2012; Kim et al., 2013; Stawarczyk et al., 2014). However, above 1600 °C, grain growth occurs which can cause yttria to be pushed out of the grains into the boundaries, as well as causing some grains to fall out causing pores (Hallman et al., 2012). This would cause instability in the zirconia as well as causing vulnerabilities in strength due to the grain pullout and pore creation.

Due to lengthy sintering times, several manufacturers have come up with high-speed sintering programs to better aid clinicians in providing restorations in one visit to their patients. A study on multilayered zirconia by chroma, a newer type of zirconia, which will be mentioned in a subsection later, published by Coskun and Sari (2019) revealed that high-speed sintering may be promising as specimens that were sintered utilizing the high-speed program showed an improvement in their translucency parameters, with no change to their surface roughness or contrast ratio. However, Kaizer et al. (2017) reported deep cracks propagating into the deeper parts of the specimens after being subjected to a high-speed, or super-speed sintering program and a wear test. This was also accompanied with exposed grain facets in the wear micropits, which can be seen in Figure 4 below (Kaizer et al., 2017). These deep cracks indicate that the material is susceptible to sliding wear fractures, due to fatigue, if subjected to a high-speed sintering program. They also reported poorer surface wear of the antagonist with fast sintered zirconia.

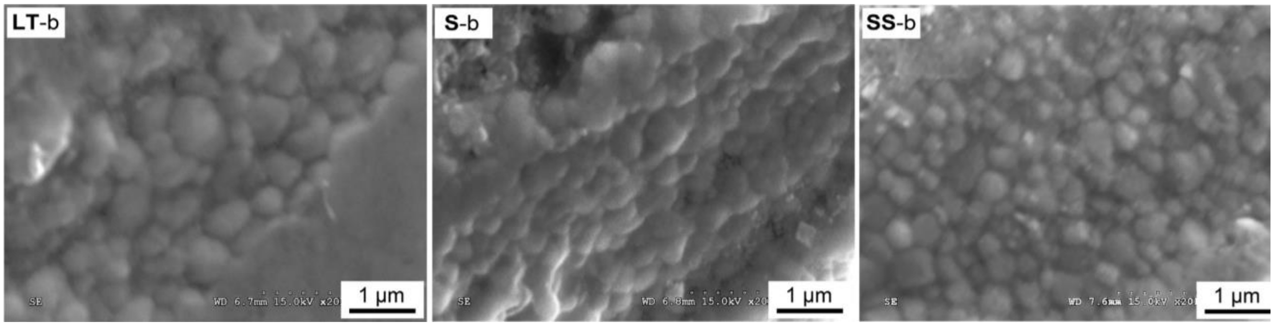

Figure 4: Microstructure of zirconia subjected to long-term (LT), speed (S), super speed (SS) sintering programs (Kaizer et al., 2017)

1.2.4 OPTICAL PROPERTIES

When it comes to optical properties, zirconia's use in the anterior region of the mouth is usually undesirable by both dentist and patient as it can be very opaque due to its crystals' birefringent nature (Zhang, 2014). 5Y zirconia with higher cubic content is used frequently in the anterior region, 3Y has low translucency but might be good when trying to mask underlying discoloration or over a metal post. Birefringence is a phenomenon exhibited by certain materials where an incident ray of light is split into two; these materials are also considered to be anisotropic in which there is a difference in the measurements depending on the angle or direction of measurement. This causes light scatter at the grain boundaries, leading to some light being absorbed, reflected, split, scattered, and transmitted. This can be visualized easily in Figure 5 (Burgess, 2018). The presence of sintering aids, oxides, and additives in the zirconia means that light will not pass through easily as each material has a refractive index of its own. Deleting these aids or additives from the composition will lead to less pores, grain boundaries, impurities and defects which are essential in improving translucency. As previously mentioned, increasing the cubic zirconia crystal concentration, with an associated increase of yttria content, leads to increased translucency of zirconia with diminished strength and toughness (Zhang, 2014). Reducing grain size would lead to a more isotropic material which would provide better translucency; however, this is limited as the grain size threshold is 1 μm where a tetragonal to monoclinic phase transformation can occur (Manziuc, 2019). Kim et al. (2013) also reported that lowering sintering times leads to small grain size, which would lead to a denser, more compact material with decreased porosity. Moreover, the thicker the zirconia is, the less translucent the material is (Vichi et al, 2016). As a result, new monolithic translucent zirconia was introduced to the market utilizing different yttria concentrations or grain size, however, this meant that there was a compromise in strength within these materials, as such they would not be suitable for all-indications.

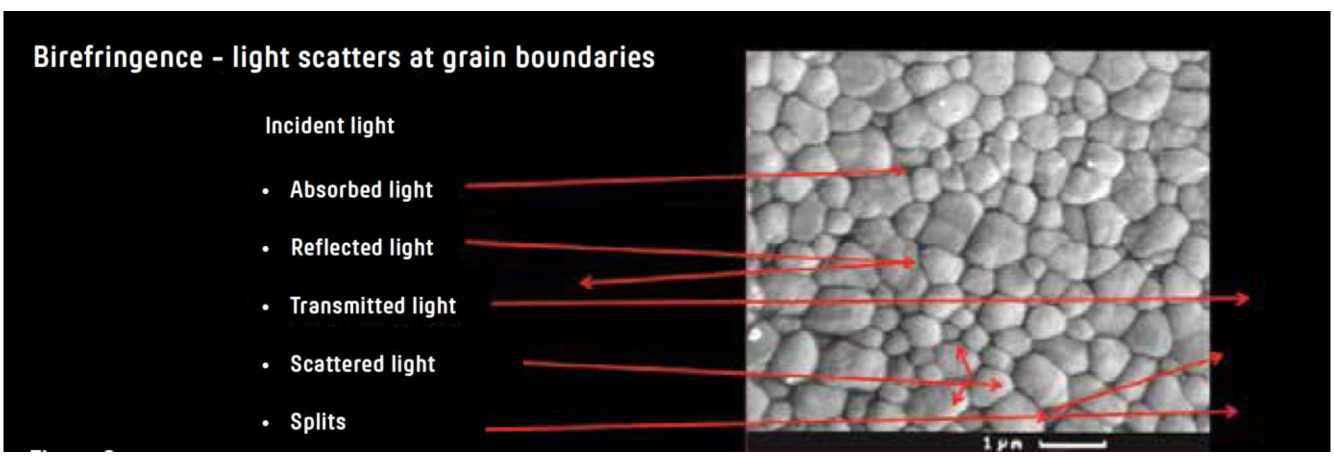

Figure 5: Birefringence of zirconia. scanning electron microscopy (SEM) of zirconia surface with irregular borders. There are differences in the index of refraction of light in different components in the zirconia, and porosity (Burgess, 2018).

1.2.5 LOW TEMPERATURE DEGREDATION

Zirconia also exhibits a unique phenomenon termed "low temperature degradation" (LTD), characterized by a spontaneous transformation of its crystal phase from tetragonal to monoclinic in the presence of water (Pekkan et al., 2020). Proposed mechanisms suggest initial chemical adsorption of water onto the zirconia surface, followed by reaction with oxygen, generating OH ions. These ions infiltrate zirconia through grain boundaries, occupying oxygen vacancies and inducing proton defect formation, eventually destabilizing the tetragonal phase (Ban, 2019). This repeated phase transformation and associated volumetric expansion contribute to micro and macro-cracking within zirconia (Ban, 2019), potentially impeding the performance of processes reliant on tetragonal crystals, such as the transformation toughening phenomenon (PTT).

Several factors, including temperature, surface defects, stabilizing oxide distribution and quantity, manufacturing methods, stress, and moisture, can influence LTD. The repercussions of LTD encompass reduced toughness, increased wear, micro-crack formation, and surface roughening, facilitating plaque accumulation (Pekkan et al., 2020). Despite these known consequences and the recognition of LTD as a risk factor for mechanical failure, a definitive correlation between LTD and zirconia failures during clinical service remains elusive (Pekkan et al., 2020). Dopants can also be used or added to decrease the effects of LTD on zirconia. Cerium oxide stabilization offers superior LTD resistance and thermal stability relative to yttria, although larger quantities are required, accompanied by drawbacks such as imparting a yellowish-brown hue to the final restoration (Bajraktarova-Valjakova et al., 2018).

1.2.6 MULTILAYERED ZIRCONIA

Although zirconia shows a number of desirable physical properties that exceeds those of other materials, there is still a high demand lead by the dentist and patient for more aesthetic and translucent restorations to be placed in the anterior regions of the mouth. Although having a restoration made purely from 5Y-ZP would result in acceptable aesthetics due to increased translucency, this comes at a major expense of strength and toughness where both are decreased greatly as the restoration becomes more cubic with the yttria content increase. As such, sacrificing physical properties of importance to get better aesthetics does not really seem to rectify this issue as another one is risen.

To solve this problem, a newer type of zirconia, dubbed as multilayer or graded zirconia, has emerged on the market. This technology involves having a different color gradient between the layers of the material, or by combining the different types of zirconia, i.e., different % by mol content of yttria, with varying properties to create one material (Zhang, 2014). These can be placed into two categories: multilayer by chroma or multilayer by composition.

In multilayer by chroma, the whole material retains the same % by mol content of yttria throughout, but the chroma gradient is reduced as you move from the incisal layer to the deeper cervical layer, therefore the material would appear to be more translucent in the enamel layer and less translucent in the dentin layer, thus mimicking the natural appearance of a tooth. However, it is not a change in translucency that occurs, just a reduction in the chroma as you move cervically. The change in shade gradient is achieved via the addition of different metal oxides in the different layers. One material that utilizes this gradient technology is Cercon XT ML made by Denstply Sirona. However, this material is made entirely from cubic zirconia, 5Y-ZP, contains 4 layers, has a transmittance rate of 43% with a reported flexural strength of 790 MPa, which can be seen below in Figure 6 (Dentsply Sirona, 2019).

Another example of this is the Katana ML range, which was the first to be introduced into the market in 2015 by Kuraray Noritake. The top of the line of the range, Katana HTML, contains four layers and is made entirely using 3Y-TZP with varying chroma. It boasts flexural strength values of up to 1125 MPa and a 31% transmittance rate. This gradational structure can be explained in Figures 7 and 8 below (Kuraray Noritake, 2019).

Figure 6: Cercon XT ML diagram showing each layer within the material (Dentsply Sirona, 2019).

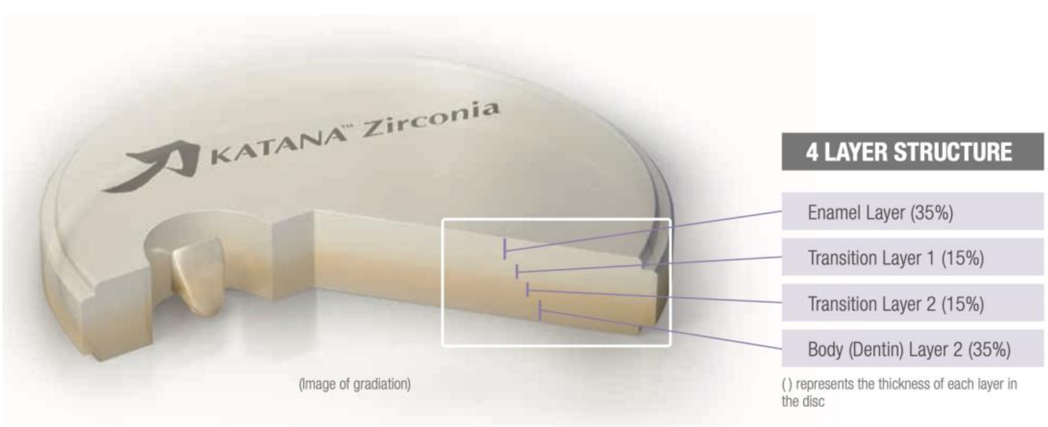

Figure 7: Katana HTML layering structure (Kuraray Noritake, 2019).

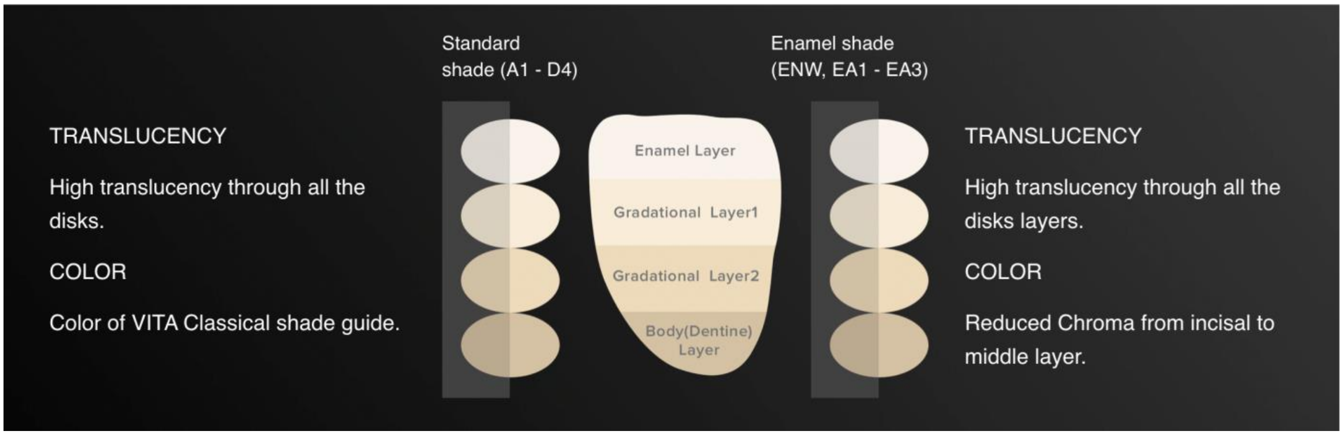

Figure 8: Katana HTML gradational structure (Kuraray Noritake, 2019).

In multilayer by composition, the material would contain different layers with each layer having a different type of zirconia. As such, this would not only cause the material to have different levels of translucency from top to bottom, but also different physical properties, which may be a cause of concern. Nevertheless, the market is still producing new products utilizing this type of technology. Ivoclar Vivadent produced a multilayered zirconia disc named "IPS Emax ZirCAD Prime", which is a result of a combination of both 3Y-TZP (high strength) and 5Y-ZP (high translucency) to produce the desirable mechanical and optical properties in a single ceramic. They claim that their "gradient technology" results in an aesthetic zirconia that is comparable with lithium disilicate with an "all-indications" label due to its 650 – 1200 MPa flexural strength and fracture toughness of greater than 5 MPa $m^{1/2}$ (Ivoclar Vivadent, 2019). It contains three layers, with the 5Y zirconia being concentrated in the enamel level and the 3Y in the dentin layer to provide strength where tensile forces are highest, with a transitional gradational layer. This can be visualized below in Figure 9.

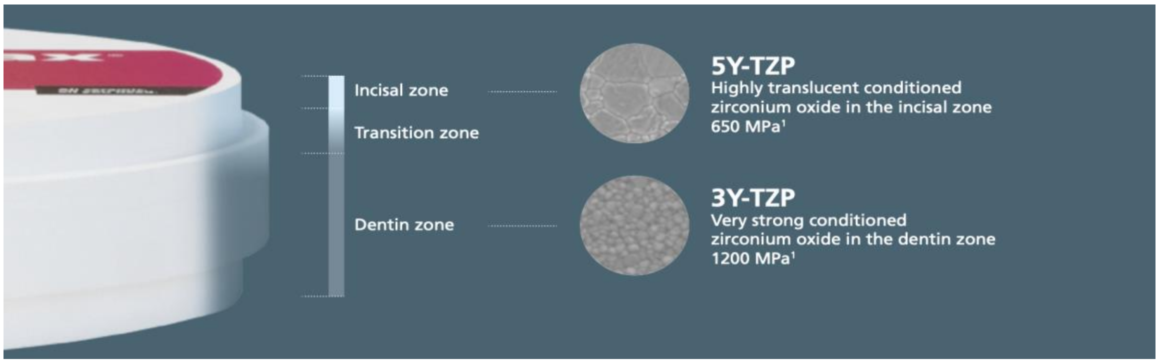

Figure 9: Layering structure of ZirCAD Prime (Ivoclar Vivadent, 2019).

Sometimes, manufacturers would combine both types of multilayered zirconia within the same material. B and D Dental Solutions have produced a ceramic disc, Origin Beyond+ Hybrid Zirconia, that contains 5Y and 4Y zirconia. It is a multilayer both by translucency and chroma, that contains six different layers with five varying translucencies that increases from 46% to 50% cervically to incisally, respectively. They report a flexural strength range between 600 - 1100 MPa, increasing as you move away from the enamel region and to the cervical region, claiming that it is strong enough to be used for posterior restorations and translucent enough to be used anteriorly, which can be seen in Figure 10 (B and D Dental Technologies, 2020).

Figure 10: Structure of Origin Beyond+ Hybrid (B and D Dental Technologies, 2020).

When it comes to producing restorations from multilayered zirconia discs or blocks, the technician would ‘nest’ the restoration in accordance to the needs of the dentist, mostly decided by location of the restoration in the mouth i.e., anterior or posterior. For example, for a posterior restoration where aesthetics do not matter as much, a molar made from ZirCAD Prime would most likely be nested, or positioned, more towards the dentin layer, where 3Y-TZP is at its highest concentrations. This is done to achieve the highest levels of strength, as opposed to it being nested closer to the enamel layer where the restoration would be more translucent but weaker. Figure 11 below helps show this nesting process.

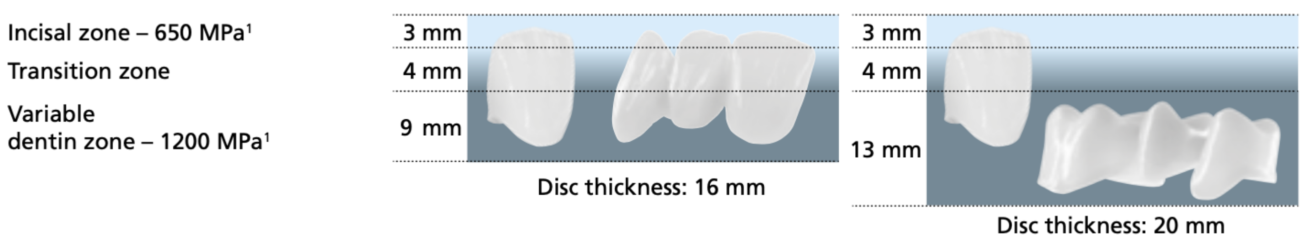

Figure 11: Nesting process showing posterior restorations position more towards the dentin zone while anterior ones positioned more towards the incisal zone (Ivoclar Vivadent, 2019).

1.3 PURPOSE OF THE STUDY

All materials mentioned strive for a superior ceramic in terms of both optical and mechanical properties. In the modern age of dentistry, a shift is happening to transition into single, monolithic type restorations where veneering a ceramic onto the core or framework is no longer needed. Recent literature shows that most failures that occur in zirconia core frameworks are a result of a failure of the bond between the veneer and the zirconia framework, or chipping or fracture of the veneered ceramic, whereas the zirconia framework remained intact (Kolakarnprasert et al., 2019).

As such, the demand for an all-indication type of restorative material has been on the rise. Aesthetically speaking, patients have been more involved in the decision-making process. It is a very demanding job for the dentist, or technician, to deliver a restoration that is appreciated by the patient and fully satisfies their needs in terms of shape, color, and shade matching. As such, restorations will be sent back to the lab, often more than once, for corrections to be made on color or shade, which involves a staining or glazing procedure followed by a firing process. O'Brien et al. (1991) reported color changes between ceramic specimens that were fired three times and ones that were fired six times. However, these color changes were lower than expected values and as such repeated firings were deemed acceptable up to ten times with regards to color change. In a more recent study that applies to monolithic zirconia, Ozdogan and Ozdemir (2020) reported that no effects occurred to color or translucency, or phase transformation of zirconia frameworks subjected to repeated firings up to four times.

However, there is little research regarding the newer novel multi-layered zirconia materials as their introduction to the market has been very recent. Kolakarnprasert et al. (2019) compared the three types of the Katana ML line in terms of microstructure, chemical composition, low temperature degradation (LTD) resistance, and translucency properties only to find differences between the material itself. Studies in this field have explored various aspects of multilayered zirconia. Cho and Seol (2022) concentrated on optical properties and phase fractions. They found significant differences between the two types of multilayered zirconia they tested, one being multilayered with different Yttria concentrations for each layer, and one being monolithic multilayered. Amongst each material, significant differences in contrast ratio and translucency parameter were seen as you move from enamel layer to dentin layer, but not between all layers. On the other hand, Heidari et al. (2022) investigated the arrangement of layers within fixed dental prostheses (FDP) connectors, focusing on optimizing strength distribution via different nesting positions on the monolithic multilayered zirconia blank, in which they found no significant differences between the strength of the layers. Machry et al. (2022) analyzed mechanical properties by sectioning individual layers of multilayered zirconia and assessing parameters like flexural strength and hardness, differing from this study where intact layers are to be maintained. They found significant differences in flexural strength, under monotonic and cyclic fatigues applications, between the layers of the material they tested with the layers that contained less yttria content were stronger than the ones that contained more of it. Winter et. al (2022) also conducted a number of tests on multilayered zirconia before and after thermal cycling, and included one of the materials that are to be used in this study, IPS e.Max ZirCAD Prime by Ivoclar Vivadent. They sectioned different layers from the multilayered zirconia, subjected to thermal cycling, and flexural strength results revealed significant differences after thermal cycling between some of the layers, but not within each layer before and after thermal cycling.

The purpose of this study is to fill these voids in the literature regarding the microstructure, mechanical and optical properties of multilayered zirconia subjected to repeated firing. It will aim to increase knowledge and understanding of this type of novel material, whether multilayered by chroma or composition, to improve their applications in the dental field and raise awareness in the dental community as well. It will help explore any shortcomings of the material, approve or refute manufacturer's claims, as well to assess their reliability as a possible superior restorative material in the field. The study will aim to test the flexural strength, contrast ratio, elemental composition and crystallographic structure to evaluate any changes that may occur after the materials are subjected to repeated firings to mimic glazing protocols.

1.4 HYPOTHESES

Null hypotheses:

1. There will be no differences in contrast ratio between the different groups after being subjected to repeated firing.
2. There will be no differences in CIELAB values between the different groups after being subjected to repeated firing.

3. There will be no differences in crystallographic structure between the different groups after being subjected to repeated firing.
4. There will be no differences in elemental composition between the different groups after being subjected to repeated firing.
5. There will be no differences in flexural strength between the different groups after being subjected to repeated firing.

Alternative hypotheses:

1. There will be differences in contrast ratio between the different groups after being subjected to repeated firing.
2. There will be differences in CIELAB values between the different groups after being subjected to repeated firing.
3. There will be differences in crystallographic structure between the different groups after being subjected to repeated firing.
4. There will be differences in elemental composition between the different groups after being subjected to repeated firing.
5. There will be differences in flexural strength between the different groups after being subjected to repeated firing.

CHAPTER 2. MATERIALS AND METHODS

2.1 MATERIALS

Three different types of zirconia will be tested in this experiment: **IPS emax ZirCAD Prime (ZP)** by Ivoclar Vivadent lot no. Z00K3M, **Origin Beyond+ Hybrid (OB)** from B & D Dental Solutions lot no. 14mm-154171, and **Katana HTML (KT)** by Kuraray Noritake lot no. EBPWQ. The disc of ZP was 16mm in thickness, comprised of 3 layers being 19% for enamel layer, 25% for transition layer, and 56% for dentin layer. The OB zirconia disc was 14 mm in thickness and is comprised of 6 layers with 23% for enamel, 23% for dentin, with each transition layer being 13.5% of the disc. KT zirconia disc was 14 mm in thickness, with 35% of it being in enamel, 35% in dentin layer, and 15% for the two transition layers each. All three zirconia discs had a diameter of 98.5 mm. Shade A2 was used for all three materials. All three materials are considered to be multilayered zirconia, with ZP being multilayer by composition, OB by composition and chroma, and KT by chroma only. A more traditional type of zirconia, **inCoris TZI (TZI)** by Dentsply Sirona was also used in this research to compare the results to, as well as to validate the methodology as this material has been on the market for quite some time and has been tested and proven. TZI comes in disc form as well in 13mm thickness, 98.5 mm diameter, and shade A3 was used.

2.2 SPECIMEN PREPARATION

Each multilayered material was sub-divided into four groups: control, 1R, 3R, and 5R each representing the initial sintering cycle, one firing cycle, three firing cycles, and five firing cycles to mimic glazing respectively. Due to the fact that the flexural strength test is a destructive test, undesirable internal stresses or flaws could be introduced into the specimen for the other tests. Moreover, the devices that were used for the various tests have certain limitations when it comes to sample size and / or thickness. As such, two different sets of specimens were fabricated: Specimens A used for the flexural strength test, and Specimens B used for the contrast ratio test, elemental composition via Energy Dispersive X-ray Spectroscopy (EDS), and X-ray Diffraction (XRD) for the analysis of the crystalline structure.

2.2.1 SPECIMENS A

An appropriate number of discs for each material was obtained so that each group of materials contained 10 identical, rectangular bars, totaling 40 specimens for ZP, 40 for OB, and 80 for KT, 160 in total. 45 bar specimens for Katana HTML were also produced, but in a smaller size than the previous 80. Katana HTML had an extra number of specimens, for reasons that will be stated later in this chapter. TZI had 10 specimens made only to serve as a reference control group. These samples were obtained by sectioning the zirconia discs using a High-Speed Precision Saw (Isomet 5000; Buehler Ltd., Lake Bluff, IL) with a diamond blade (15 HC diamond; Buehler Ltd., Lake Bluff, IL) for gross sectioning, and Slow-Speed Saw (Isomet 11-1180; Buehler Ltd., Lake Bluff, IL) for finer cuts using a diamond blade (Buehler Ltd., Lake Bluff, IL). The discs were oriented in a manner where the enamel would face the top and the dentin layer would face the bottom, and the saw would be cutting the disc from the side of it. The specimens were sectioned at predetermined dimensions, which were amplified in size before sectioning due to the 20-25% shrinkage that occurs in these materials as reported by the manufacturers. The specimens were then grinded manually using serial silicon carbide abrasive paper from a coarser grain, 320 grit, to a finer grain, 600 grit (CarbiMet; Buehler Ltd., Lake Bluff, IL). This was done to help achieve dimensions as close as possible to the wanted presintered size, as well as to remove any large, gross scratches that may have been introduced into the specimens in the sectioning process via the sectioning blades. This process can be seen below in Figures 12 and 13.

Figure 12: Sectioned disc

Figure 13: Isomet 11-1180 Low Speed Saw sectioning the zirconia disc.

Once the specimens were all sectioned and ground down to size from any deep scratches, they were subsequently cleaned in an ultrasonic bath (Quantrex; L&R Ultrasonics, Kearny, NJ) for 30 seconds then blot dried with cloth. This was done to remove any possible contamination that may have happened during the sectioning and grinding process, i.e., any loose diamonds from the sectioning blades or contaminants from the abrasive paper, as well as to remove any loose powder than may have stuck on to the specimen in the process. This can be seen in Figure 14 below. Due to the possible water sorption that may have occurred during the sectioning and grinding process, the samples were dried in a convection oven (3511FSQ; Fisher Scientific, Pittsburgh, PA) at 70 °C for 24 hours shown in Figure 15. The specimens were then sintered immediately after drying, as per each material's manufacturer's instructions in a zirconia furnace (Hotspot 110L; Zircar, Florida, NY). The sintering protocol for each material can be seen below in Tables 1, 2, 3, and 4.

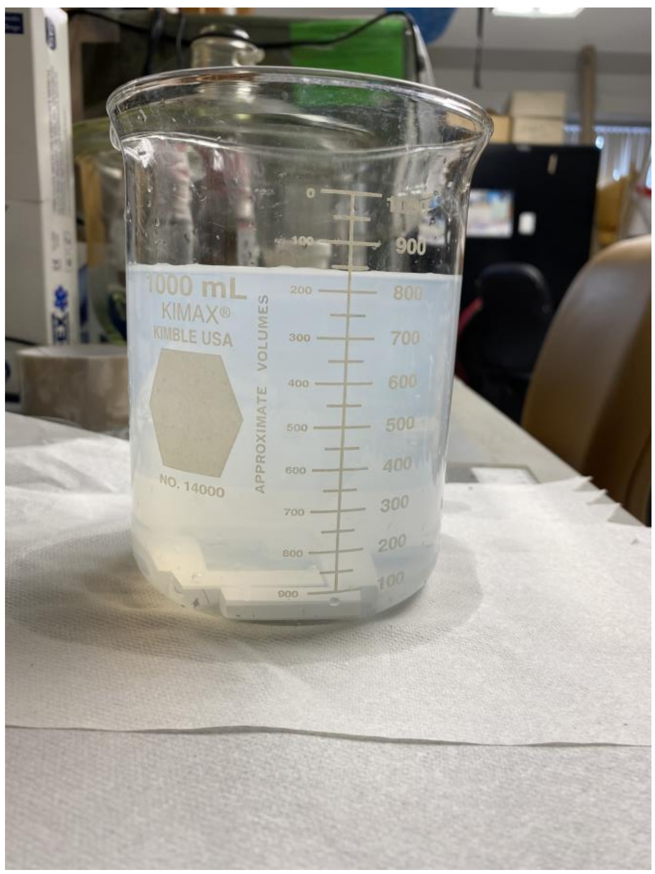

Figure 14: Murky water caused by loose powder that was stuck on the zirconia specimens after ultrasonic bathing.

Figure 15: Specimens being dried in a convection oven

Table 1: Katana HTML Sintering Program

Starting Temperature (ºC)	Heating Rate (ºC / min)	Cooling Rate (ºC / min)	Target Temperature (ºC)	Holding Time (min)
25	10	-	1500	-
1500	-	-	1500	120
1500	-	10	25	-

Table 2: ZirCAD Prime Sintering Program

Starting Temperature (ºC)	Heating Rate (ºC / min)	Cooling Rate (ºC / min)	Target Temperature (ºC)	Holding Time (min)
20	10	-	900	-
900	-	-	900	30
900	3.3	-	1500	-
1500	-	-	1500	120
1500	-	10	900	-
900	-	8.3	300	-

Table 3: Origin Beyond+ Hybrid Sintering Program

Starting Temperature (^oC)	Heating Rate (^oC / min)	Cooling Rate (^oC / min)	Target Temperature (^oC)	Holding Time (min)
25	20	-	1050	-
1050	-	-	1050	30
1050	2	-	1480	-
1480	-	-	1480	180
1480	-	5	1000	-
1000	-	10	250	-

Table 4: inCoris TZI Sintering Program

Starting Temperature (^oC)	Heating Rate (^oC / min)	Cooling Rate (^oC / min)	Target Temperature (^oC)	Holding Time (min)
25	25	-	800	-
800	15	-	1510	-
1510	-	-	1510	120
1510	-	30	200	-

After sintering, the specimens were polished using 70, 45, 15, 6, and 0.5 µm diamond discs (DGD Ultra disc, Buehler Ltd., Lake Bluff, IL) to achieve a mirror-like surface using the Grinder / Polisher machine (EcoMet 250; Buehler Ltd., Lake Bluff, IL). ZP, OB, and 40 KT large specimens were all polished manually using two finger pressure along the long axis of the specimen. Only two groups of the Katana HTML small bar specimens were polished, the last group was not polished to be used as a comparison.

The remaining 40 large specimens of Katana HTML, and the 10 inCoris TZI specimens were sectioned and grinded in the same manner as the other specimens, but it was decided to polish them in an automated fashion to allow for a more uniform polishing to help achieve flatter and more parallel specimens. This was decided after initial testing of the four groups of KT samples, which revealed a big difference in flexural strength from what was reported by the manufacturers than what was observed during experimentation. This was also the reason why it was decided to fabricate small specimens of KT to help compare the specimen size to determine if size had an effect on the strength. TZI was used in this case to help validate the large size of the KT specimens, adopting the same automated polishing technique. The automated polishing involved gluing the specimens onto a polishing disc using a crystal adhesive (Crystalbond 509 Mounting Adhesive; Ted Pella Inc., Redding, CA). The adhesive was heated up to a maximum temperature of 185 ºC to avoid introducing any potential phase transformation in the zirconia specimens. The specimens were glued in an even circle so that the path of rotation on the polishing discs would be the same across all specimens to ensure an even surface finish. Once air cooled to ambient room temperature, the polishing plate was mounted onto the EcoMet 250 Grinder / Polisher machine using a maximum starting force of 60 N, and a speed of 180 RPM for the head and 60 RPM for the base rotating in opposite directions. The force was decreased by 10 N each time, in a serial manner, from a coarser disc to a finer one to a minimum of 25 N on the 0.5 µm disc. The same diamond grinding disc protocol and sequence was used in this case as well, i.e., from 70 to 0.5 µm. Both methods of polishing were done under continuous water irrigation, and all sides of the specimens were polished to a mirror-like finish. A 45º bevel was added onto all sides of each specimen at a 0.5 µm finish. Figures 16-19 show the polishing process and outcome.

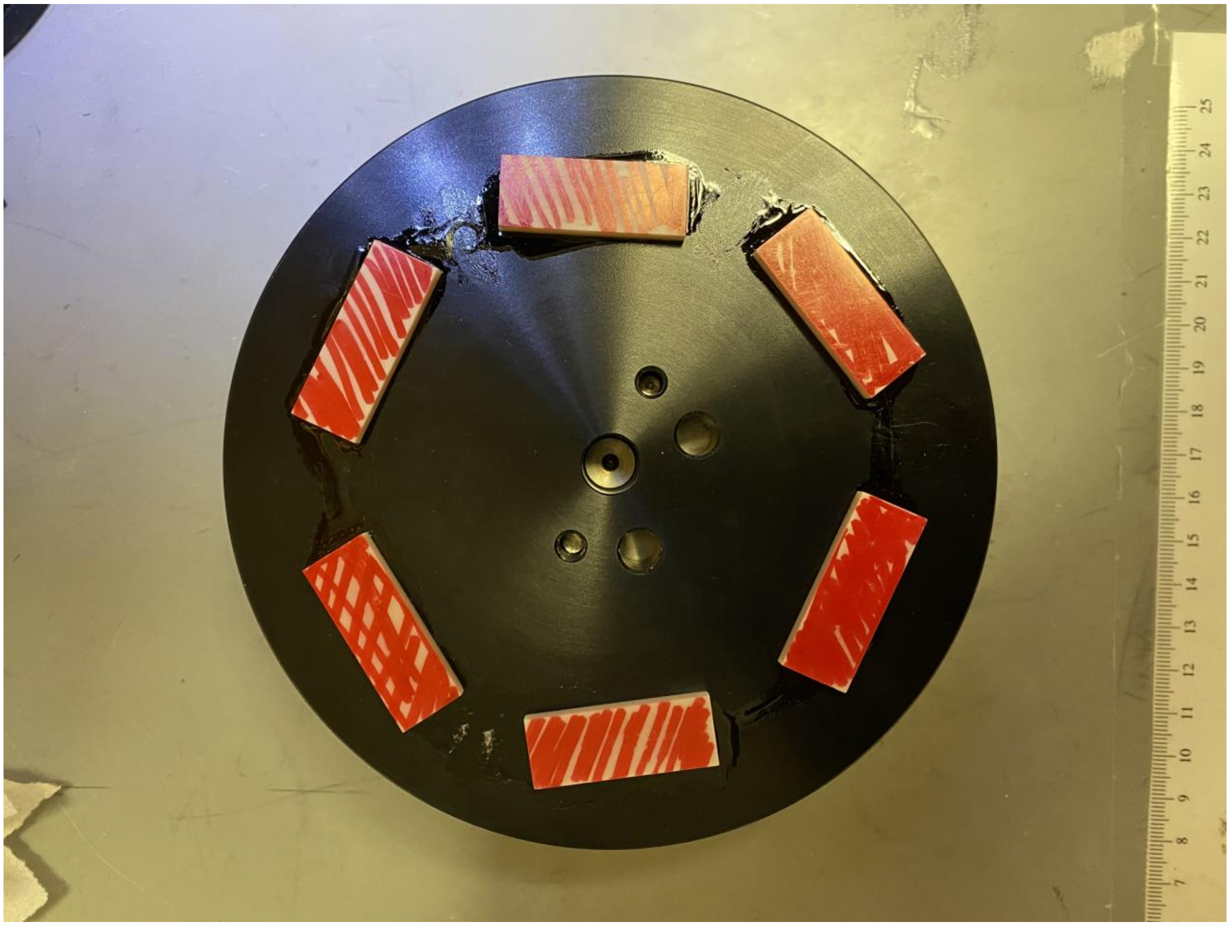

Figure 16: KT specimens mounted onto the polishing disc. Red markings were placed to serve as a guide to ensure an even, polished flat surface.

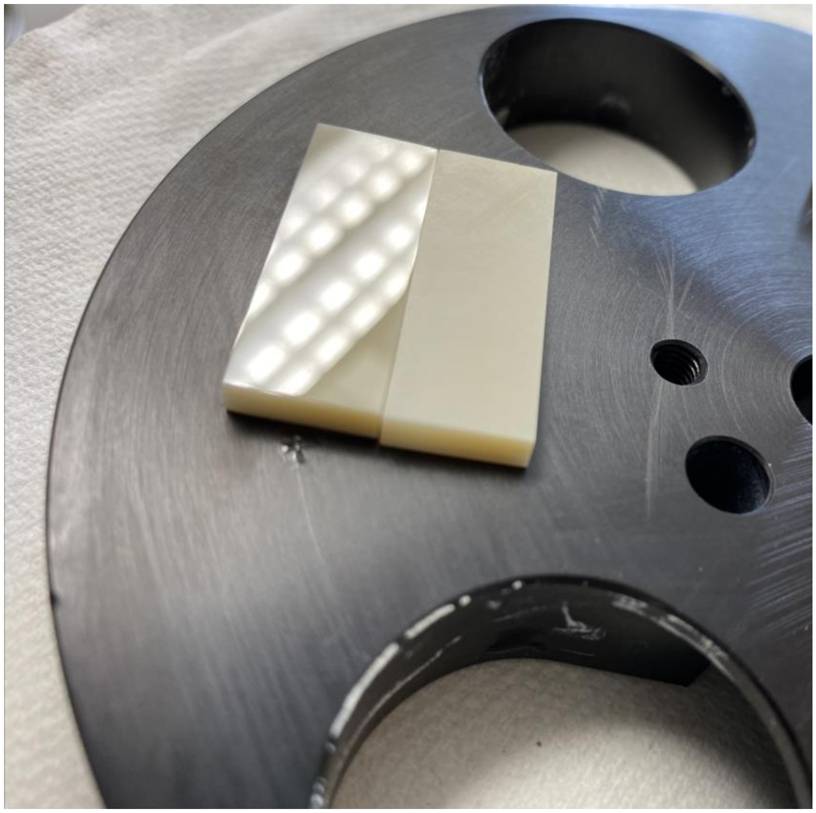

Figure 17: Comparison between a polished an unpolished KT specimen. Notice the reflection on the polished specimen (left) and the dullness of the unpolished one (right). Note: unpolished specimen here was placed next to the polished one for demonstration purposes only.

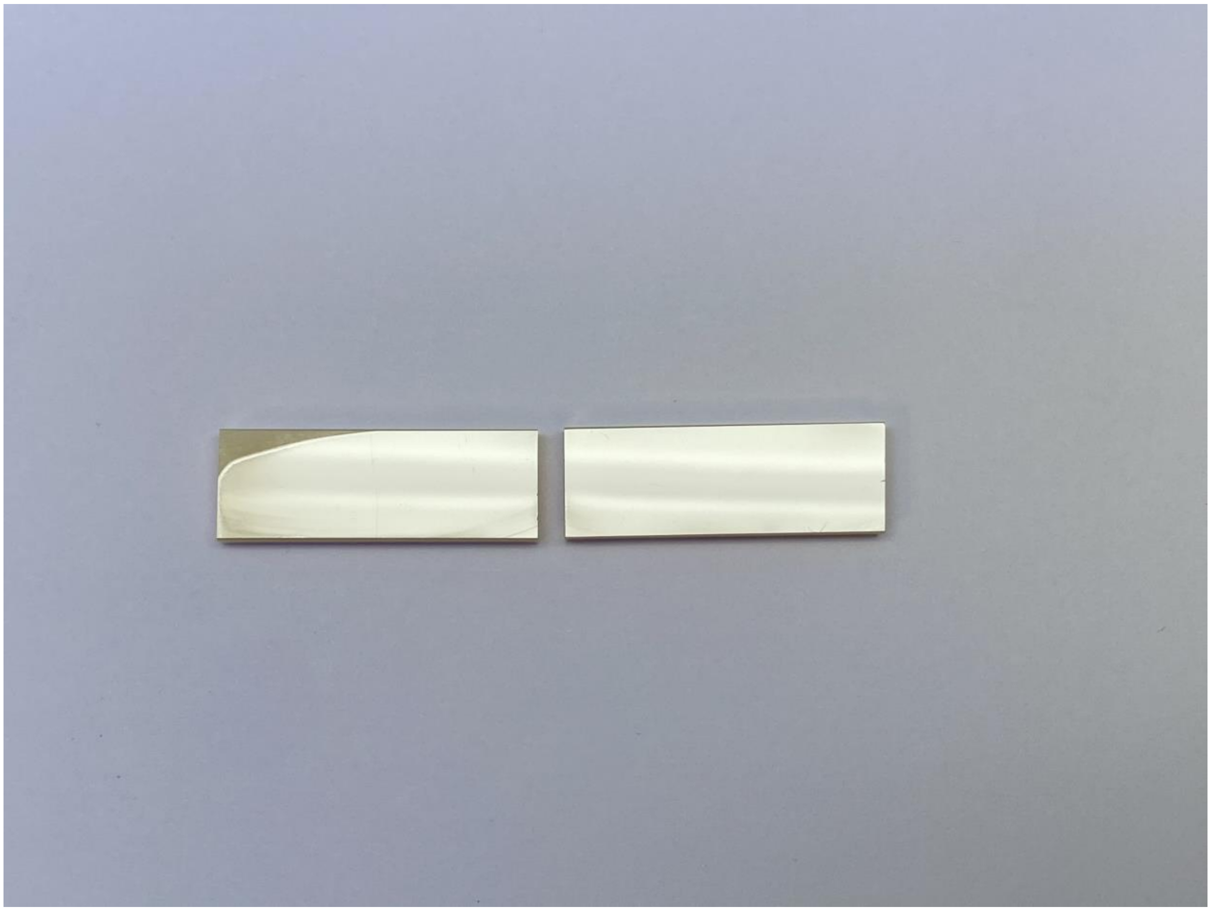

Figure 18: KT specimen deemed to have an uneven finish (left) vs. evenly polished surface finish (right) free of any scratches or defects.

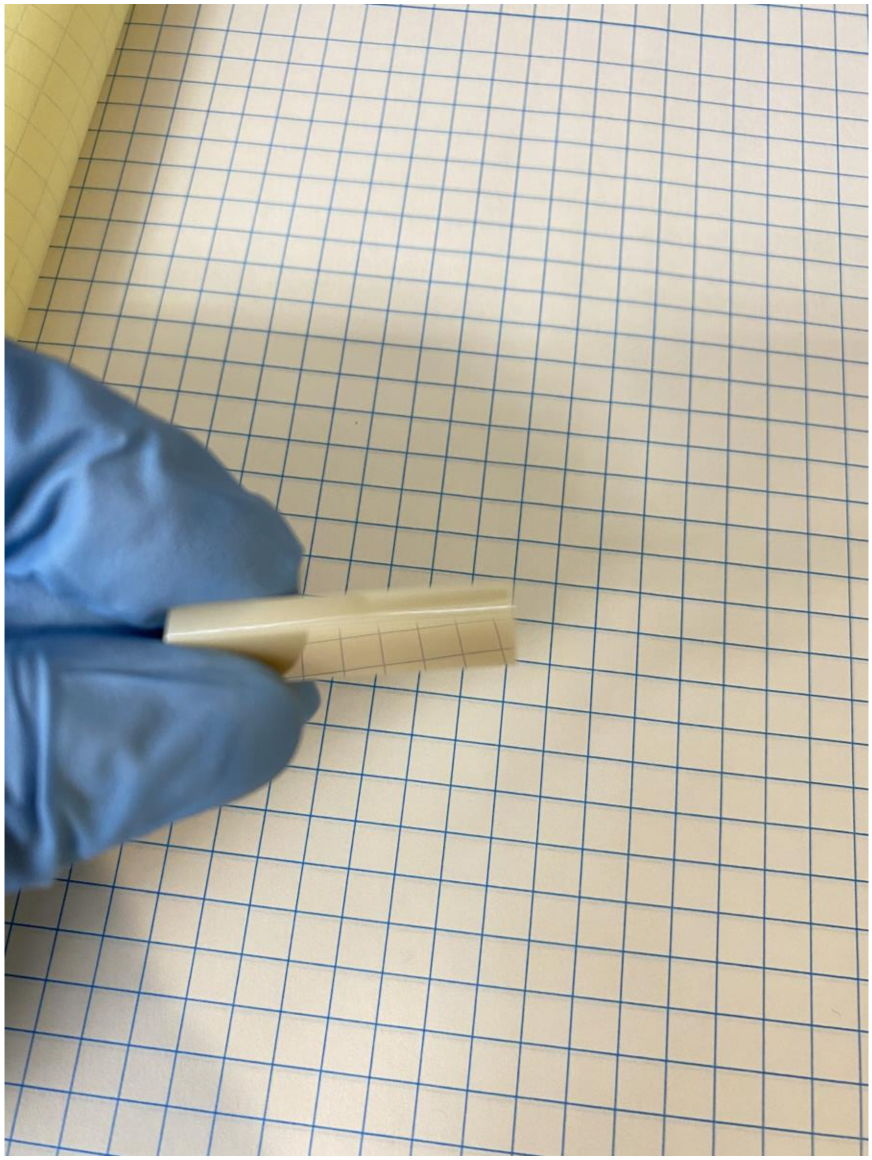

Figure 19: KT specimen with a mirror-like final finish. Notice the grid marks reflecting on the specimen.

Once an evenly polished surface finish was achieved and a bevel was placed, the specimens were cleaned in an ultrasonic acetone bath for 2 minutes to remove any leftover traces from the marker and adhesive on the samples. All groups, with the exception of two of the small sized Katana HTML groups, were subsequently annealed to remove any phase transformation effects that may have occurred from the polishing process. This was done using a Speed furnace (Sirona InFire HTC; Dentsply Sirona, York, PA), using the following protocol shown in Table 5, which was adapted from VITA Zahnfabrik (2011).

Table 5: Regeneration firing procedure (annealing)

Starting Temperature (°C)	**Heating Rate (°C / min)**	**Final Temperature (°C)**	**Holding Time (min)**	**Cooling**
500	100	1000	15	Natural cooling with furnace

Once the annealing process was done, the specimens were divided into plastic bags according to their material and treatment groups. Groups 1R, 3R, and 5R correspond to 1 repeated firing, 3 repeated firings, and 5 repeated firing cycles as to mimic glazing or staining. The TZI and small sized Katana HTML specimens were just used as a control and no repeated firings were done on them. The protocol for the repeated firing process was adapted from Ivoclar Vivadent for the IPS Ivocolor Staining Technique (2019). The furnace used was Programat CS (Ivoclar Vivadent, Schaan, Liechtenstein). A maximum of 3 specimens were treated in each cycle, which were cooled to room temperature before starting the next firing cycle. The protocol can be seen in Table 6. Figure 20 shows the specimens as soon as the cycle finishes. Specimens were considered ready for flexural strength testing once this process was done. A diagrammatic representation of specimens A can be seen in Figure 21. Specimen A sizes before and after specimen preparation can be seen in Table 7.

Table 6: Repeated firing protocol

	Stand-by Temperature B (°C)	**Closing TIMES (min)**	**Heating Rate T ↗ (°C / min)**	**Firing Temperature T_1 (°C)**	**Holding Time H_1 (min)**	**Vacuum 1 (°C)**	**Vacuum 2 (°C)**	**Long-term cooling L (°C)**
Stains and Glaze Firing	403	6:00	15	710	1:00	450	709	450

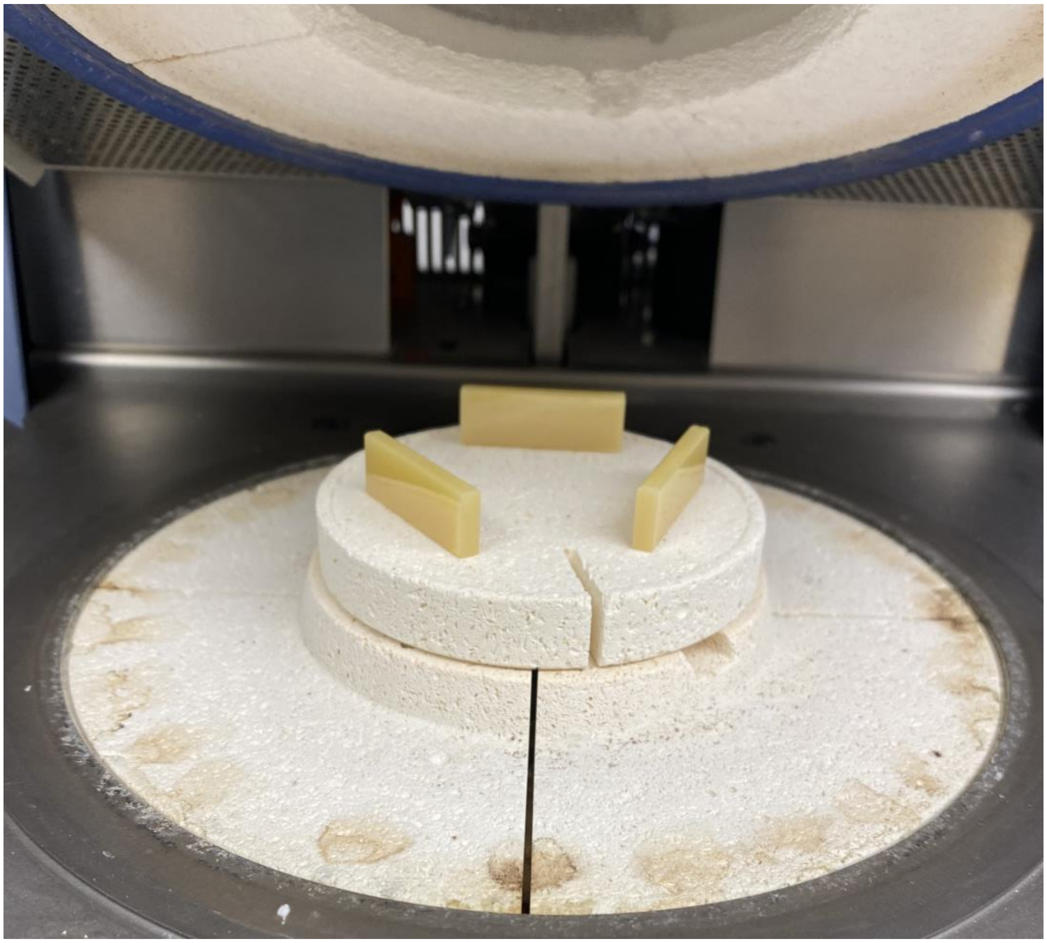

Figure 20: KT specimens showing a creamy color the moment the repeated firing cycle is done.

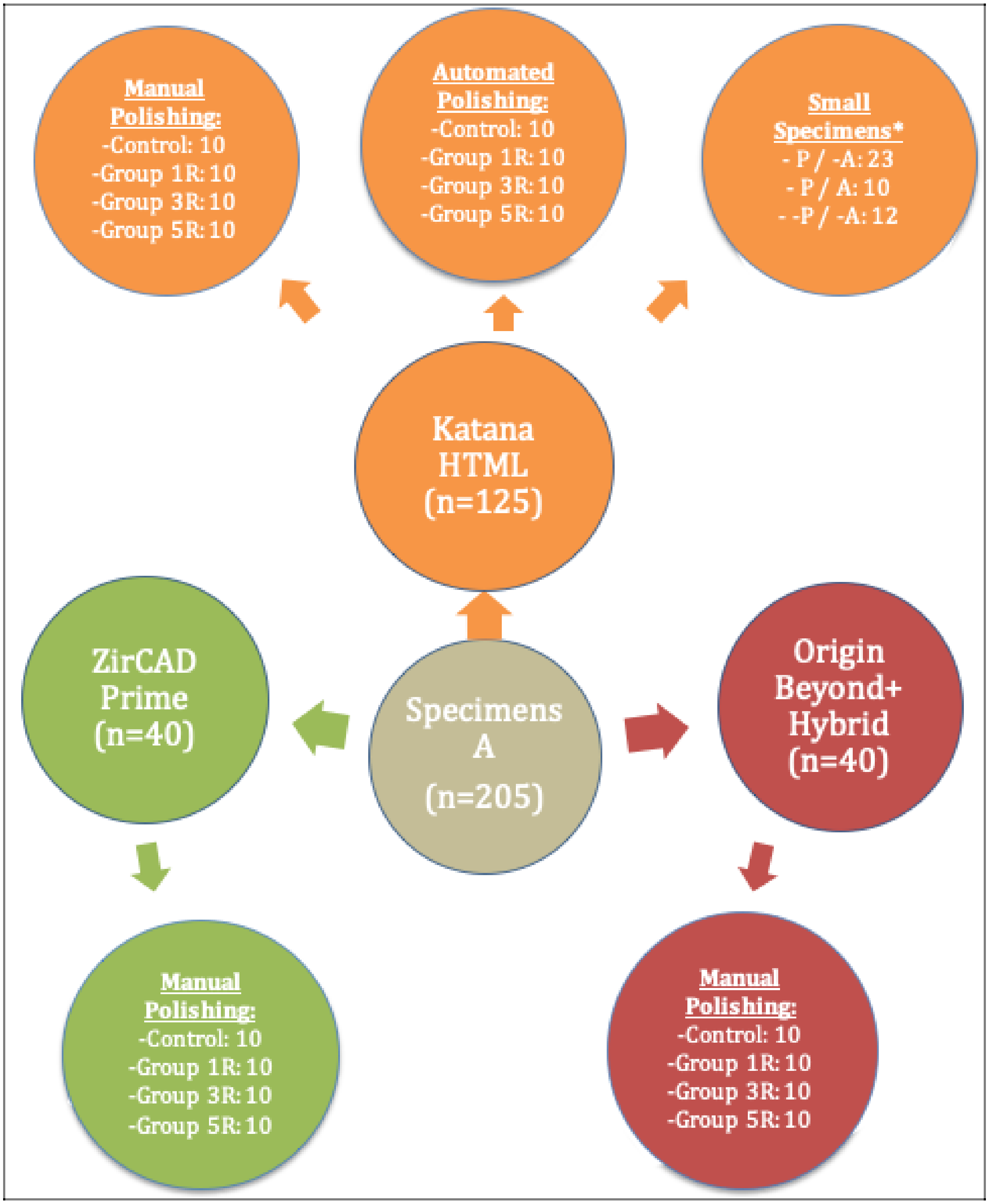

Figure 21: Specimens A. *P: polished, A: annealed, -P: not polished, -A: not annealed.

2.2.2 SPECIMENS B

As mentioned previously, a second set of specimens was made for the remainder of the tests to avoid introducing any faults into the specimens from the flexural strength test, as well as machine limitations when it came to specimen size and width. Due to the remainder of the tests being non-destructive, one set of samples was made and used for all these tests. With the exception to the number and size of specimens, Specimens B were prepared in the same steps that were used to prepare Specimens A, utilizing the automated polishing technique described earlier. This was done to ensure an even and flat surface so that each specimen had uniform width, as any discrepancies would have introduced variations and inaccuracies during testing. A total of 24 samples were machined, each material had 8 specimens divided equally into their 4 groups. Specimens B were cleaned using an isopropyl alcohol bath submerged in ultrasonic water for 2 mins to ensure no residues of any sorts were left on the specimens. A graphic representation of this can be seen in Figure 22. Specimens B were used for the contrast ratio test, crystallographic changes via XRD, and elemental composition via EDS. Specimen size before and after sintering can be seen in Table 8 for this group of specimens.

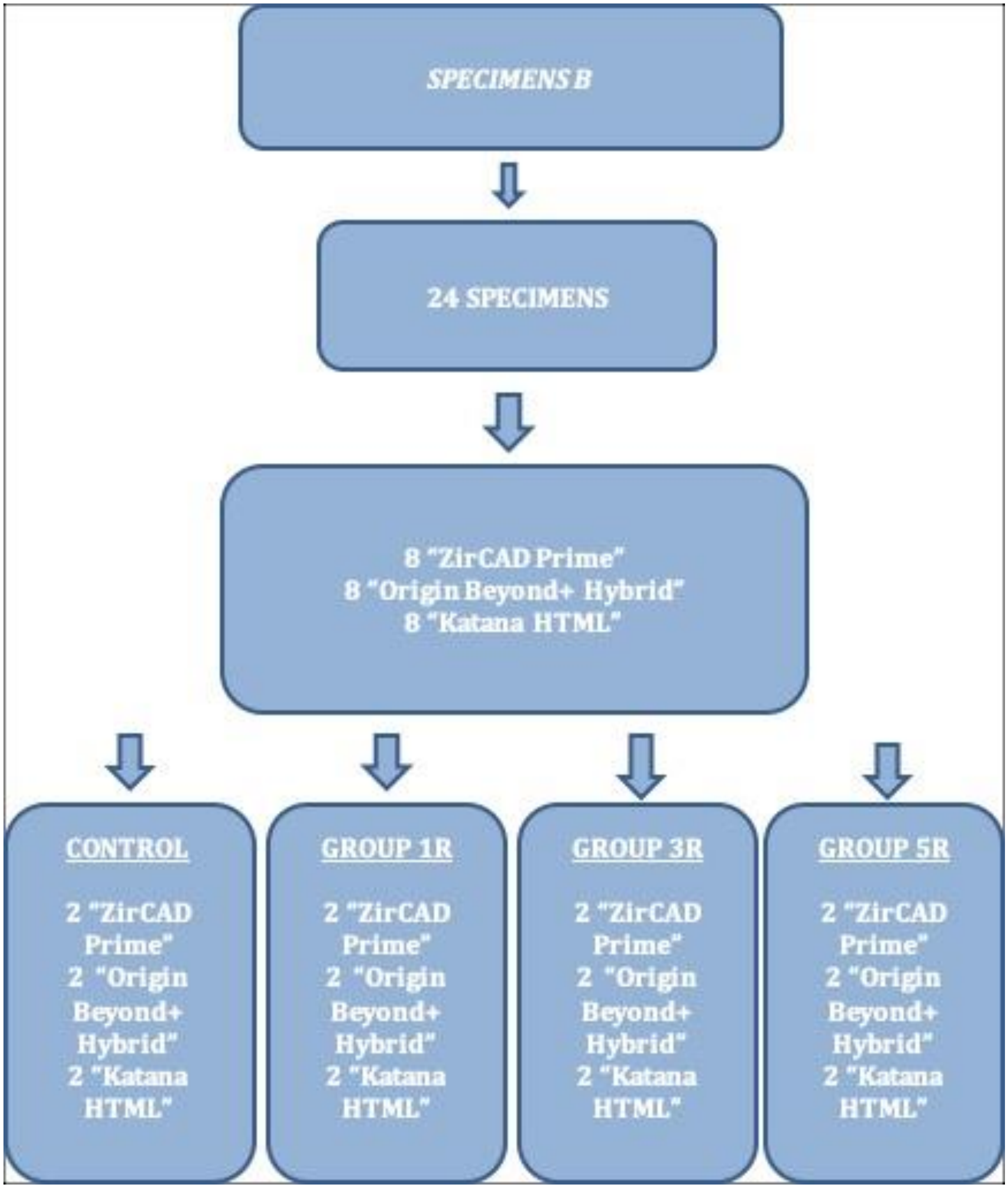

Figure 22: Specimens B diagrammatic representation

2.2.3 SPECIMEN SIZE

For the purposes of this study, all layers were to be included for the various multilayered zirconia. As per ISO 6872 Dentistry – Ceramic Materials guidelines, the final size of the bars for Specimens A should have had a width of 4mm, thickness of 3mm and length of 25mm, since they are to be used for a three-point flexural strength test (International Organization for Standardization, 2014). However, the final measurements of each specimen bar surpassed the recommended dimensions as listed by the ISO 6872 standard due to the increased thickness of the discs. If adhered to the ISO 6872 standard, that would have meant that each layer would have been sectioned separately and the tests conducted on each layer individually to comply with their sizing measurement since the suggested thickness is only 3mm. This would have not given an accurate representation of the material since these materials would more likely be used in partial or full thickness during the nesting process in dental restoration fabrication. As such, the rationale in including all layers, i.e., enamel, transition, and dentin, would give a more accurate clinical representation of the material and how they would perform in the oral environment. Considering the testing machine's ability to fracture the specimens, an increase to the width and length of the specimens was necessary to accommodate the increased thickness of the specimens.

Both the Origin Beyond+ Hybrid and Katana Zirconia HTML zirconia discs measured 14mm each in thickness with all layers included. The ZirCAD Prime disc measured 16mm in thickness. As such, the bars that were obtained had all layers included as a priority over the ISO 6872 guidelines, therefore resulting in much thicker specimens. TZI bars were fabricated to have the same size as OB and KT to validate the size used. ZP's size was previously validated in an internal study at Boston University's Department of Restorative Sciences and Biomaterials. With regards to the small sized KT bar specimens, they were sectioned from various parts of the disc and as such, specimens do not include all the layers in the disc. Note that whenever thickness is mentioned in regards to Specimens A, it refers to the side that will be held perpendicular to the crosshead in the flexural test.

As for Specimens B, they were fabricated to be much smaller to accommodate the various tests. However, all layers of each multilayered material were included for testing. Thickness in Specimens B would refer to the side that will be held perpendicular to the light beam in the contrast ratio test. Note that specimens B only included ZP, OB, and KT in one size for the purposes of this study.

As previously mentioned, due to material shrinkage varying between 20-25%, the pre-sintered size of the bars must be determined prior to sectioning the discs and polishing the bars. All these measurements might vary slightly from one specimen to another since manual grinding / polishing was used in certain cases. However, each individual specimen was measured using a digital caliper to account for this minor variation.

Table 7: Specimens A Mean Dimensions

Material	Thickness (mm)	Width (mm)	Length (mm)	Support Span (mm)
ZirCAD Prime (presintering)	16	6.4	66	-
ZirCAD Prime (final)	13.1	5.3	54	40
Origin Beyond+ (presintering)	14	4.56	40.5	-
Origin Beyond+ Hybrid (final)	11.1	3.6	32	20
Katana HTML (large – presintering)	14	4.3	39.0	-
Katana HTML (large - final)	11.5	3.6	32	20
Katana HTML (small – presintering)	2.5	3.6	30.5	-
Katana HTML (small - final)	2.1	3	25	20
inCoris TZI (presintering)	13	4.1	36.3	-
inCoris TZI (final)	11.5	3.6	32	20

Table 8: Specimens B Mean Dimensions

Material	Thickness (mm)	Width (mm)	Length (mm)
ZirCAD Prime (presintering)	1.1	6.6	16.1
ZirCAD Prime (final)	0.9	5.4	13.2
Origin Beyond+ Hybrid (presintering)	1.1	6.6	14
Origin Beyond+ Hybrid (final)	0.9	5.2	11.1
Katana HTML (presintering)	1.1	6.3	14.0
Katana HTML (final)	0.9	5.2	11.5

2.3 OPTICAL PROPERTIES

Specimens B were used for this test and placed in the Ci7600 Benchtop Spectrophotometer holders (X-Rite, Grand Rapids, MI). CIE standard illuminant D65 was used to represent average daylight. The test was conducted by determining a range for each layer, in mm, across all multilayered zirconia materials. This range was used in order to get more accurate results by aiming to focus most of the light beam on each layer separately during the scans, avoiding overlapping layers as much as possible. However, due to the smallest aperture available being 3.5 mm in diameter, the scans can include more than one layer at a time during the scan depending on the layer's size. For example, ZP's enamel layer measured 2.48 mm in length after sintering and as such it would have to overlap with the transition layer during the test since the aperture's diameter is 3.5 mm. The determined size of each layer can be seen in Table 9 below.

The specimens were moved manually in the holder to allow the test of each layer or prespecified range. Specimens were centered for each scan, making sure the 3.5 mm wide aperture hole was covered completely. The sides of each specimen were avoided due to the presence of the chamfer, which may have interfered with the test. Transition layers that measured less than 3 mm in length were grouped into one for the scans as it was impossible to obtain accurate results trying to isolate each transition layer. Two specimens were used for each group. Two scans were taken for each layer: enamel, transition, and dentin once using a black background and another using a white background, giving a total of three readings per specimen and a total of six per group per material, which can be seen in Figure 24. The spectrophotometer was calibrated before each scan. The contrast ratio ($CR = Y^b/Y^w$) was determined from the luminous reflectance over black (Y^b) and white (Y^w) backgrounds using the spectrophotometer for each group. Figures 23 - 25 help visualize this process. The results were gathered and compared using JMP Pro 17 software for statistical analysis (SAS Institute, Cary, NC). The "0" value was considered to be transparent and "1" value was considered to be completely opaque.

Color values were measured for L*, a*, and b* as part of the CIELAB system. The calculations done were performed on white and black backgrounds using the same

Ci7600 Benchtop Spectrophotometer (X-Rite, Grand Rapids, MI). Statistical analysis was done using JMP Pro 17 software (SAS Institute, Cary, NC).

Table 9: Width range of each layer in fully sintered Specimens B

Material	Enamel Layer (mm)	Transition Layer (mm)	Dentin Layer (mm)
ZirCAD Prime	0 - 2.48	2.48 – 5.78	5.78 – 13.2
Origin Beyond+ Hybrid	0 - 2.58	2.58 – 8.64	8.64 - 11.1
Katana HTML	0 - 4.04	4.04 – 7.51	7.51 – 11.5

Figure 23: A ZP specimen being positioned for an enamel layer scan.

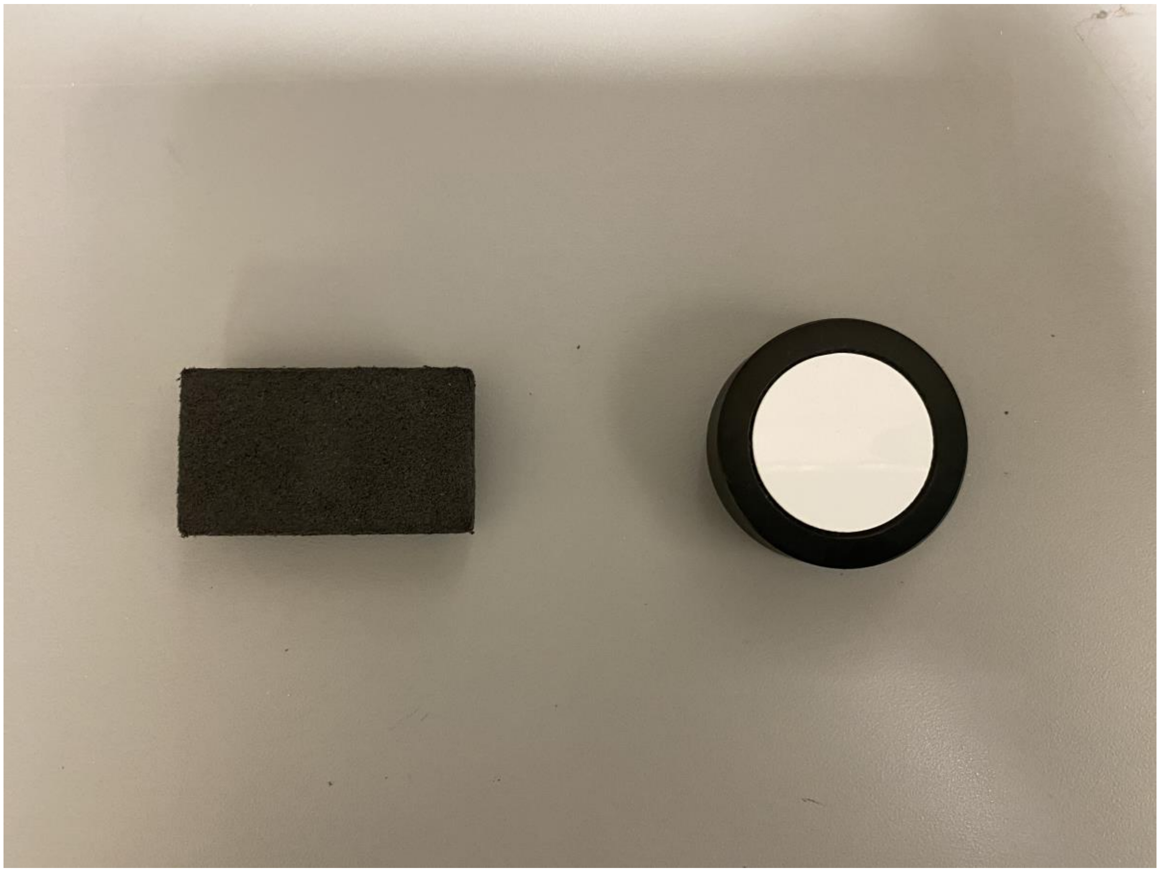

Figure 24: Black background (left) and white background (right)

Figure 25: Scan being conducted on a white background

2.4 CRYSTALLOGRAPHIC ANALYSIS

Crystallographic analysis was performed on Specimens B of the multilayered zirconia to evaluate phase composition and any crystallographic changes that may have occurred from the repeated firing process using XRD (D8 Discover; Bruker, Billerica, MA). Using the same rationale that was employed in the contrast ratio test, the analysis was done on each individual layer using the same values listed in Table 9. With the use of a 1 mm pinhole and a 1 mm collimator, it was achievable to successfully target each layer individually without having any overlap since the diameter of the target beam was 1mm only. The parameters used were as following: Cu tube with wavelength of 1.5418 (Kα) at 40 kV and 40 mA, utilizing a Coupled Two Theta / Theta scan with a 2-theta range from 20^o to 85^o, a step size of 0.01979^o, and a 1.0 second count time. A Z-scan was done before each scan to ensure proper positioning. Rietveld Analysis and graphs of the crystallographic phases were obtained using open source GSAS II software. Figure 26 shows the positioning of the laser beam onto one of the layers on the specimen. All readings were taken from the center of the specimen avoiding any edges or corners. Statistical analysis was done using JMP Pro 17 software (SAS Institute, Cary, NC).

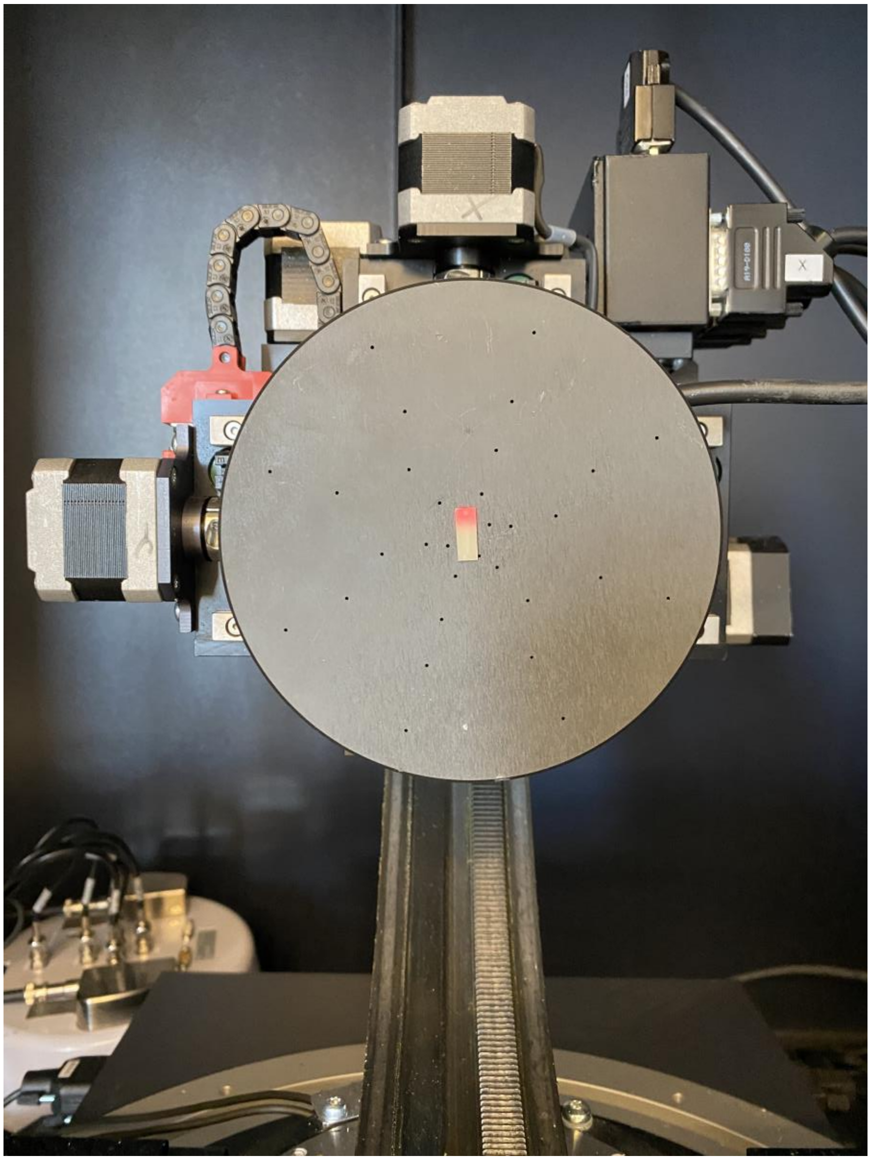

Figure 26: Laser beam pointed at the top layer, enamel, of a specimen.

2.5 ELEMENTAL COMPOSITION

As mentioned in the previous chapter, the amount of yttria in zirconia can have a varied effect depending on its concentration. Since these are multilayered zirconia to be tested, which can have different yttria amounts between their layers, it was decided to investigate how this concentration changes across each layer when subjected to repeated firing. Yttria content was measured for each layer using the Scanning Electron Microscope (SEM, Hitachi) and its Energy-Dispersive X-Ray Spectroscopy (EDS) (Aztec 50 SDD Detector, Oxford Instruments). These specimens were bathed in cleaned with isopropyl alcohol right before the test was conducted. Variable Pressure (VP) mode was used on the SEM with a 15 kV and 10 mm working distance.

An individual point scan method was utilized on the EDS software, Aztec 4.1 SP1. Utilizing the measurements from Table 9 to position the specimen onto the layer of interest, an individual point scan was made. Since the objective was to see how the yttria content changes across each layer, it was decided to conduct these individual point scans on 5 locations on the specimen: enamel, enamel-transition junction, transition, transition-dentin junction, and dentin layer. 4 individual point scans were made on each location to yield better, more accurate results. These results were obtained then analyzed to get the yttria mol % by comparing it to the zirconia and hafnium concentrations. Statistical analysis was done using JMP Pro 17 software (SAS Institute, Cary, NC).

2.6 FLEXURAL STRENGTH (THREE-POINT)

A three-point flexural strength test was used to assess the strength of the specimens. Since the test was to include all of the layers in the multilayered zirconia disc, this resulted in an increased thickness of Specimens A being tested. As such, this meant that an increased amount of force was needed in order to break each specimen. The Universal Testing Machine (5566A; Instron, Norwood, MA) has a load cell with a maximum load capacity of 10,000N. A simple reverse calculation that was made meant that the Instron was not capable of breaking these samples and required a higher amount of force. Therefore, a force amplifier was used and set up on the Instron testing stage, which effectively multiplied the load applied onto the specimens by 2.5 times, increasing the maximum load of 10,000N to 25,000N. This meant that there was enough force available to break the specimens.

A blunt attachment was placed into the Instron crosshead, which would in turn transfer the force onto the amplifier's arm. A hardened steel roller was attached on the arm of the amplifier, using a hot glue gun, which would direct the force onto the specimen. Two platforms were available to attach onto the amplifier base, with the distance between the support span rollers being 40mm and 20mm respectively. The 40mm platform was used for ZP specimens and the 20mm was used for the OB and KT large specimens. The two bottom rollers were also fixated onto their respective platforms using a hot glue gun. The thickness of all rollers was 4.75mm, measured using a digital caliper. The specimens were placed horizontally onto the two rollers, oriented so that the enamel layer surface was facing the top, where the highest compressive forces are, and the dentin layer surface at the bottom, where the highest tensile stresses are. Once the specimen was positioned so that there was at least 2mm on either side of the rollers, to comply with the ISO 6872 Dentistry – Ceramic Materials Standards, the third roller would apply constant force directly into the middle of the specimen at a 0.5mm/min until the specimen fractured, for which the fracture load was obtained and subsequently analyzed. Figure 27 shows this setup.

As for the small KT specimens, a similar procedure was performed. They were placed onto a premade fixture that was attached into the Instron, with a 20mm support span. Since these specimens were small in thickness, there was no need to include the amplifier in the test. As such, an attachment that had a roller was inserted into the Instron, which would direct the force onto the specimen directly. The Instron crosshead continuously applied force onto the specimens at a rate of 0.5mm/min, until the specimens fractured. All three rollers had a diameter of 3.2mm. Figure 28 shows the setup for the small specimens.

Care was taken so that specimens were positioned in the center on the rollers, avoiding any angulations, or touching the glue that was used to fixate the rollers onto the platform. Rollers that were scratched or showed signs of deformities after a few tests were replaced with new rollers. An enclosure casing was also made for safety purposed to avoid any flying projectiles once the specimens were fractured.

Once the results were obtained, the flexural strength was calculated using the following formula:

$$\sigma = \frac{3Pl}{2wb^2}$$

Where σ= flexural strength in, MPa, *P* is the breaking load in Newtons; *l* is the test span (center-to-center distance between support rollers), in millimeters; *w* is the width of the specimen, in millimeters *b* is the thickness of the specimen, in millimeters. Statistical analysis was performed using JMP Pro 17 software (SAS Institute, Cary, NC).

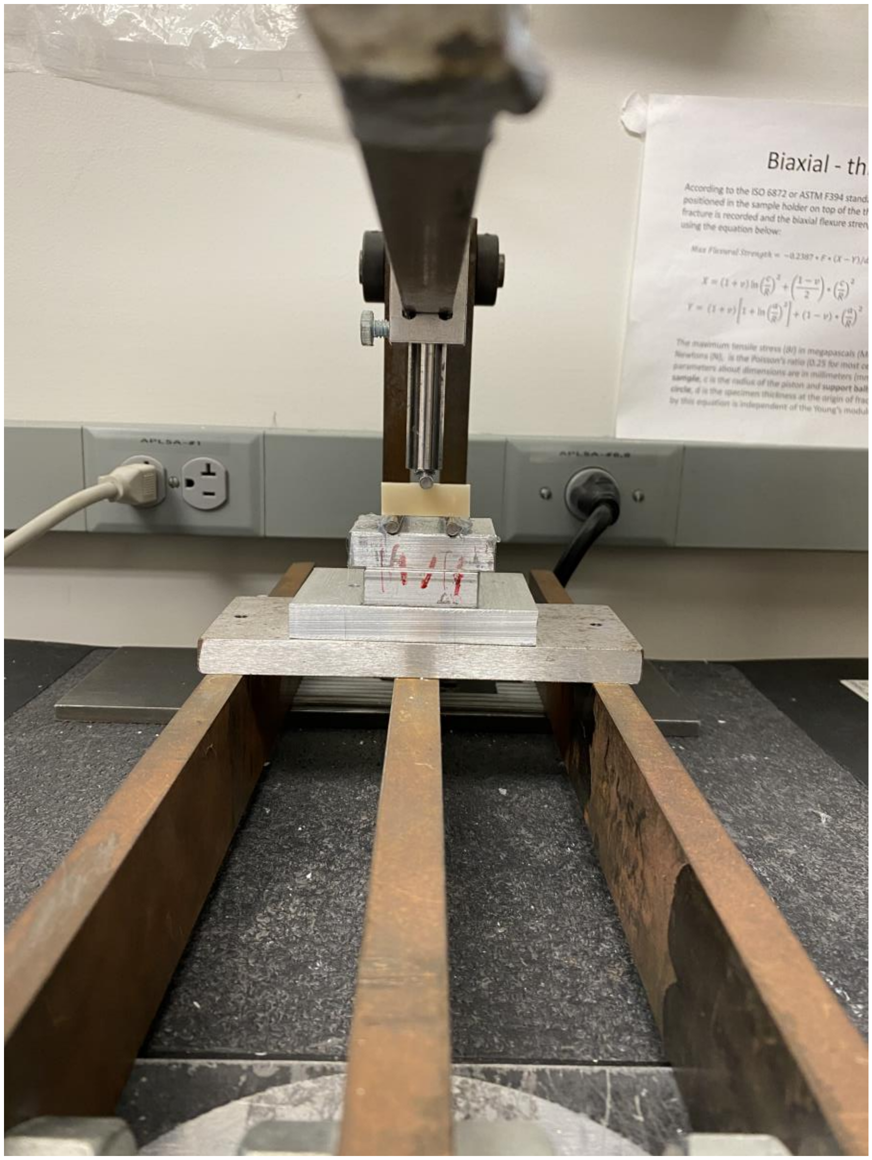

Figure 27: Katana HTML specimen (11.5 x 3.6 x 32mm) positioned onto the rollers on the amplifier.

Figure 28: Katana HTML small specimens (2.1 x 3 x 25mm) positioning.

CHAPTER 3. RESULTS

3.1 OPTICAL PROPERTIES

Contrast ratio results expressed are multiplied by 100 to be reflected as percentage value. ZP showed the highest contrast ratio value 73.66, while KT showed the lowest value of 87.88. Contrast ratios of different layers in OB and KT showed relatively close values without significant differences, as opposed to ZP. Table 10 shows the mean contrast ratio values by material and repeated firing effect, while Figure 29 shows the gradual decrease in translucency of each material from the enamel layer to the dentin layer. The values shown in both Table 10 and Figure 29 here represent opacity. Fit of Least Squares (FLS) Tukey HSD statistical test revealed that there was a significant difference ($p<0.0001$) in contrast ratio between the materials, namely between KT and ZP and OB; the latter two showed no significant difference between them. There was also a significant difference ($p<0.0001$) of contrast ratio values between the layers of the same material. These significant differences between materials and layers can be seen in Table 11. However, no significant differences were observed as a result of the repeated firing treatment on the materials or the individual layers within each material ($p =0.107$). The highest levels of translucency were seen in the enamel layer of each material, while the lowest levels of translucency were evident in the dentin layer. Table 12 shows the values for each layer and each material with the repeated firing treatment associated with it.

A Fit of Least Squares test (FLS) was conducted to see if any significant differences existed in the spectral reflectance values. L*, which represents lightness, was significantly different between materials and the different layers ($p<0.0001$) shown in Table 13. When adding the repeated firing treatment into the equation, it was significantly different only between the KT 1R group and KT 5R group, $p = 0.0006$, shown in Table 14. For a*, which represents the green-red color scheme, significant differences were found between the different layers and materials as well ($p<0.0001$), which can be seen in Table 15. No significant effect was seen from the repeated firing treatment on either layers or material. For b*, which represents the blue-yellow color scheme, there was also a significant difference between the different materials and layers ($p<0.0001$), which can be seen in Table 16. Repeated firing showed no significant difference on the materials or layers. Table 17 shows the mean L*, a*, and b* values across all materials and layers.

Table 10: Mean Contrast Ratio Values

		Contrast Ratio – Opacity %			
Material	**Treatment**	**N**	**Mean**	**Std Dev**	**CV**
Katana HTML	**Control**	6	85.94	1.86	2.17
	1R	6	86.25	1.51	1.75
	3R	6	86.35	1.23	1.43
	5R	6	86.40	1.01	1.17
Origin Beyond+ Hybrid	**Control**	6	79.00	2.67	3.38
	1R	6	79.81	2.68	3.35
	3R	6	78.74	2.83	3.60
	5R	6	79.41	2.28	2.87
ZirCAD Prime	**Control**	6	79.85	5.28	6.62
	1R	6	79.85	4.72	5.92
	3R	6	78.62	4.68	5.95
	5R	6	79.08	4.26	5.39

Table 11: LSMeans Differences Tukey HSD for Contrast Ratio in Materials and Layers

Level	Significance*						Least Sq Mean
Katana HTML,Dentin	A						87.62
Katana HTML,Transition	A						86.33
Katana HTML,Enamel		B					84.74
Zircad Prime,Dentin		B					84.74
Origin Beyond+ Hybrid,Dentin			C				81.91
Origin Beyond+ Hybrid,Transition				D			79.52
Zircad Prime,Transition				D			78.67
Origin Beyond+ Hybrid,Enamel					E		76.28
Zircad Prime,Enamel						F	74.63

Connecting Letters Table showing contrast ratio differences between materials and layers. *Levels not connected by the same letter are significantly different. ***p <0.0001***

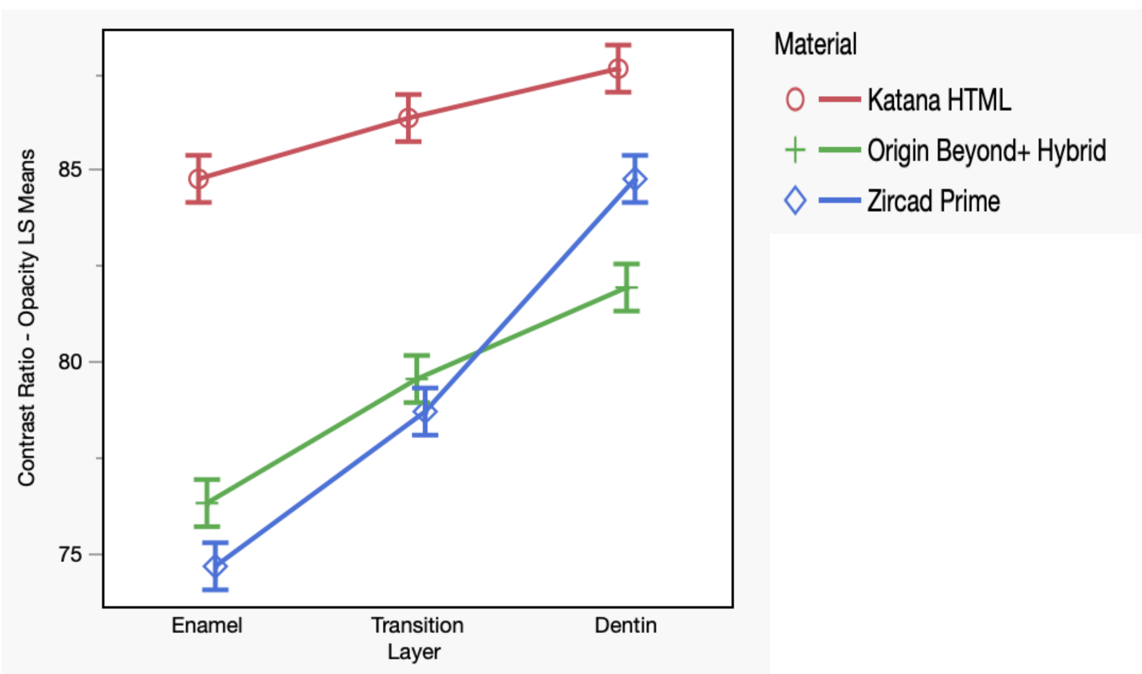

Figure 29: LSM Plot showing an increasing opacity is shown in each material as you proceed from enamel to dentin layer, regardless of treatment done.

Table 12: Contrast Ratio Opacity Values

				Contrast Ratio – Opacity %		
Material	**Treatment**	**Layer**	**N**	**Mean**	**Std Dev**	**CV**
Katana HTML	**Control**	Enamel	2	83.89	0.48	0.57
		Transition	2	86.05	0.57	0.67
		Dentin	2	87.88	0.92	1.05
	1R	Enamel	2	84.86	0.92	1.08
		Transition	2	86.33	0.77	0.89
		Dentin	2	87.57	1.61	1.83
	3R	Enamel	2	84.94	0.6	0.71
		Transition	2	86.54	0.35	0.4
		Dentin	2	87.59	0.01	0.01
	5R	Enamel	2	85.3	0.59	0.69
		Transition	2	86.43	0.24	0.28
		Dentin	2	87.47	0.13	0.15
Origin Beyond+ Hybrid	**Control**	Enamel	2	76.42	1.62	2.12
		Transition	2	78.51	0.22	0.28
		Dentin	2	82.09	0.34	0.41
	1R	Enamel	2	76.52	0.29	0.38
		Transition	2	80.59	0.21	0.26
		Dentin	2	82.31	0.51	0.62
	3R	Enamel	2	75.5	1.02	1.35
		Transition	2	79.09	0.07	0.09
		Dentin	2	81.62	1.14	1.39
	5R	Enamel	2	76.7	0.81	1.05
		Transition	2	79.9	0.55	0.69
		Dentin	2	81.63	0.15	0.18
ZirCAD Prime	**Control**	Enamel	2	73.66	0.4	0.54
		Transition	2	80.72	1.23	1.52
		Dentin	2	85.17	1.8	2.11
	1R	Enamel	2	74.6	0.08	0.1
		Transition	2	79.83	0.41	0.51
		Dentin	2	85.11	0.89	1.05
	3R	Enamel	2	75.21	1.02	1.35
		Transition	2	76.07	0.85	1.12
		Dentin	2	84.59	0.33	0.38
	5R	Enamel	2	75.07	1.83	2.44

		Transition	2	78.07	1.21	1.55
		Dentin	2	84.11	1.04	1.24

Table 13: LS Means Differences Tukey HSD for L*.

Level	Significance*						Least Sq Mean
Katana HTML,Enamel	A						72.92
ZirCAD Prime,Dentin		B					70.69
Katana HTML,Transition		B	C				70.26
Katana HTML,Dentin			C				69.51
ZirCAD Prime,Enamel				D			68.15
ZirCAD Prime,Transition				D	E		67.23
Origin Beyond+ Hybrid,Dentin					E	F	66.91
Origin Beyond+ Hybrid,Enamel					E	F	66.70
Origin Beyond+ Hybrid,Transition						F	66.25

Connecting Letters Table showing differences between materials and layers. Levels not connected by the same letter are significantly different. *p <0.0001*

Table 14: LSMeans Differences Tukey HSD for L* after repeated firing.

Level	Significance*				Least Sq Mean
Katana HTML,1R	A				71.72
Katana HTML,3R	A	B			70.96
Katana HTML, Control	A	B			70.57
Katana HTML,5R		B			70.31
Zircad Prime,5R			C		68.91
Zircad Prime,1R			C		68.71
Zircad Prime,3R			C		68.64
Zircad Prime, Control			C		68.48
Origin Beyond+ Hybrid, Control				D	67.12
Origin Beyond+ Hybrid,3R				D	66.69
Origin Beyond+ Hybrid,5R				D	66.59
Origin Beyond+ Hybrid,1R				D	66.07

Connecting Letters Table showing differences between materials and layers as a result of repeated firing treatment. *Levels not connected by the same letter are significantly different. *p = 0.0006*

Table 15: LSMeans Differences Tukey HSD for a*.

Level	Significance*							Least Sq Mean
Origin Beyond+ Hybrid,Dentin	A							0.07
ZirCAD Prime,Dentin		B						-0.19
Origin Beyond+ Hybrid,Transition			C					-1.09
Origin Beyond+ Hybrid,Enamel				D				-1.32
ZirCAD Prime,Transition				D	E			-1.37
Katana HTML,Dentin				D	E			-1.38
ZirCAD Prime,Enamel					E			-1.48
Katana HTML,Transition						F		-1.63
Katana HTML,Enamel							G	-1.92

Connecting Letters Table showing differences between materials and layers. *Levels not connected by the same letter are significantly different. *p <0.0001*

Table 16: LSMeans Differences Tukey HSD for b*.

Level	Significance*							Least Sq Mean
Katana HTML,Dentin	A							12.46
Katana HTML,Transition		B						10.59
Origin Beyond+ Hybrid,Dentin			C					9.55
ZirCAD Prime,Dentin			C					9.05
Katana HTML,Enamel				D				7.87
Origin Beyond+ Hybrid,Transition					E			5.85
Origin Beyond+ Hybrid,Enamel					E			5.46
ZirCAD Prime,Transition						F		3.02
ZirCAD Prime,Enamel							G	1.83

Connecting Letters Table showing differences between materials and layers. *Levels not connected by the same letter are significantly different. *p <0.0001*

Table 17: Mean L* a* b* values for each material and layer

	L*			a*			b*		
	Layer			Layer			Layer		
	Enamel	Transition	Dentin	Enamel	Transition	Dentin	Enamel	Transition	Dentin
Material	Mean (SD)	Mean (SD)	Mean (SD)	Mean (SD)	Mean (SD)	Mean (SD)	Mean (SD)	Mean (SD)	Mean (SD)
Katana HTML	72.92 (1.05)	70.26 (0.61)	69.51 (0.81)	-1.92 (0.08)	-1.63 (0.12)	-1.38 (0.08)	7.87 (0.24)	10.60 (0.53)	12.46 (0.47)
Origin Beyond+ Hybrid	66.70 (0.57)	66.25 (0.53)	66.91 (0.52)	-1.32 (0.04)	-1.09 (0.11)	0.07 (0.12)	5.47 (0.31)	5.85 (0.31)	9.55 (0.45)
ZirCAD Prime	68.15 (0.81)	67.23 (0.45)	70.69 (0.45)	-1.48 (0.11)	-1.37 (0.08)	-0.19 (0.07)	1.83 (0.44)	3.03 (0.61)	9.05 (0.32)

3.2 CRYSTALLOGRAPHIC CHANGES – XRD

A Rietveld Analysis was conducted using the free open-source software GSAS II (Toby and Von Dreele, 2013), of which a summary of results is reported in Table 18 and Figure 30. The tetragonal phase was the highest in the dentin layers, with the highest value being present in ZP group 1R, 85.7% by phase, and lowest in the enamel layers with the lowest value being in OB group 1R, 44.05%. The cubic phase was highest in the enamel layers, with the highest being in the ZP group 1R, 60.69% by phase, and lowest in the dentin layer, with the lowest being in ZP group 3R, 12.71% by phase. The monoclinic phase was also present with no particular aggregation in any layer but was the highest in KT group 5R with a concentration of 1.31% by phase, with the lowest value of 0% by phase being present across different materials and groups. An incidental finding was observed with the rhombohedral phase being present in all three materials, generally being highest in the enamel layers of ZP and OB, and dentin layer of KT. The highest value recorded for the rhombohedral phase was present in the enamel layer of ZP group 5R with a 11.93% by phase concentration, and was lowest in the enamel layer of KT group 1R with a 1.59% by phase concentration.

FLS Tukey HSD statistical tests were run across all materials and groups to see if there were any significance to the results. Comparing the three materials, there was a significant difference in tetragonal phase content ($p=0.0001$) and cubic phase content ($p=0.0014$) among the different materials and among layers within each material. For rhombohedral phase content, there was only a significant difference between the enamel layer of ZirCAD Prime and the other materials and layers, (p=0.0033). For monoclinic phase content, no significant differences were noted between materials and layers (p=0.3536). All these values can be seen in Tables 19-22. When it came to test for significant of the effects of the repeated firing treatment across layers of each material, no significance was found (p = 0.12). Figures 31-33 show representative XRD phase peaks for each layer of the three materials.

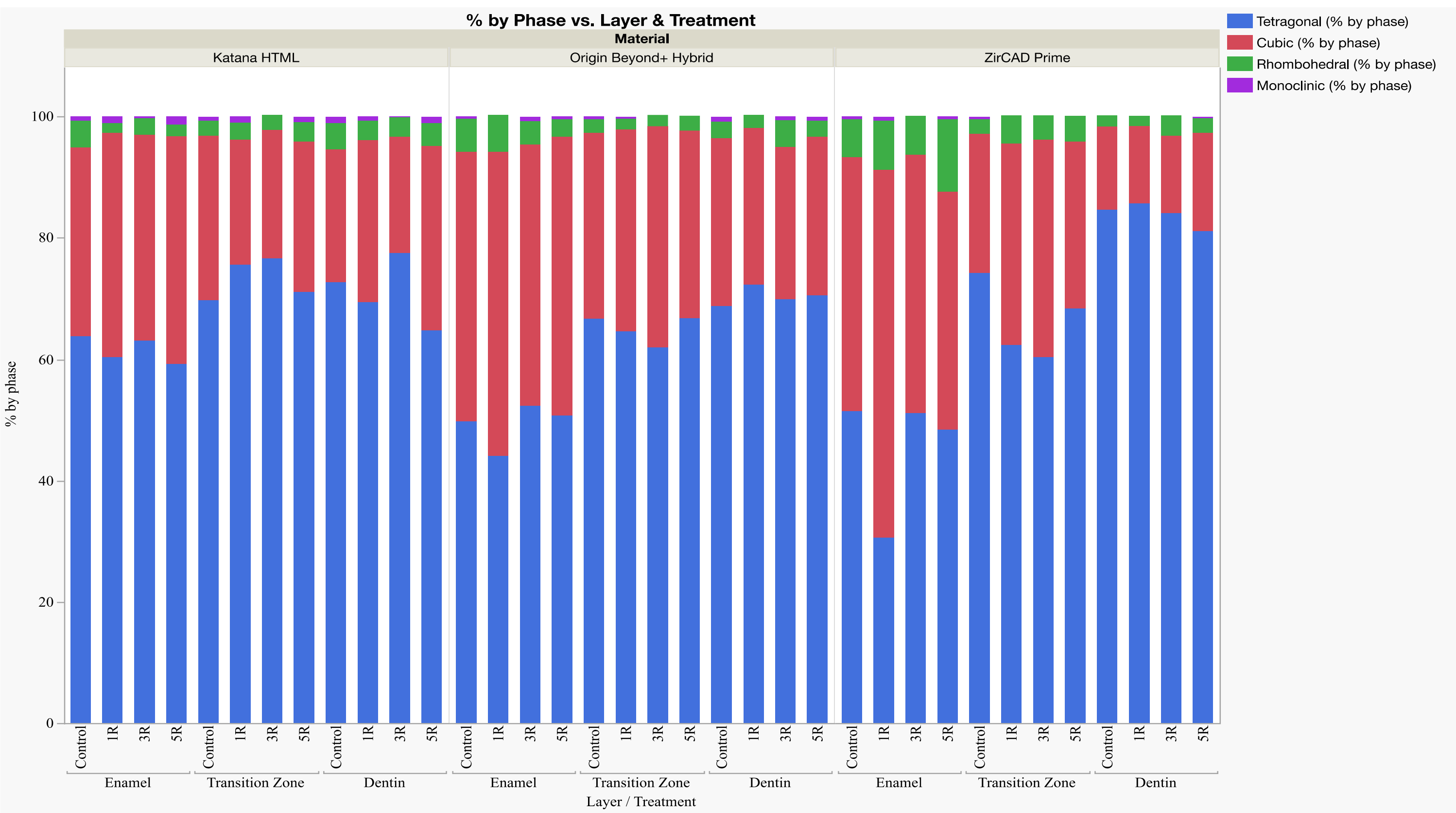

Figure 30: Phase Composition vs. Layer and Treatment

Table 18: Summary of Rietveld Analysis for Phase Composition

Cubic (% by phase)												
Layer												
Material	Enamel				Transition Zone				Dentin			
	Treatment				Treatment				Treatment			
	Control	1R	3R	5R	Control	1R	3R	5R	Control	1R	3R	5R
	Mean	Mean	Mean	Mean	Mean	Mean	Mean	Mean	Mean	Mean	Mean	Mean
Katana HTML	31.13	37.03	33.99	37.58	27.12	20.6	21.11	24.82	21.89	26.68	19.2	30.45
Origin Beyond+ Hybrid	44.51	50.17	43.14	46.02	30.72	33.3	36.5	30.95	27.68	25.82	25.04	26.13
ZirCAD Prime	41.94	60.69	42.63	39.3	22.91	33.15	35.83	27.56	13.72	12.78	12.71	16.15
Tetragonal (% by phase)												
Layer												
Material	Enamel				Transition Zone				Dentin			
	Treatment				Treatment				Treatment			
	Control	1R	3R	5R	Control	1R	3R	5R	Control	1R	3R	5R
	Mean	Mean	Mean	Mean	Mean	Mean	Mean	Mean	Mean	Mean	Mean	Mean
Katana HTML	63.79	60.32	63.07	59.24	69.76	75.61	76.69	71.08	72.7	69.45	77.51	64.74
Origin Beyond+ Hybrid	49.73	44.05	52.31	50.7	66.65	64.6	61.91	66.74	68.78	72.31	69.95	70.52
ZirCAD Prime	51.43	30.58	51.13	48.36	74.24	62.4	60.39	68.36	84.65	85.7	84.15	81.15
Monoclinic (% by phase)												
Layer												
Material	Enamel				Transition Zone				Dentin			
	Treatment				Treatment				Treatment			
	Control	1R	3R	5R	Control	1R	3R	5R	Control	1R	3R	5R
	Mean	Mean	Mean	Mean	Mean	Mean	Mean	Mean	Mean	Mean	Mean	Mean

Katana HTML	0.66	1.06	0.25	1.31	0.63	1	0	0.89	1.03	0.71	0.1	1.02
Origin Beyond+ Hybrid	0.34	0	0.72	0.46	0.41	0.27	0	0	0.8	0	0.58	0.63
ZirCAD Prime	0.42	0.64	0	0.4	0.4	0	0	0	0	0	0	0.24
Rhombohedral (% by phase)												
Layer												
Material	**Enamel**				**Transition Zone**				**Dentin**			
	Treatment				**Treatment**				**Treatment**			
	Cont-rol	**1R**	**3R**	**5R**	**Cont-rol**	**1R**	**3R**	**5R**	**Con-trol**	**1R**	**3R**	**5R**
	Mean	**Mean**	**Mean**	**Mean**	**Mean**	**Mean**	**Mea-n**	**Mea-n**	**Mea-n**	**Mean**	**Mean**	**Mean**
Katana HTML	4.43	1.59	2.69	1.87	2.49	2.79	2.47	3.21	4.38	3.17	3.19	3.79
Origin Beyond+ Hybrid	5.42	6.05	3.83	2.83	2.22	1.8	1.87	2.45	2.74	2.13	4.43	2.72
ZirCAD Prime	6.21	8.09	6.39	11.93	2.45	4.64	3.98	4.24	1.82	1.68	3.32	2.46

Table 19: LS Means Differences Tukey HSD for % Tetragonal in Material and Layer.

Level	Significance*				Least Sq Mean
ZirCAD Prime,Dentin	A				83.91
Katana HTML,Transition Zone		B			73.28
Katana HTML,Dentin		B	C		71.10
Origin Beyond+ Hybrid,Dentin		B	C		70.39
ZirCAD Prime,Transition Zone		B	C		66.34
Origin Beyond+ Hybrid,Transition Zone		B	C		64.97
Katana HTML,Enamel			C		61.60
Origin Beyond+ Hybrid,Enamel				D	49.19
ZirCAD Prime,Enamel				D	45.37

Connecting Letters Table showing differences between materials and layers for % tetragonal. *Levels not connected by the same letter are significantly different. ***p* = *0.0001***

Table 20: LSMeans Differences Tukey HSD for % Cubic in Material and Layer.

Level	Significance*				Least Sq Mean
ZirCAD Prime,Enamel	A				46.14
Origin Beyond+ Hybrid,Enamel	A				45.96
Katana HTML,Enamel		B			34.93
Origin Beyond+ Hybrid,Transition Zone		B	C		32.86
ZirCAD Prime,Transition Zone		B	C		29.86
Origin Beyond+ Hybrid,Dentin		B	C		26.16
Katana HTML,Dentin			C		24.55
Katana HTML,Transition Zone			C	D	23.41
ZirCAD Prime,Dentin				D	13.84

Connecting Letters Table showing differences between materials and layers for % cubic. *Levels not connected by the same letter are significantly different. *$p = 0.0014$*

Table 21: LSMeans Differences Tukey HSD for % Monoclinic in Material and Layer

Level	Significance*				Least Sq Mean
Katana HTML,Enamel	A				0.82
Katana HTML,Dentin	A	B			0.71
Katana HTML,Transition Zone	A	B	C		0.63
Origin Beyond+ Hybrid,Dentin	A	B	C	D	0.50
Origin Beyond+ Hybrid,Enamel	A	B	C	D	0.38
ZirCAD Prime,Enamel	A	B	C	D	0.36
Origin Beyond+ Hybrid,Transition Zone		B	C	D	0.17
ZirCAD Prime,Transition Zone			C	D	0.10
ZirCAD Prime,Dentin				D	0.06

Connecting Letters Table showing differences between materials and layers for % monoclinic. *Levels not connected by the same letter are significantly different. *$p = 0.3536$*

Table 22: LSMeans Differences Tukey HSD for % Rhombohedral in Material and Layer.

Level	Significance*		Least Sq Mean
ZirCAD Prime,Enamel	A		8.15
Origin Beyond+ Hybrid,Enamel		B	4.53
ZirCAD Prime,Transition Zone		B	3.82
Katana HTML,Dentin		B	3.63
Origin Beyond+ Hybrid,Dentin		B	3.00
Katana HTML,Transition Zone		B	2.74
Katana HTML,Enamel		B	2.64
ZirCAD Prime,Dentin		B	2.32
Origin Beyond+ Hybrid,Transition Zone		B	2.08

Connecting Letters Table showing differences between materials and layers for % rhombohedral. *Levels not connected by the same letter are significantly different. ***P = 0.0033***

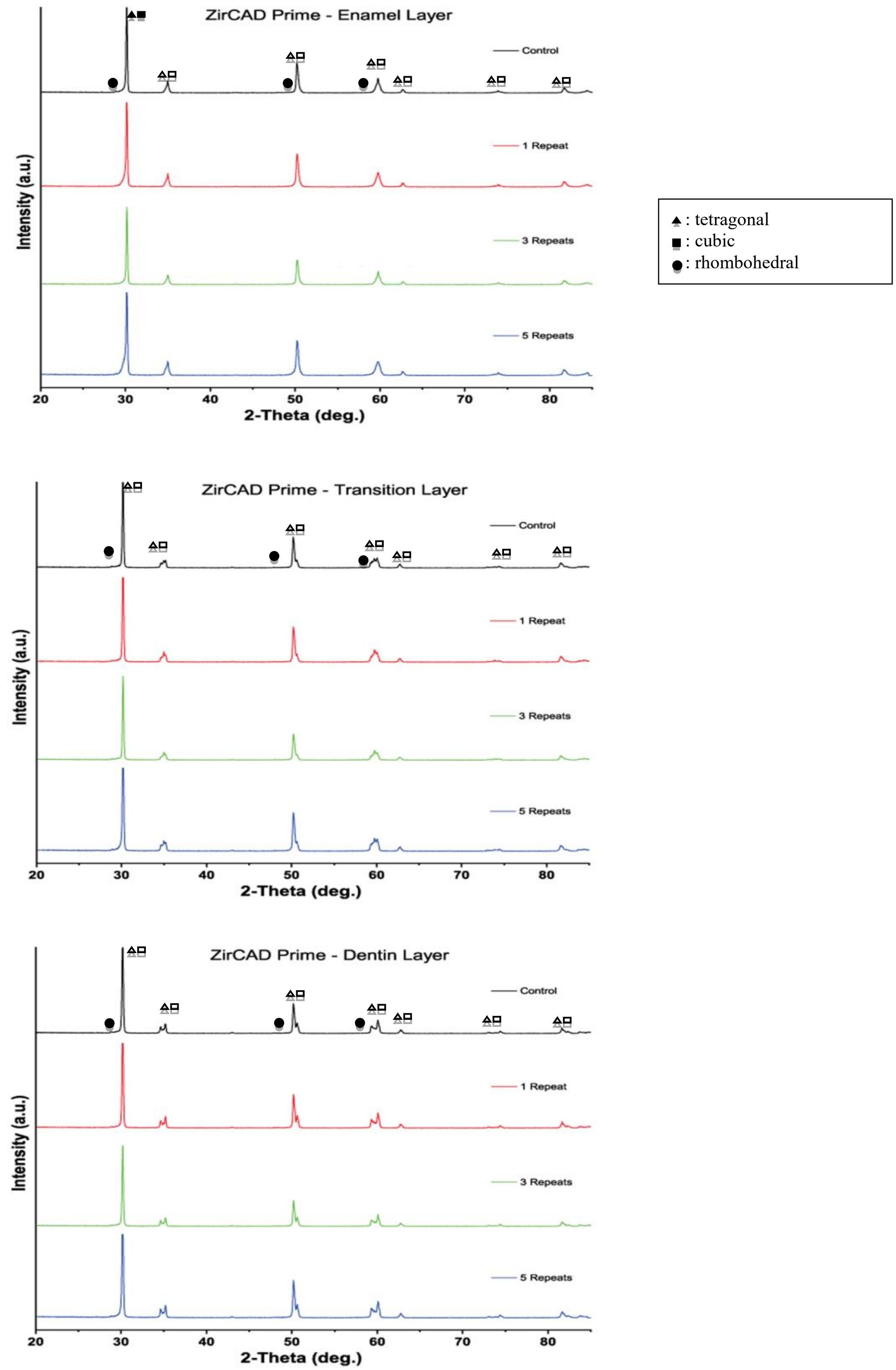

Figure 31: Representative XRD graph showing ZirCAD Prime crystallographic phase peaks for each layer.

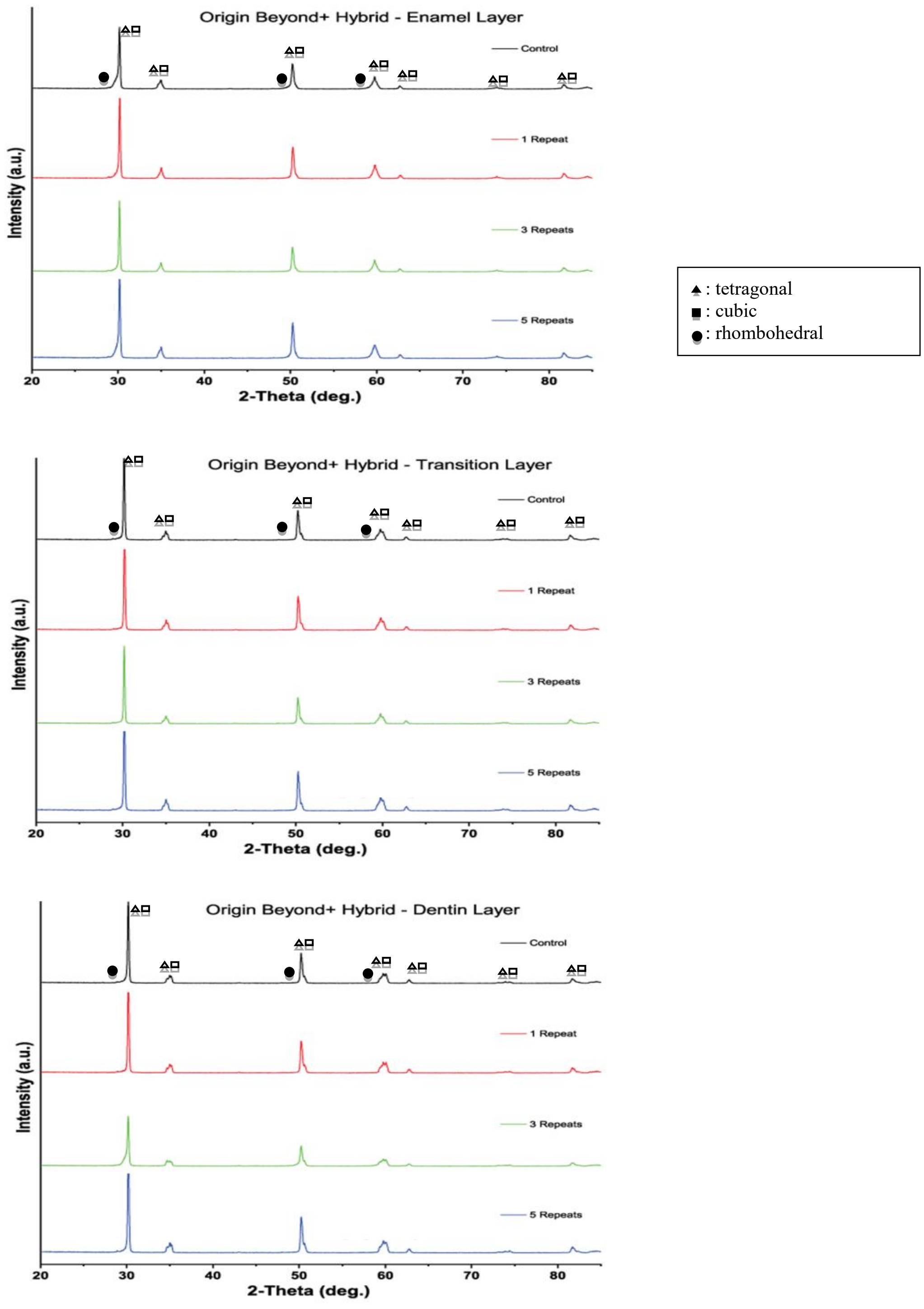

Figure 32: Representative XRD graph showing Origin Beyond+ Hybrid crystallographic phase peaks for each layer.

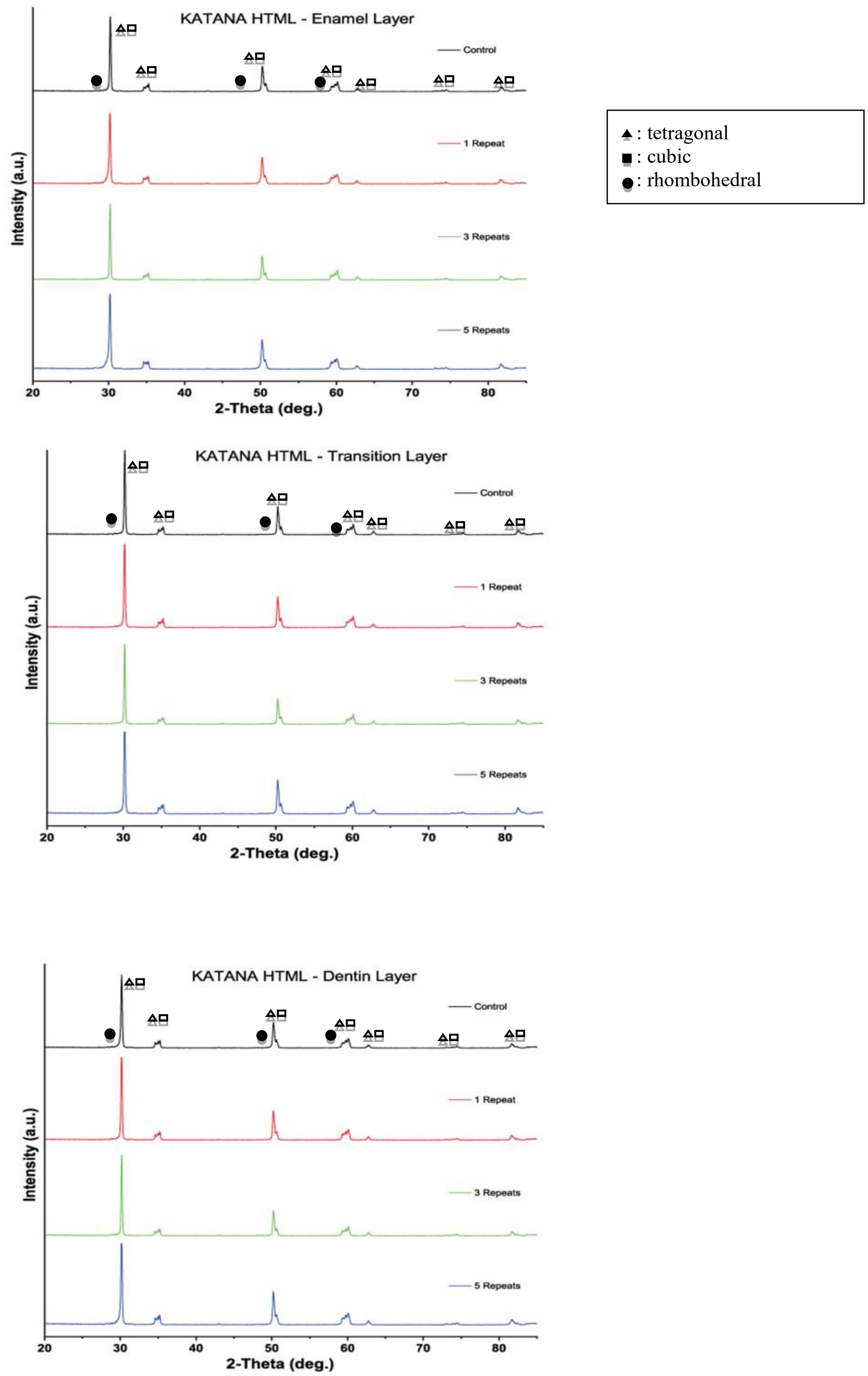

Figure 33: Representative XRD graph showing Katana HTML crystallographic phase peaks for each layer.

3.3 ELEMENTAL COMPOSITION

Through the use of the SEM and its Aztec software, the Y_2O_3 mol % in each of the three materials across their multilayers was measured. Regarding the repeated firing treatment, significant differences existed between the different type of materials ($p=0.0106$), but no significant effects were seen across the layers between each treatment group; which can be seen in Figure 34. A FLS test revealed that there were significant differences between the materials, $p<0.0001$, and layers within each material for OB and ZP only, $p<0.0001$, which can be seen in Figure 35 and Table 24. The Y_2O_3 mol % ranged from 2.81% to 3.13% in KT, 3.54% to 4.75% in OB, and 2.06% to 4.91% in ZP, shown in Table 23. There is a noticeable trend where the Y_2O_3 mol % gradually decreases moving from the enamel layer towards the transition, and then dentin layer in both OB and ZP; this was not the case for KT as it remained fairly in a tight range throughout its layers, which can be seen in Figure 35. It is worth noting that the significant differences that existed were between the enamel, transition, and dentin layer and no significant differences were found at the junctions between enamel / transition or dentin / transition layers.

Table 23: Yttria mol % content

				Yttria mol %
Material	**Treatment**	**Layer**	**N**	**Mean**
Katana HTML	**Control**	Enamel	4	2.91
		Enamel / Transition	4	3.10
		Transition	4	3.13
		Transition / Dentin	4	3.05
		Dentin	4	3.13
	1R	Enamel	4	2.95
		Enamel / Transition	4	2.91
		Transition	4	3.13
		Transition / Dentin	4	2.90
		Dentin	4	2.81
	3R	Enamel	4	2.98
		Enamel / Transition	4	2.83
		Transition	4	3.02
		Transition / Dentin	4	3.09
		Dentin	4	3.05
	5R	Enamel	4	2.91
		Enamel / Transition	4	2.90
		Transition	4	2.81
		Transition / Dentin	4	3.04
		Dentin	4	2.93
Origin Beyond+ Hybrid	**Control**	Enamel	4	4.75
		Enamel / Transition	4	4.38
		Transition	4	3.86
		Transition / Dentin	4	3.63
		Dentin	4	3.54
	1R	Enamel	4	4.72
		Enamel / Transition	4	4.66
		Transition	4	4.01
		Transition / Dentin	4	3.60
		Dentin	4	3.57
	3R	Enamel	4	4.69
		Enamel / Transition	4	4.58
		Transition	4	3.97
		Transition / Dentin	4	3.66
		Dentin	4	3.75
	5R	Enamel	4	4.73
		Enamel / Transition	4	4.45
		Transition	4	4.12
		Transition / Dentin	4	3.72

		Dentin	4	3.68
ZirCAD Prime	**Control**	Enamel	4	4.75
		Enamel / Transition	4	4.68
		Transition	4	3.27
		Transition / Dentin	4	2.32
		Dentin	4	2.36
	1R	Enamel	4	4.70
		Enamel / Transition	4	4.75
		Transition	4	3.46
		Transition / Dentin	4	2.23
		Dentin	4	2.25
	3R	Enamel	4	4.72
		Enamel / Transition	4	4.91
		Transition	4	2.86
		Transition / Dentin	4	2.37
		Dentin	4	2.06
	5R	Enamel	4	4.89
		Enamel / Transition	4	4.84
		Transition	4	3.67
		Transition / Dentin	4	2.36
		Dentin	4	2.22

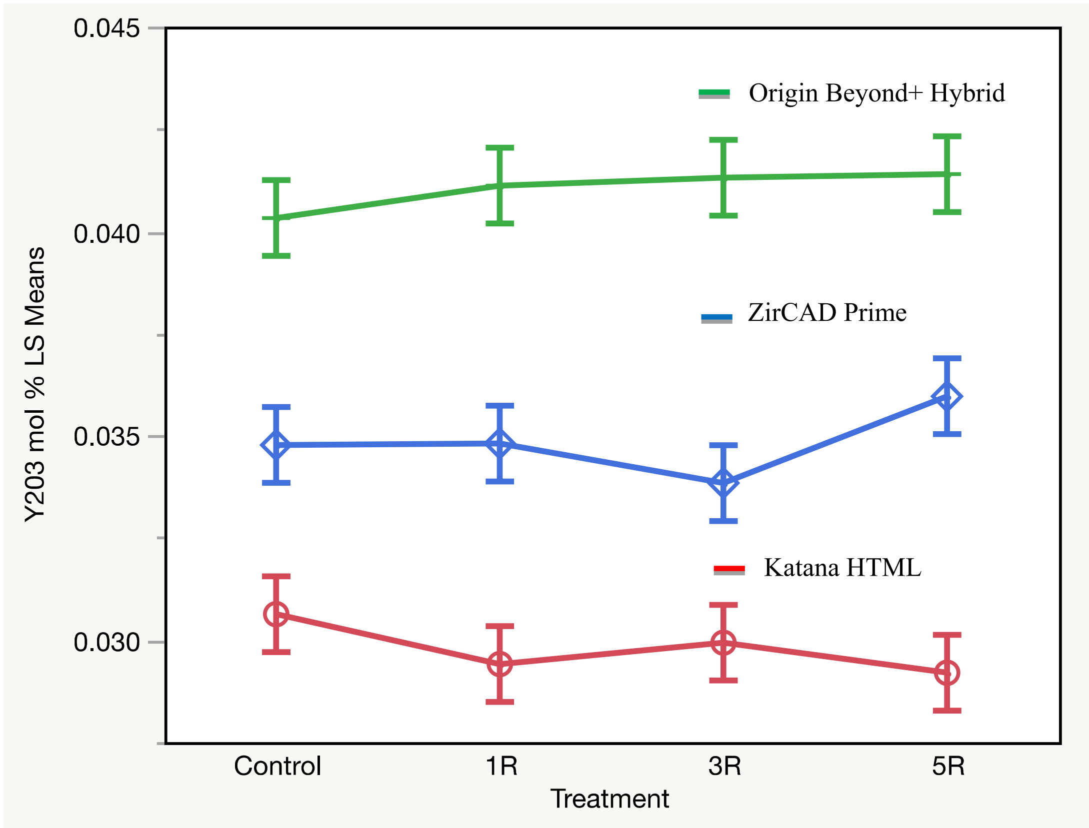

Figure 34: LSM plot showing the Y_2O_3 % by mol concentration against repeated firing treatment for the three materials: ZP, OB, KT.

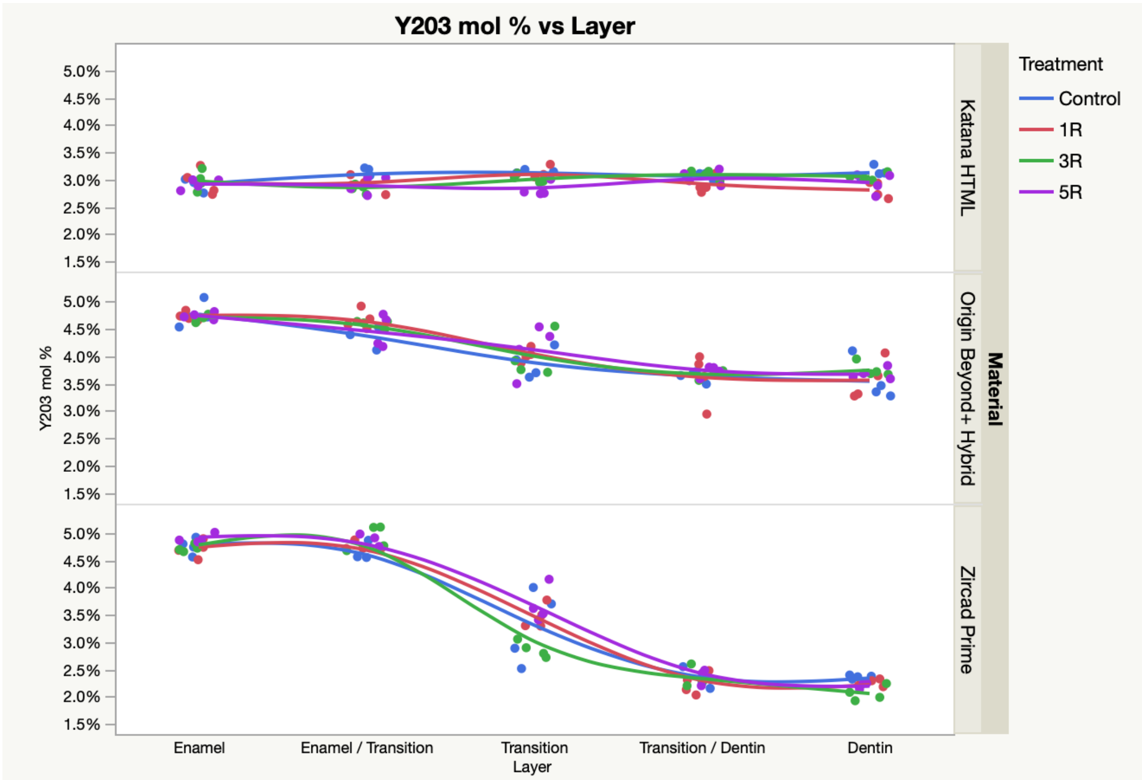

Figure 35: General pattern where Y_2O_3 mol % decreases as you move from the enamel layer towards the dentin layer, with no significant effects resulting from the repeated firing treatment.

Table 24: LSMeans Differences Tukey HSD for Yttria mol % between materials and layers.

Level	Significance*							Least Sq Mean
ZirCAD Prime,Enamel / Transition	A							0.047
ZirCAD Prime,Enamel	A	B						0.047
Origin Beyond+ Hybrid,Enamel	A	B						0.047
Origin Beyond+ Hybrid,Enamel / Transition		B						0.045
Origin Beyond+ Hybrid,Transition			C					0.039
Origin Beyond+ Hybrid,Transition / Dentin				D				0.036
Origin Beyond+ Hybrid,Dentin				D				0.036
ZirCAD Prime,Transition					E			0.033
Katana HTML,Transition						F		0.030
Katana HTML,Transition / Dentin						F		0.030
Katana HTML,Dentin						F		0.029
Katana HTML,Enamel						F		0.029
Katana HTML,Enamel / Transition						F		0.029
ZirCAD Prime,Transition / Dentin							G	0.023
ZirCAD Prime,Dentin							G	0.022

Connecting Letters Table showing differences between materials and layers for yttria mol % content. *Levels not connected by the same letter are significantly different. ***p <0.0001***

3.4 THREE-POINT BEND FLEXURAL STRENGTH

The last set of results that will be presented are the three-point flexural strength test ones. Due to the different number of tests that were conducted and factors considered for this experiment, this section will have a more detailed presentation of results compared to the previous tests. ZP, OB, and KT had 40 large specimens, all manually polished, each divided in four groups evenly to be subjected to repeated firing treatment. Another set of specimens, KT2, divided evenly into four groups, $n=40$, and inCoris TZI, $n=12$, the latter material used only to validate the specimen size, were fabricated in a large size, polished in an automated fashion, and tested in the same manner as the previous samples. Last, three control groups of KT with small bar specimens, with one group not polished and not annealed, $n=11$, a second polished but not annealed, $n=22$, and the third polished and annealed, $n=9$ were fabricated. Five specimens were considered outliers and were excluded from all statistical tests. Table 25 shows the mean flexural strength results for all groups and materials. Figures 36 and 37 show visual representation of these results in bar charts for the large specimens and small specimens respectively.

Table 25: Mean flexural strength (MPa) results for all groups and materials

		Flexural Strength (MPa)			
All Materials	**Glaze Firing**	**N**	**Mean**	**Std Dev**	**CV**
ZirCAD Prime	Control	10	839.12	91.85	10.95
	1R	10	689.45	148.55	21.55
	3R	10	722.63	149.30	20.66
	5R	10	764.90	170.03	22.23
Origin Beyond Hybrid+	Control	10	733.61	123.44	16.83
	1R	10	756.03	142.25	18.81
	3R	10	785.28	109.19	13.91
	5R	10	744.83	108.48	14.56
Katana HTML (manual polishing)	Control	10	637.74	163.99	25.71
	1R	10	603.42	80.83	13.40
	3R	10	560.89	82.15	14.65
	5R	10	677.23	122.16	18.04
Katana HTML 2 (automated polishing)	Control	9	873.42	107.06	12.26
	1R	9	821.19	59.53	7.25
	3R	10	761.97	185.57	24.35
	5R	10	833.70	166.46	19.97
inCoris TZI	Control	12	933.89	96.66	10.35
Katana HTML small (-P / -A)	Control	11	898.67	46.61	5.19
Katana HTML small (P / -A)	Control	22	1135.93	89.83	7.91
Katana HTML small (P / A)	Control	9	1011.16	55.05	5.44

P: polished, A: annealed, -P: not polished, -A: not annealed

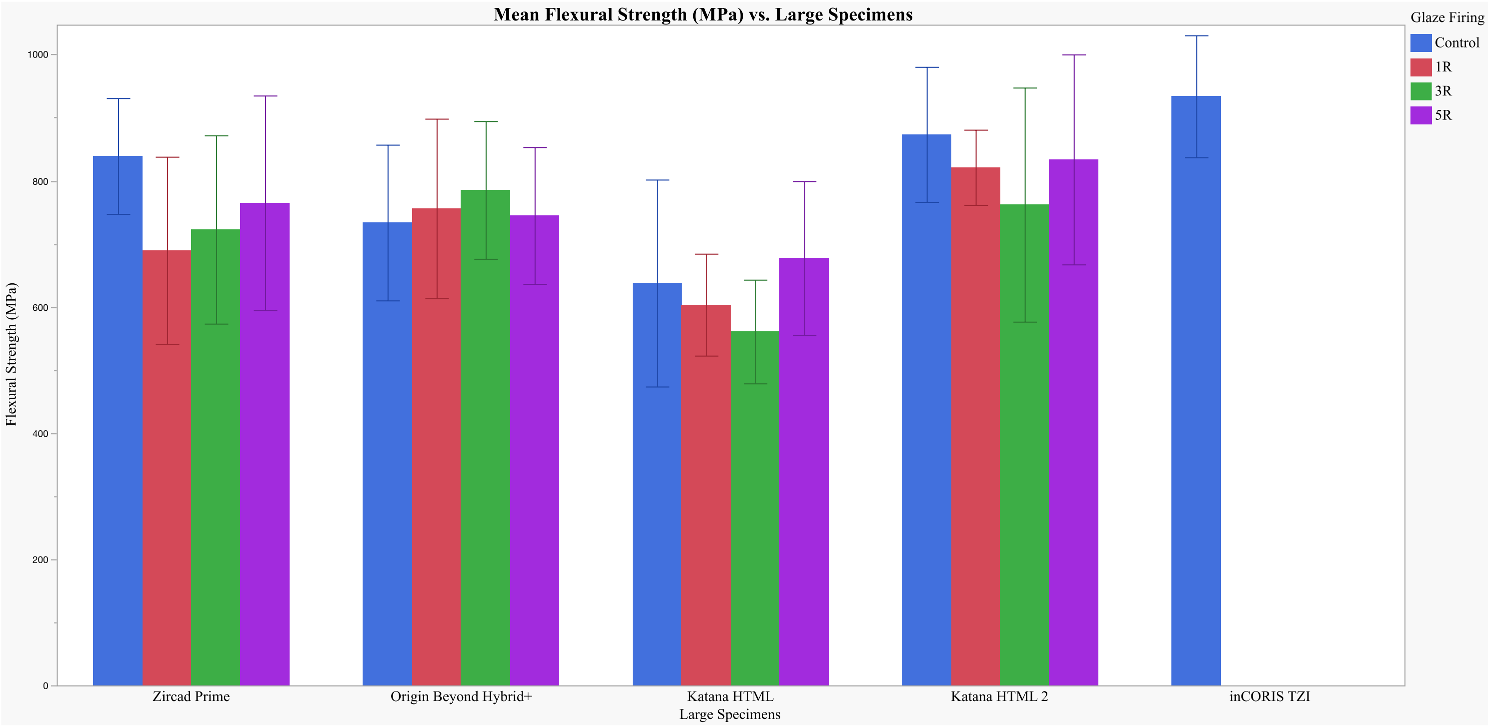

Figure 36: Mean flexural strength (MPa) of all large specimens.

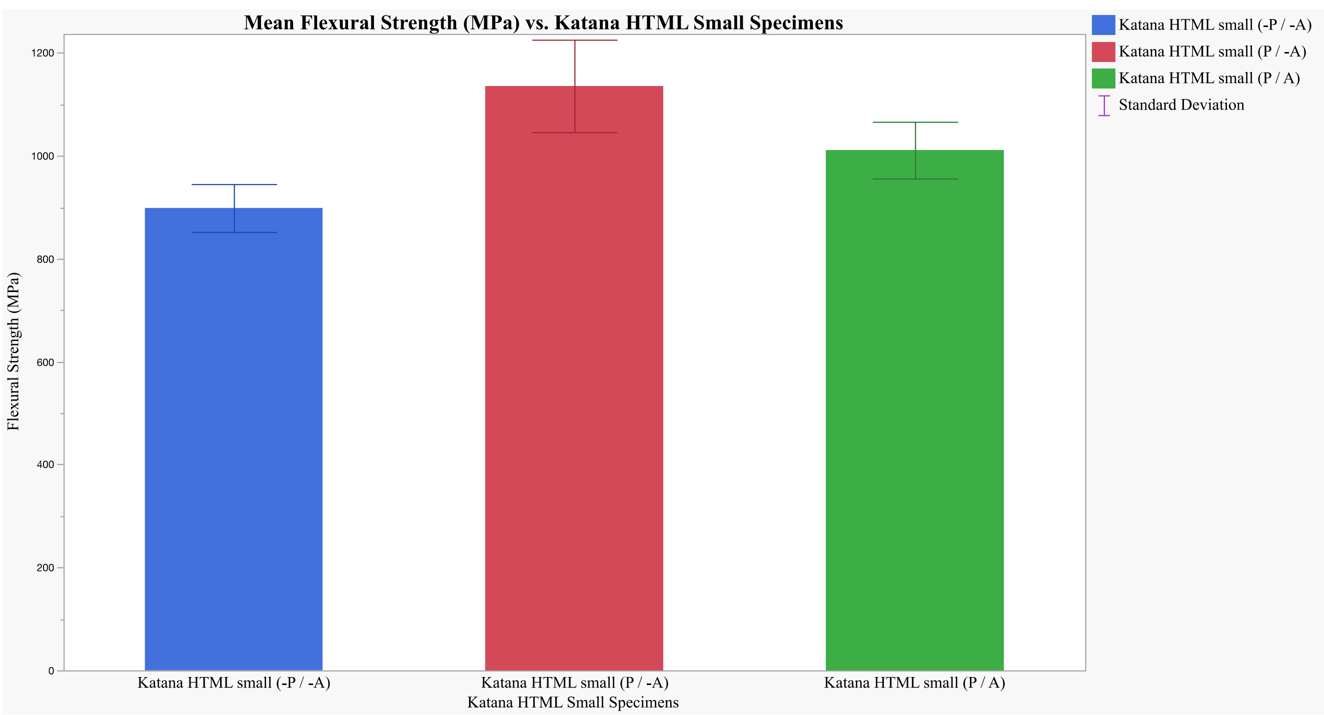

Figure 37: Mean flexural strength (MPa) of Katana HTML small specimens. P: polished, A: annealed, -P: not polished, -A: not annealed

3.4.1 LARGE SPECIMENS

This subsection will be discussing the results of all large specimens. Considering the specimens that were manually polished, ZP control group had the highest mean flexural strength of 839.12 MPa, with the lowest reading of 560.89 MPa being attributed to KT 3R group. When comparing the effects of the repeated firing treatment on materials and on the different layers, no significant differences were seen on the materials or their layers. Table 27 shows a connecting letter report to describe the non-significant effect of the repeated firing treatment on the materials and layers, excluding KT2.

On the other hand, the materials that were polished in an automated fashion yielded higher flexural strength results, with the highest being 933.89 MPa in the inCoris TZI control group, and the lowest being in the KT2 3R group with a value of 761.97 MPa, shown in Table 25. Differences resulting from the effect of repeated firing treatment on KT2 were measured and appeared to be non-significant. Comparing the differences in flexural strength between the control groups of KT2 and inCoris TZI, they also were non-significant.

Utilizing the FLS test, there was a significant difference between KT2 and KT, but none between KT2, ZP, and OB ($p<0.0001$) shown in Table 28. The authors would like to emphasize that it is an unfair comparison to compare KT2, polished automatically, with the manually polished ZP and OB, especially since all three materials are different from each other, so the non-significance in between the three materials should not be viewed as a defining conclusion since a number of different factors are involved. The significant difference between KT2 and KT only existed between the materials, $p<0.0001$, but any differences related to the repeated firing treatment were non-significant. This gives a conclusion that the different polishing techniques utilized in this experiment have a significant effect on the flexural strength results.

Table 27: LSMeans Differences Tukey HSD in Material and Layer after repeated firing.

Level	Significance*			Least Sq Mean (MPa)
Control,ZirCAD Prime	A			839.12
3R,Origin Beyond Hybrid+	A	B		785.28
5R,ZirCAD Prime	A	B		764.90
1R,Origin Beyond Hybrid+	A	B		756.03
5R,Origin Beyond Hybrid+	A	B	C	744.83
Control,Origin Beyond Hybrid+	A	B	C	733.61
3R,ZirCAD Prime	A	B	C	722.63
1R,ZirCAD Prime	A	B	C	689.45
5R,Katana HTML	A	B	C	677.23
Control,Katana HTML		B	C	637.74
1R,Katana HTML		B	C	603.42
3R,Katana HTML			C	560.89

Connecting letter report comparing repeated firing treatment effects on material and layer. *Levels not connected by the same letter are significantly different. ***p* =0.1858**

Table 28: LSMeans Differences Tukey HSD in Material for large specimens after repeated firing.

Level	Significance*		Least Sq Mean
Katana HTML 2	A		822.57
Origin Beyond Hybrid+	A		754.93
Zircad Prime	A		754.02
Katana HTML		B	619.82

Connecting letter report comparing repeated firing treatment effects on large specimens. *Levels not connected by the same letter are significantly different. ***p* <0.0001**

3.4.2 COMPARISON BY SIZE

Since two different sized specimens of the same material were fabricated, Katana HTML, it was seen as an opportunity to compare the effects of size on flexural strength. Comparing KT, KT2, and Katana HTML small (P / A) resulted in significant differences between KT and Katana HTML small (P / A), but none between KT2 and the small specimen group, $p<0.0001$, seen in Table 29. Note that the small bar specimens were all manually polished, as KT was, so a size comparison between these two groups would prove to be more accurate than KT2 being involved in the calculation since KT2 was polished in an automated fashion. However, it is interesting to see that there were no significant differences between KT2 and Katana HTML small (P / A). Figure 38 helps visualize this comparison. Table 30 shows the mean values for all Katana HTML specimens in the control group with regards to specimen size.

Table 29: LSMeans Differences Tukey HSD for Katana HTML by size.

Level	Significance*		Least Sq Mean
Katana HTML small (P / A)	A		1011.15
Katana HTML 2 (automated polishing)	A		873.41
Katana HTML (manual polishing)		B	637.74

Connecting letter report comparing flexural strength of Katana HTML by size. *Levels not connected by the same letter are significantly different. *p <0.0001*

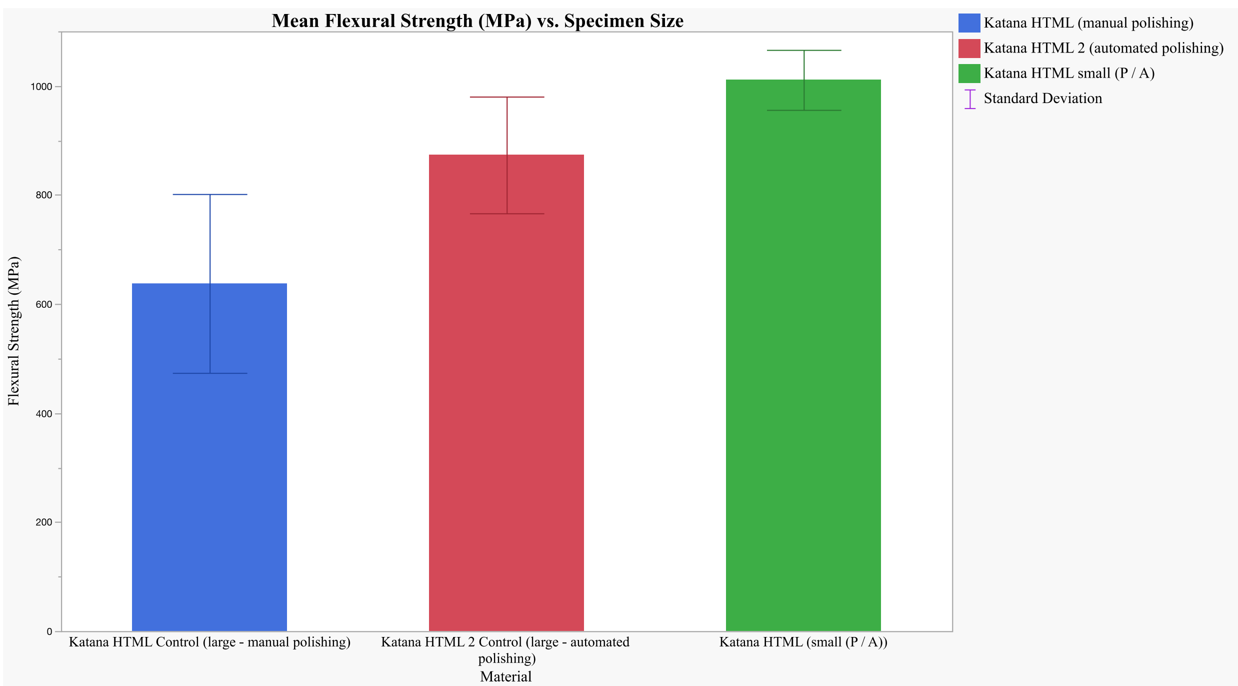

Figure 38: Mean flexural strength (MPa) vs Specimen Size

Table 30: Mean flexural strength (MPa) of Katana HTML with regards to specimen size

	Flexural Strength (MPa)			
Material	**N**	**Mean**	**Std Dev**	**CV**
Katana HTML (manual polishing)	10	637.74	163.99	25.71
Katana HTML 2 (automated polishing)	9	873.42	107.06	12.26
Katana HTML small (P / A)	9	1011.16	55.05	5.44

3.4.3 COMPARISON BY POLISHING

Flexural strength of small sized Katana HTML specimens was also compared using one-way ANOVA statistical test. The specimens included in this statistical test were not annealed. The test revealed a significant difference in strength when it came to compare the polished specimens with the unpolished ones, $p < 0.0001$, shown in Figure 39. The polished specimens yielded larger strength results, 1135.93 MPa, than the unpolished ones, 898.67 MPa. Table 31 and Figure 40 help quantify and visualize this data respectively.

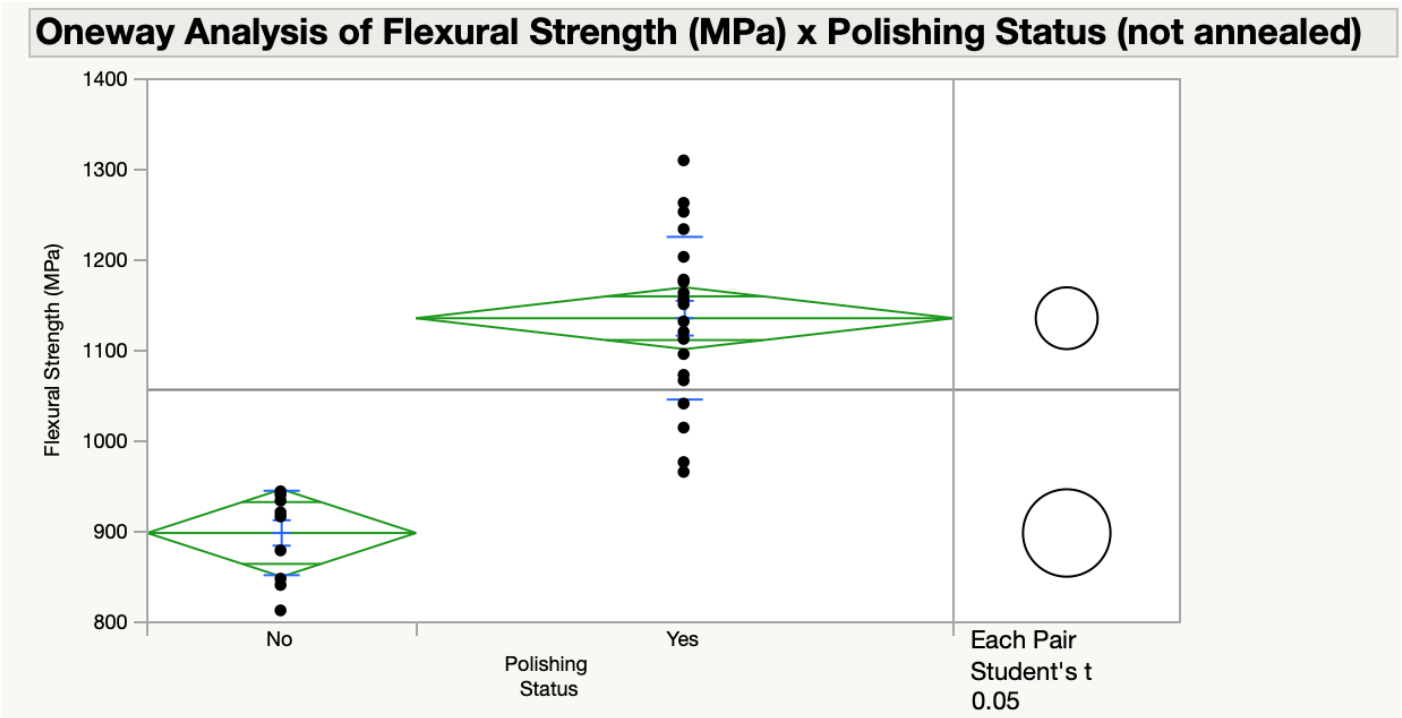

P <0.0001

Figure 39: Comparing Katana HTML small specimens by polishing. Note that all specimens included in this test were not annealed.

Table 31: Mean flexural strength (MPa) of Katana HTML small specimens comparing polishing status. Specimens here have not been annealed.

	Flexural Strength (MPa)			
Polishing Status	**N**	**Mean**	**Std Dev**	**CV**
Not Polished	11	898.67	46.61	5.19
Polished	22	1135.93	89.83	7.91

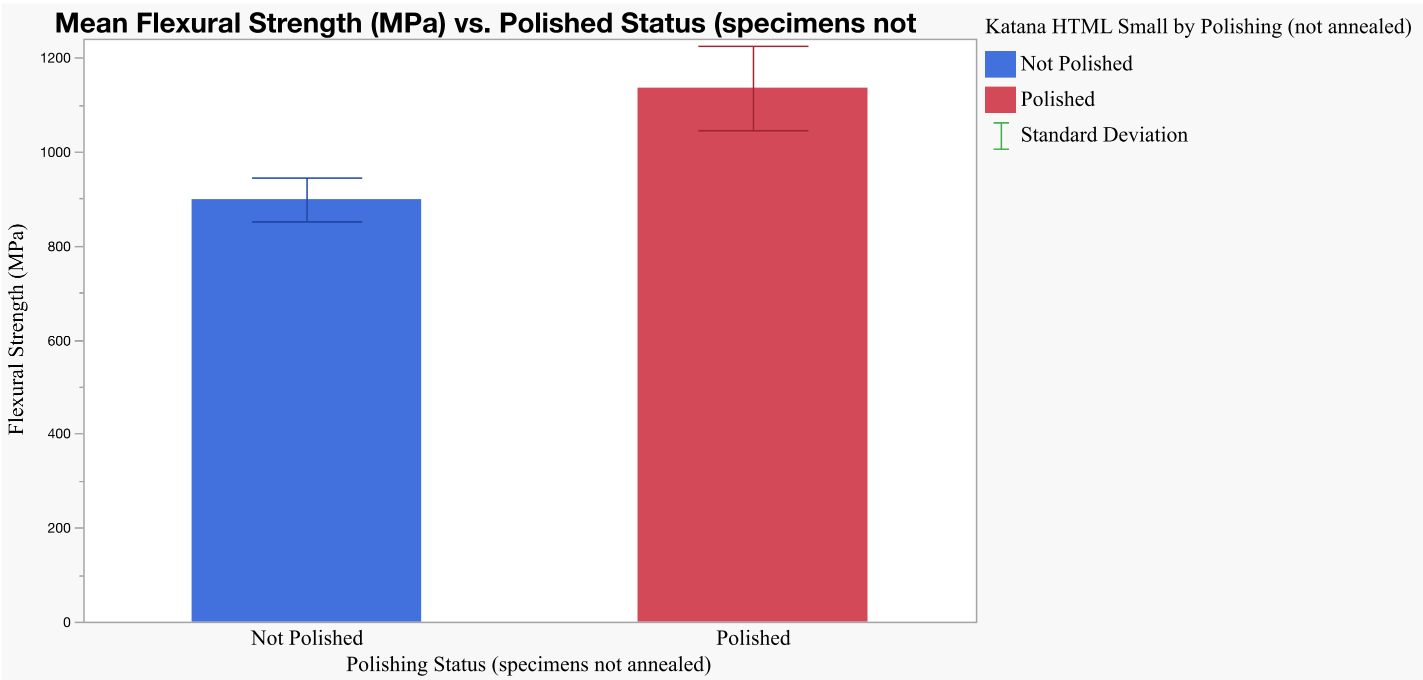

Figure 40: Mean flexural strength (MPa) vs. Katana HTML small specimens by polishing (specimens not annealed).

3.4.4 COMPARISON BY ANNEALING

The comparison for the flexural strength test was done by comparing Katana HTML small specimens by their annealing status. All specimens used in this statistical test were polished. ANOVA statistical test revealed a significant difference between the two groups, p=0.0006, seen in Figure 41. The annealed group had a lower mean flexural strength result, 1011.16 MPa, than the group that was not annealed, 1135.93 MPa. Figure

42 shows a bar chart representation of this relationship and Table 32 presents the quantitative data for it.

Table 32: Mean flexural strength of annealed specimens. Note that all specimens included here were polished.

	Flexural Strength (MPa)			
Annealing Status	**N**	**Mean**	**Std Dev**	**CV**
Annealed	9	1011.16	55.05	5.44
Not Annealed	22	1135.93	89.83	7.91

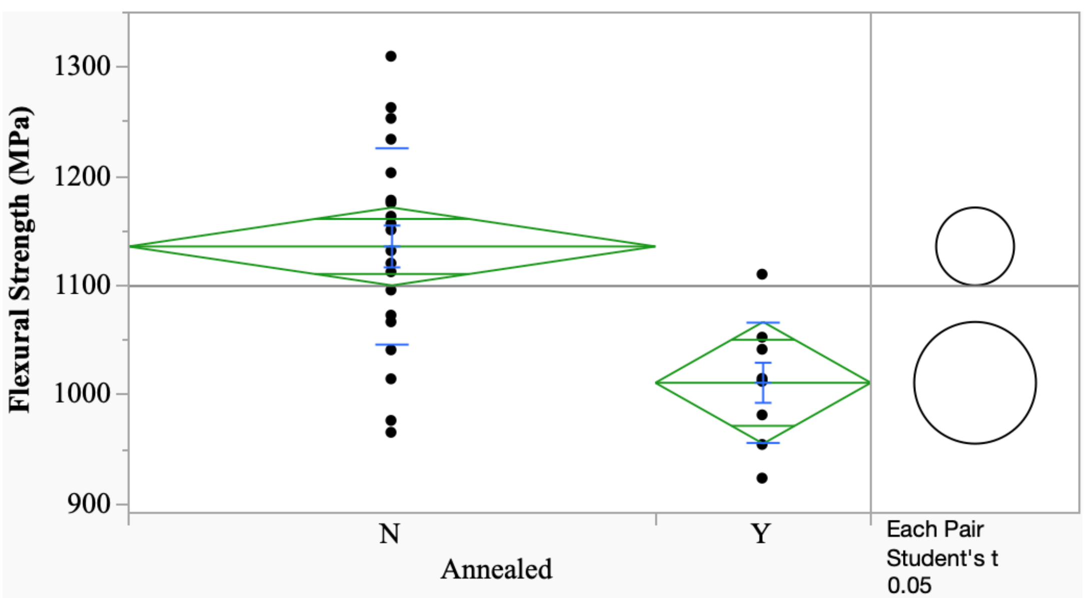

p =0.0006

Figure 41: Oneway ANOVA of Flexural Strength vs Katana HTML by annealing

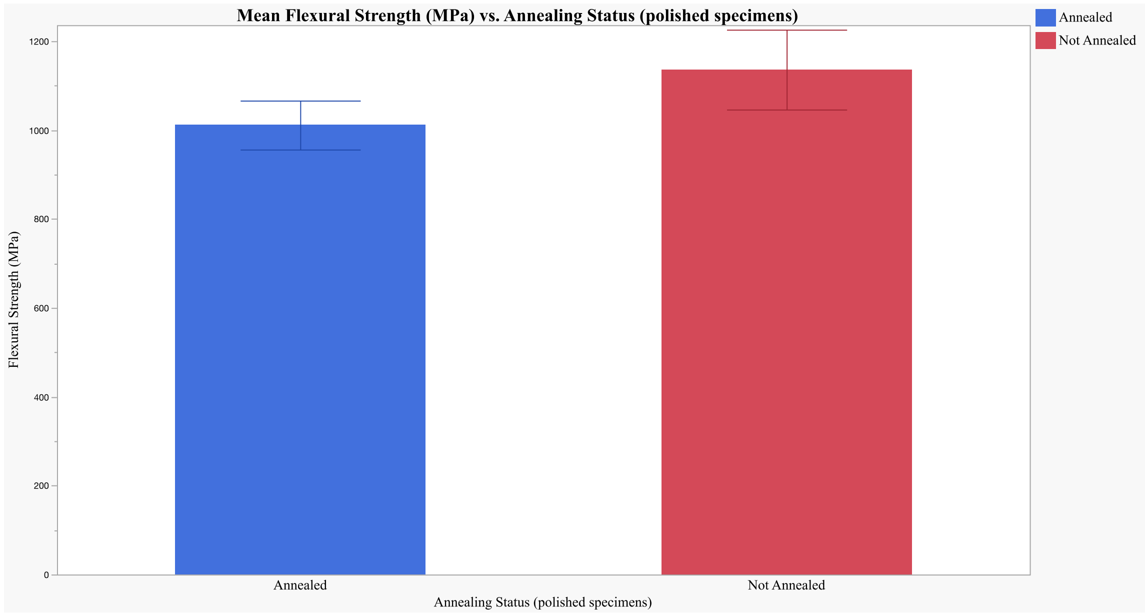

Figure 42: Mean flexural strength (MPa) vs. Material by annealing (Katana HTML small polished specimens).

CHAPTER 4: DISCUSSION

4.1 OPTICAL PROPERTIES

As can be seen from the results, the repeated firing treatment had no significant effects on the contrast ratio of the different materials. As such, the null hypothesis that repeated firing does not affect contrast ratio cannot be rejected. Significant differences existed only between the different brands of material and the layers within each material, $p<0.0001$ for the contrast ratio test. These results do make sense since all three materials have been made using different compositions and yttria content. Although both ZP and

OB have 5Y in their enamel layer, ZP had the highest levels of translucency, and both were more translucent than their 3Y shaded zirconia counterpart, KT.

It has been known and reported in the literature that higher yttria concentrations would result in more translucent zirconia (Zhang, 2014). This can be supported by the EDS analysis done in this study showing the different yttria concentrations across each layer of each material, which can be seen in Table 23. The highest yttria mol % was present in ZP followed by OB then KT, and these values existed in larger concentrations in the enamel layer and decreased moving towards the dentin layer for ZP and OB only. Since OB contains both 5Y and 4Y, it is reasonable to see that the translucency values obtained in this study are closer in range across all layers, and this correlates directly with the yttria concentrations found in its layers. The same can be said for ZP, where 5Y exists in the enamel layer and 3Y in the dentin layer, and both translucency and yttria mol % content decrease moving from the enamel towards the transition layer, with a bigger difference in the layers than was present in OB. Regarding KT, which is a 3Y zirconia multilayered by chroma, the contrast ratio values were all relatively close to each other across its layers when comparing it with the other two materials. This makes sense as the yttria mol % concentration was generally the same across its layers. The minor difference in translucency across its layers can be attributed to the various additives or oxides that were added to allow this subtle transition, which can further hinder light passing through the material by acting as contaminants (Burgess, 2018; Ghodsi and Jafarian, 2018; Shah et al., 2008).

Higher yttria concentrations generally contain more of the cubic phase of zirconia, which also supports the results of this study. This can be supported by the results of the XRD analysis that was conducted, which shows that the higher cubic % by mol concentrations across all three materials was in ZP, followed by OB with KT coming last. The highest cubic concentrations were also present in the enamel layer, tapering down towards the dentin layer across all materials. The lowest cubic % by mol levels were present in KT, and this would make sense since it was the least translucent out of all three materials. This is reflected in the opacity values shown above in the results section. The more cubic the zirconia is, the more translucent it would be (Ghodsi and Jafarian, 2018; Manziuc et al., 2019). This is due to the larger grains generally seen in cubic zirconia, which would facilitate the passage of light with the least amount of grain boundary interference (Stawarczyk et al., 2013; 2014).

With respect to evaluating color changes, CIELAB color space values are generally used. Based on the results of this study, the null hypothesis can only partially be rejected as repeated firing only had a significant effect in one of the CIELAB color space values for one of the groups only. After repeated firing, the significant difference that existed in L* between the KT 1R and 5R groups is unclear given all the other results that have been obtained, and this could be attributed to the normal percentage error in the spectrophotometer readings. All values, L*, b*, and a* were significantly different between all materials and their layers. This is justified since all three materials are made from a different composition with various colorants being used. Moreover, the small sample size for each group, n=2, makes it difficult to generalize the result as a bigger sample would have. However, there are a few general trends that could be seen. Moving from enamel to dentin, L* values tend to decrease, with the exception existing in OB and ZP where it increased in the dentin layer; a* and b* values increase as you move away from the enamel layer towards the dentin layer. This translates into the materials being darker, redder, and yellower, respectively, moving from enamel to dentin layer (Bachhav and Aras, 2011). These values change as different oxides are added into the material to allow for life-like color changes to occur. These color changes would definitely have an effect on light transmittance by acting as contaminants due to their different refractive indices, which would cause light to scatter or absorbed (Burgess, 2018; Ghodsi and Jafarian, 2018; Shah et al., 2008).

There have been very few studies conducted on multilayered zirconia in the literature, and none include any of the materials used in this study with respect to contrast ratio. As such, the results of this study will be compared to those that exist in the literature. Bachhav and Aras evaluated the effects of ceramic thickness and repeated firing the color of zirconia based ceramic systems (2011). They reported significant differences in L* a* b* values in both repeated firing, repeated 3,5,7, and 9 times; and thickness of specimens. Although this study reported significant differences that were resulting from the repeated firing only for L*, between KT 1R and 5R, it could be attributed to the different materials used and repeated firing protocol implemented, as different sintering temperatures can result in different color shades or translucency (Ahmed et al., 2019; Stawarczyk, 2013). Cho and Seol (2022) found significant differences between the two types of multilayer zirconia that they used in terms of contrast ratio and spectral reflectance. The results of their study agree with the patterns found here in this study as contrast ratio decreased moving from the dentin layer towards the enamel layer, and translucency parameter increased when moving from the dentin layer towards the enamel layer. However, in their study, they sectioned each layer of each multilayered zirconia, and did not include any transition boundaries in their testing. Ozdogan and Ozdemir (2020) reported no significant differences to color or translucency parameters after repeated firing done on zirconia frameworks, which are in agreement with this study's results. No study on repeated firing was conducted to assess contrast ratio of zirconia was present in the literature to compare the results of this study to.

With respect to materials, a few studies have conducted experiments to evaluate the translucency of multilayered zirconia, with most using light transmittance or translucency parameters and none using contrast ratio. This is mostly due to the fact that there has been no standard method to measure optical properties in dental ceramics (Stawarczyk et al., 2014). Ueda et al. (2015) evaluated the transmittance of light through four different layers of Katana ML, a type of shaded multilayered zirconia with specimens having a thickness of 1.00mm +/- 0.05mm. The shade chosen was A-light, which corresponds to Vita Shade A1.5-2. They reported mean light transmittance values of 32.8% for the enamel layer, 31.2% for the first transition layer, 25.4% for the second transition layer, and 21.7% for the dentin layer. Although the reported translucency values were reported as light transmittance and not contrast ratio values, the general trend of decreasing translucency seen moving from the enamel layer towards the dentin body layer is also consistent with the results of this study across all three multilayered materials. They reported significant differences in light transmittance values between the layers of the material, which is consistent with the results of this study as well. They also reported a decrease in L* values, and an increase in a* b* values moving from enamel towards dentin, which was also seen in this study with the exception of L* values for OB and ZP. These results make sense given the reasons explained in this section. Although the size of the sample that was used in this study for the contrast ratio test, *n*=2 per group, was not large, the trend can be seen clearly. Moreover, the overlap between the layers due to the size of the aperture hole being 3.5mm meant that there was going to be overlap in ZP's enamel layer and transition layer during the measurement, as well as OB's enamel layer with the transition layer and dentin layer overlapping with the transition layer. This overlap could explain why the L* values in ZP and OB did not follow the trend seen in the study conducted by Ueda et al. (2015) since their study sectioned and measured each layer separately. On the other hand, the specimen's thickness was controlled precisely in this study and as such this would allow for less variation and more consistent results to be produced in this test. Thickness definitely has an effect on translucency, as reported by a number of studies in the literature (Bachhav and Aras, 2011; Manziuc et al., 2019; Matsukazi et al., 2015). Moreover, as more pigments and oxides are added to produce the gradational change in color between the layers, a change in translucency can be seen which was noted in both studies (Ueda et al., 2015). However, this can be more specifically applied to KT since the translucency change in OB and ZP may be more attributed to the yttria concentration changes between the layers as opposed to the pigments.

In another study conducted by Harada et al. (2016), total transmittance (T_t%) was measured in two thicknesses 0.5mm and 1.0mm with the study using different types of zirconia, including different shaded multilayered zirconia, and comparing them to lithium disilicate. The results of the study found that Katana UTML (5Y-ZP) and Katana STML (4Y-ZP) both had significantly higher T_t% than Katana HT (3Y-TZP) yielding values of 23.37+/- 0.27, 21.86 +/- 0.39, and 20.18 +/- 0.39 respectively for the 1.0mm groups. Note that Katana HT differs from Katana HTML, used in this study, in which the latter is shaded zirconia while the former is traditional unshaded monochromatic. The results of their study corroborate the results of this study by agreeing with the fact that the higher yttria concentration, the more translucent the material is, and this trend can be seen in both studies where OB (5Y and 4Y) and ZP (5Y and 3Y) were both more translucent than KT (3Y). Their study also concluded that Katana UTML and Katana STML were significantly more translucent than BruxZir, a more traditional type of zirconia, 20.13 +/- 0.22 T_t%; but less than E.max CAD LT, a lithium disilicate, 27.05 +/- 0.56 T_t%. Another study reported contrast ratio values of InCoris TZI with a thickness of 0.9mm, having values of 0.81 +/- 0.1 (Kanchanavasita et al., 2013). Comparing that value to this study, the multilayered zirconia in this study appears to be more translucent than this translucent type of zirconia even with the slight difference in thickness, since the thickness utilized in this study was 0.95mm +/- 0.2. Although the multilayered zirconia was less translucent than lithium disilicate, the advancements in aesthetics in the zirconia field have been noteworthy with current multilayered zirconia already showing improved results than more traditional ones.

Limitations in the optical experiment in this in vitro study, as mentioned, include the overlap in between the layers during measurement as well as the relatively small sample size. The relatively small sample size was due to it being a pilot study to see whether it would be worth continuing on a larger scale. It would be worth conducting the experiment where each layer has been sectioned separately completely and measured to avoid the overlap between layers during measurement, as conducted in the Ueda et al. study (2015). Moreover, it’s worth noting that the measurements in this study had a separate specimen for each group that was measured, and not the same specimen having been measured and then exposed to repeated firing and measured continuously. Although the author believes that the variation in the way this study was conducted would be minute, it would still be worth to see if there would be an effect if conducted in the aforementioned manner. Moreover, more clinical studies are needed to assess the color-masking abilities and translucency of these novel multilayered zirconia.

4.2 CRYSTALLOGRAPHIC ANALYSIS

As mentioned previously in the results section, repeated firing resulted in no significant differences on the materials or their layers. As such, the null hypothesis cannot be rejected as there were no crystallographic changes seen after repeated firing. However, there were significant differences in the phase fraction between the layers of each material where all phases showed significant differences with the exception of the monoclinic phase. The results of the XRD analysis make sense in this study and correlate to the EDS analysis that was done as well. A general pattern can be seen where the tetragonal phase exists highest in the dentin levels, where there is a lower yttria content, and cubic phase existing mostly in the enamel layers, where the yttria content was highest in the multilayer by composition materials, ZP and OB. It is noteworthy that KT, which is a 3Y multilayered by chroma, contained 20-30% of the cubic phase in its various layers. This is most likely because there was a need to increase translucency in this material, and that was done by making the material more cubic with the addition of oxides and colorants as well. When it comes to ZP and OB, the enamel layer was more cubic to allow for more translucency, and the dentin layer was more tetragonal to provide strength.

The presence of rhombohedral zirconia was an interesting finding that has been reported in the literature, resulting from mechanical stresses from abrasion in the grinding or polishing process (Denry and Holloway, 2006; Kitano et al., 1988). A shoulder can be seen in the main tetragonal peaks between 27-30º 2Ø. This hump is usually identified as rhombohedral zirconia, or strained tetragonal zirconia that results due to a distorted lattice (Denry and Holloway, 2006; Hasegawa et al., 1985; Kondoh, 2004).

The representative XRD graphs for KT are all identical across all layers and repeated firings, which makes sense since the material is completely made up of 3Y. KT peaks were seen at $2\theta = 35^{o}$ and 50^{o}. OB has a slight difference in its peaks at $2\theta = 35^{o}$, 50^{o} and 60^{o} between its layers, with the differences being clearer between the enamel and dentin layer. This makes sense since the enamel layer is reported to be 5Y and dentin body layer is 4Y. ZP had similar differences in peaks at 2Ø = 35°, 50°, and 60° between its layers as well, which correlates to the enamel layer being 5Y and dentin body layer being 3Y.

The absence of the monoclinic phase was interesting since it is expected that some tetragonal to monoclinic phase transformation happening due to the various grinding and polishing stages. The annealing process that was applied, as well as the wet polishing could have very well reversed this transformation completely, leaving only trace amounts (Denry and Holloway, 2006; Kitano et al., 1988).

Inokoshi et al. conducted XRD analysis on the Katana multilayer line which includes HT, UTML, and STML (2018). They reported that the main peaks were found at 2Ø = 30° and 50°, which agree with the results of this study. They also noted three separate peaks at 2Ø = 35° for the Katana HT. Although it's a different material, this finding was also seen in this study in Katana HTML at the same location. However, they did report a broader shoulder for the specimens that were sandblasted, implying the existence of rhombohedral zirconia at 2Ø = 50° and 60°. This finding cannot be clearly seen in this study even though it has been reported that sandblasting and polishing after sintering can yield similar phase transformations (Denry and Holloway, 2006; Inokoshi et al., 2018; Kitano et al., 1988). Ozdogan and Ozdemir (2020) reported that the main peaks were found at 2Ø = 30° and 50° at, which agree with the results of this study. They found no significant differences in the phases or peak levels when the zirconium framework was subjected to repeated firings, which is in agreement with the results of this study as well.

4.3 ELEMENTAL COMPOSITION

As mentioned in the results section, the repeated firing treatment had no significant effect on the yttria % by mol concentration across all brands of multilayered zirconia used in this experiment. As such, the null hypothesis cannot be rejected with respect to changes to the yttria % by mol concentration after repeated firing. However, yttria % by mol was significantly different between the different brands of materials, and within each layer of each brand of material, with the exception of KT for the latter. Layers bordering the transition layer had no significant differences between them, i.e., enamel-transition layer junction and transition-dentin layer junction. These results do make sense since ZP is advertised as having 5Y in the enamel layer and 3Y in the dentin layer, while OB is reportedly 5Y in the enamel layer and 4Y in the dentin layer, whereas KT is a 3Y-TZP throughout its layers. A general trend is seen where the yttria % by mol concentration decreases moving from the enamel layer towards the dentin layer in both OB and ZP. The measurements recorded in this study roughly translate into the advertised yttria % by mol that is advertised by all these companies. The gradual decrease in yttria % by mol concentration is because more strength is needed where tensile stresses are the highest, i.e., the dentin body layer, whereas the yttria concentration is higher in the enamel section since higher concentrations lead to a more translucent zirconia (Zhang, 2014). In KT, however, the yttria % by mol remained fairly the same across all of its layers, which supports the fact that more pigments and oxides are being used in this material to allow for the life-like, gradational color change in the material; hence being called multilayer by chroma, or shaded zirconia, as opposed to multilayer by composition for the other two brands.

Moreover, higher yttria concentrations usually translate into more cubic phase of zirconia being present as opposed to the tetragonal phase (Zhang, 2014). This agrees with the results of crystallographic composition analysis done in this study where most of the cubic phase was found in the enamel layers of the materials and tetragonal phase was present in higher quantities in the dentin body layer. The contrast ratio test also conforms with the results of the elemental analysis as the enamel layers, which contained higher yttria concentrations, were more translucent than their dentin counterpart, which had lower yttria concentrations.

No studies in the literature have conducted any elemental analysis for yttria % by mol for the materials used in this study. Kolakarnprasert et al. (2019) reported yttria % by mol for the Katana multilayered zirconia by chroma line, which included UTML, STML, and ML, arranged from most translucent to least translucent. Their results found that UTML contained 5.4% by mol, STML contained 4.8% by mol yttria, and ML contained 3.7% by mol yttria. Translucency levels were significantly lower for ML than UTML and STML, with no significant differences between the latter two. There were no differences in translucency between the layers of each material. They also reported that UTML had the highest cubic fraction out of the three materials, with ML having the lowest amount of cubic zirconia. These results conform to the patterns observed in this study where higher yttria concentrations yield more translucent and cubic fractions in the enamel layers of OB and ZP, both multilayer by composition, and were consistent between the layers for KT which is a multilayer by chroma. The results of their study agreed with the one done by Inokoshi et al. (2018), where the UTML and STML yttria % by mol concentrations were 5.4% and 4.8% respectively. They were also in agreement with the cubic and tetragonal fraction % by wt. for both UTML and STML.

4.4 FLEXURAL STRENGTH

As previously mentioned in the results section, there were no significant effects resulting from the repeated firing treatment on the strength of the materials. As such, the null hypothesis cannot be rejected in terms of flexural strength changes after repeated firing. In this study, the enamel layer was positioned in compression where the force was being exerted by the Instron, and dentin layer was positioned in tension. ZP had a difference of 149.67 MPa between its strongest mean value, 839.12 MPa (control group), and weakest, 689.45 MPa (1R group). These values, although on the lower end, are still within the advertised range as reported by the company of 650-1200 MPa (Ivoclar Vivadent, 2019). However, the 1200 MPa value reported by the company was based on the body dentin layer, containing 3Y-TZP, utilizing a biaxial flexural strength test, which usually yield higher flexural strength values than a three-point test that was used in this study (Xu et al., 2015). OB's strongest group yielded a mean flexural strength of 785.28 MPa (3R group), and its weakest being 733.61 MPa (control group), with a difference of 51.67 MPa. This was situated well within the advertised range made by the company of 600-1100 MPa. It is interesting to note that OB's control group, which was the weakest in that material, was stronger than two of ZP's groups, 1R and 3R. It is expected to observe ZP have significantly higher flexural strength results across all its groups since the dentin body layer, which contains 3Y-TZP, made up more than 50% of the material, whereas OB is made from 4Y and 5Y. According to the literature, 3Y would yield stronger flexural strength results than 4Y or 5Y due to the lower yttria content (Denry and Kelly, 2008). However, the specimen size difference between the two materials most likely had an effect, which will be explained later in this section. KT's strongest group yielded 677.23 MPa (5R group), while the weakest group had a mean flexural strength of 560.89 MPa (3R group), giving a difference of 116.34 MPa. KT2, which were polished in an automated fashion, had the highest mean strength of 873.42 MPa (control group) with its weakest group reporting 761.97 MPa (3R group), having a difference of 111.45 MPa. In both cases, KT and KT2 fell well below the advertised strength of the material of 1125 MPa as reported by the company (Kuraray Noritake, 2019). This could be because their specimens were smaller in size, 3x4x40mm, than the ones tested in this study. Moreover, given the fact that the material is fully made of 3Y-TZP, it is expected to consistently observe higher results in strength across all their groups when compared to ZP and OB, which were multilayered by composition and contained a combination of different yttria levels. When comparing all materials to the InCoris TZI control group, which yielded 933.89 MPa, they were all weaker, which is something expected to be seen since the material is made of 3Y-TZP and free of any colorants, which may hinder flexural strength (Shah et al., 2008). Moreover, when comparing the results of inCoris TZI of this study with other studies, the results seem to be comparable with those in the study conducted by Vichi et al. (2016), which reported a flexural strength result of 1098 ± 118 MPa for the same material even though the specimen size that was used in their study, 1.2 x 4 x 15mm, were smaller than the ones used in this study.

As can be seen by the results obtained, the effect of specimen size can have a considerable effect on the material's flexural strength. All the Katana HTML small specimens that were tested in this study yielded consistently higher flexural strength results than all the other multilayered materials with less variation. Given the fact that all layers within the multilayered zirconia were to be tested together, the use of a biaxial flexural strength test was not a viable option due to size constraints. As such, the three-point bending test was chosen, which meant that beam shaped specimens were to be used instead of discs, as well as having a size that well exceeds the recommendations of the ISO-6872. Beam shaped specimens have more edge flaws than disc shaped ones, which are used in the biaxial test. These flaws can grow and propagate, leading into fracture of the material as soon as one of these flaws grows and propagates (Xu et al., 2015). Moreover, in a three-point or four-point bending test, there is bigger effective volume being tested and as such, the probability of the specimen containing a critical flaw or defect would be higher, leading to a lower flexural strength (Schatz et al., 2015). Therefore, it is necessary to take the size of the specimens into consideration when comparing the results of this study with the actual or advertised strengths reported by the various manufacturers.

With respect to polishing, the results of this study show significant differences in strength between polished specimens and unpolished ones, as well as significant differences when utilizing different polishing techniques, i.e., automated, and manual polishing. Schatz et al. (2016) reported the influence of different specimen preparation types by comparing the flexural strength of specimens polished before and after sintering. The results of their study show specimens that were wet polished after sintering produced higher flexural strength results than those that were polished before sintering, and those that were dry polished before sintering had an increased surface roughness, which could attribute to a lower flexural strength (Schatz et al., 2016). They also noted that the reliability of the monolithic zirconia, measured by the Weibull modulus, was not affected by the different specimen preparations. In this study, all specimens were polished or ground before sintering, and with the exception of one group of the small specimens, all were wet polished after sintering as well. The weakest link theory can help explain why the significant differences existed between the polished and unpolished specimens in this study, where a fault or defect that is left on the surface can grow and propagate leading to failure of the material (Schatz et al., 2016). Although polishing after sintering can help decrease the surface defects, it can still induce flaws especially when there is a large volume of material is involved, leading to an increase in critical flaw detection during the bending tests (Hatanaka et al., 2017). On the other hand, several studies reported a decrease in flexural strength and Weibull modulus when the specimens underwent a grinding process (Kosmač et al., 1999; 2000; Luthardt et al., 2002). This can help explain the large variation seen in the samples in this study. Moreover, Inokoshi et al. (2021) reported that the strength of zirconia after Al_2O_3-sandblasting is controlled by the harmony between microcrack arrangement, which leads to diminished strength, and surface compressive pressure resulting from tetragonal to monoclinic phase transformation, which would increase strength. Kosmač et al. (1999) also reported an increase in the flexural strength of Y-TZP zirconia ceramics with a decrease in reliability. Although the specimens in this study were not sandblasted, grinding or polishing can have similar resulting effects as sandblasting, triggering a monoclinic phase transformation to yield higher strength (Kosmač et al., 2000). However, the crystallographic phase analysis that was conducted in this study showed little to no monoclinic phase being present in the surface of the specimens. The polishing procedure after sintering may have removed the layer of monoclinic zirconia, and this effect was also seen in a study conducted by Guazatto et al. (2005). A noticeable amount of rhombohedral zirconia was found instead in the specimens in this study, which will be discussed later in this section. With respect to the different polishing techniques utilized in this study, it is seen that the automated technique gives rise to more consistent samples in terms of size and dimensions since most of the specimens are polished simultaneously together. Manual polishing requires a high-level of operator skill and varies between operator to operator greatly. As such, a rise in variation and decrease in reliability can be noted.

The results of the crystallographic analysis in this study revealed the presence of rhombohedral zirconia. Since it was present across all groups in this study, it can be deduced that the rhombohedral phase resulted from the grinding or polishing process in this study, and this is also in agreement with other studies in the literature (Denry and Holloway, 2006; Ruiz and Readey, 1996). It has been reported by Kitano et al. (1988) that the rhombohedral zirconia results from the cubic phase, resulting in an increased volume of 5.2% (Denry and Holloway, 2006). On the other hand, Ruiz and Readey (1996) suggested that the rhombohedral phase was formed from the tetragonal phase when the material is subjected to mechanical stresses, also resulting in an increase in volume by 3.9% (Denry and Holloway, 2006). In this study, the higher amount of rhombohedral zirconia was present mostly in the enamel layers of the multilayered zirconia by composition, OB and ZP. As such, it may be inferred that the rhombohedral transformation resulted from the cubic phase. The presence of cubic zirconia in 3Y-TZP has also been documented in the literature, and can be seen in this study as well in ZP's dentin layer and KT. The increase in volume resulting from this transformation may lead to grain pullout, which would cause surface and subsurface damage (Denry and Holloway, 2006). This could introduce flaws and defects, such as microcraters and roughness, into the specimens, leading to an increased probability of critical flaw detection during a bending test and subsequent failure. This can help explain the high amount of variance in the samples as well. Moreover, Kondoh (2004) reported that the hump seen in the tetragonal peak is caused by lattice distortion and not by the presence of rhombohedral zirconia. As such, the term strained tetragonal zirconia is also used, which would suggest that the strained tetragonal phase is more vulnerable and as such might have decreased strength. Annealing the specimens at 1000ºC for 1 hour should completely reverse the cubic or tetragonal phase transformation into the rhombohedral one (Denry and Holloway, 2006; Hatanaka et al., 2017). Song et al. (2013) reported that annealing for 1000ºC for 15 minutes would cause a complete reversal of tetragonal to monoclinic transformation. In this study, the annealing process was at 1000ºC for 15 minutes only, which may explain the absence of the monoclinic phase but presence of the rhombohedral or strained tetragonal phase. The absence of monoclinic phase would indicate that the tetragonal phase, the most mechanically advantageous stage, would be present in higher concentrations, leading to higher flexural strength. Even with annealing, however, the grain pullout and subsurface damage that resulted from the volumetric increase is irreversible. In this study, annealed specimens were significantly weaker than ones that were not annealed with a decrease in strength of about 11%, seen in Table 32. These results agree with Kosmač et al. (2000) where their annealed specimens resulted in a 10% decrease in strength than ones that were not annealed.

Considering these multilayered materials are relatively new to the market, it may be of importance in assessing the way they are manufactured. It is common to fabricate zirconia pucks by pressing the ZrO_2 powder to obtain the blank. However, given the fact that these multilayers include different colorants, oxides, and yttria concentrations, that means that the pressing technique would be done in increments and not in a single uniform step. This is most likely to introduce defects, impurities, poorly sintered regions, and critical flaws in between the layers, which would cause the material to be vulnerable (Kaizer et al., 2020). Although the sintering programs utilized in this experiment were all for multi-units to compensate for the large size of the specimen, poorly sintered areas within the material are more than likely to exist given the volume of each specimen. Kaizer et al. (2020) tested the strength of the Katana multilayer line including ML, UTML and STML. They conducted a flexural strength test isolating the enamel layer, dentin layer, and again including all layers. Their results were consistent when it came to test the separate enamel and dentin layers only, with no significant differences in strength between the two layers for their respective materials. This was consistent with the yttria content levels, with ML having the lowest, and UTML the highest amounts, i.e., ML was the strongest, 800-900MPa, then STML, 560-650 MPa, and UTML, 470-500MPa, was the weakest of the three materials. These were comparable with results reported by Flinn et al. (2017) and Pereira et al. (2018). However, when all layers were included in the test, the resultant flexural strength decreased by about 30% across all three materials (Kaizer et al., 2020). This was also confirmed by their analysis of the effects of impurities or poorly sintered regions on flexural strength using the relationship $K_C = 1.12\sigma F(\pi c F)^{1/2}$. Applying this 30% decrease in strength to this study, all three multilayered materials are well within the range of their advertised flexural strengths. The results of their study agree with this study as well in terms of specimen size, since the separate enamel and dentin layers were smaller in size during testing as opposed to testing with all layers included. A study conducted by Shah et al. (2008) reported that an increase in colorants, such as cerium or bismuth salts, resulted in a decrease in flexural strength of the material. All the aforementioned factors can help explain the large variance that exists in these materials in this study. Therefore, it is important that manufacturers take these things into consideration when producing these CAD/CAM zirconia pucks since the purpose of these multilayered materials are to be used as a whole clinically, and not just an isolated layer or two of the material to create the restoration. However, in the clinical setting, the size of the restorations that will be used are generally much smaller than the specimen sizes used in this study, and as such the overall strength of the material should be more consistent.

CONCLUSION

Within the limitations of this study, the following can be concluded:

- Repeated firing has no significant effects on the contrast ratio or CIELAB values.
- Repeated firing has no significant effects on the crystallographic structure.
- Repeated firing has no significant effects on the elemental composition.
- Repeated firing has no significant effects on flexural strength.
- There is a significant difference in flexural strength in terms of specimen size, where smaller specimens generally produce stronger results.
- There is a significant difference in flexural strength in terms of polished status, where polished samples yield stronger results than non-polished ones.

- There is a significant difference in flexural strength in terms of annealing, where annealed samples produce weaker specimens.
- There is a significant difference in flexural strength in terms of type of polishing, where automated polishing produces stronger samples than non-polished.
- There are significant differences in Yttria concentrations between enamel, transition, and dentin layer for ZP and OB, but not at the junctions of each layer. With KT, the Yttria concentration was consistent between all layers with no significant difference. There are significant differences between the 3 materials tested.
- There are significant differences between each layer in terms of crystallographic phase, where tetragonal phase was present mostly in dentin layer and cubic phase mostly present in the enamel layers for all materials. No significant differences were noted for monoclinic phase between the layers. There are significant differences between the 3 materials tested.
- There are significant differences in flexural strength between the 3 multilayered materials tested, with KT being significantly different than ZP and OB. In-Coris TZI, not multilayered, was significantly stronger than the other 3 materials.
- A general conclusion can be made across all materials tested in this study, where higher Yttria concentrations equate to increased translucency, and reduced strength; and vice-versa where low Yttria concentrations reflect into stronger and less translucent restorations.

- Multilayered zirconia is a new and viable type of material that can be used in the dental setting; however, manufacturers need to consider the different processing techniques implemented in making this novel material. Further research is still required both in-vitro and in-vivo.

BIBLIOGRAPHY

1. Ahmed, W. M., Troczynski, T., McCullagh, A. P., Wyatt, C. C. L., & Carvalho, R. M. (2019). The influence of altering sintering protocols on the optical and mechanical properties of zirconia: A review. *Journal of Esthetic and Restorative Dentistry*, *31*(5), 1–8. https://doi.org/10.1111/jerd.12492

2. Al-Juaila, E., Osman, E., Segaan, L., Shrebaty, M., & Farghaly, E. A. (2018). Comparison of translucency for different thicknesses of recent types of esthetic zirconia ceramics versus conventional ceramics … (in vitro study). *Future Dental Journal*, *4*(2), 297–301. https://doi.org/10.1016/j.fdj.2018.05.003

3. Alkurt, M., Yeşil Duymus, Z., & Gundogdu, M. (2016). Effects of multiple firings on the microstructure of zirconia and veneering ceramics. *Dental Materials Journal*, *35*(5), 776–781. https://doi.org/10.4012/dmj.2015-429

4. Bachhav, V. C., & Aras, M. A. (2011). The effect of ceramic thickness and number of firings on the color of a zirconium oxide based all ceramic system fabricated using CAD/CAM technology. *Journal of Advanced Prosthodontics*, *3*(2), 57–62. https://doi.org/10.4047/jap.2011.3.2.57

5. Ban, S. 2019. Chemical durability of high translucent zirconia. *Dental Materials Journal*. 39(1), pp. 12-23.

6. B and D Dental Technologies. (2020). Origin Beyond+ Multi. [Online]. [Accessed March 5th, 2022]. Available from: web.archive.org/, https://bnddental.com/assets/web_originproductcatalog_072320.pdf

7. Bajraktarova-Valjakova, E., Korunoska-Stevkovska, V., Kapusevska, B., Gigovski, N., Bajraktarova-Misevska, C., & Grozdanov, A. (2018). Contemporary Dental Ceramic Materials, A Review: Chemical Composition, Physical and Mechanical Properties, Indications for Use. Open Access Macedonian Journal of Medical Sciences, 6(9). doi:10.3889/oamjms.2018.378

8. Burgess, J. O. (2018). Zirconia: The Material, Its Evolution, and Composition. [Online]. [Accessed November 11th, 2020]. Available from: https://www.aegisdentalnetwork.com/cced/special-issues/2018/10/zirconia-the-material-its-evolution-and-composition

9. Carrabba, M., Keeling, A. J., Aziz, A., Vichi, A., Fabian Fonzar, R., Wood, D., & Ferrari, M. (2017). Translucent zirconia in the ceramic scenario for monolithic

restorations: A flexural strength and translucency comparison test. *Journal of Dentistry*, *60*, 70–76. https://doi.org/10.1016/j.jdent.2017.03.002

10. Carver, G. (2018). The History of Zirconia in Dentistry. [Online]. [Accessed Sep 28th, 2020]. Available from: web.archive.org/, https://blog.ddslab.com/history-of-zirconia

11. Cekic-Nagas, I., Egilmez, F., & Ergun, G. (2012). Comparison of light transmittance in different thicknesses of zirconia under various light curing units. *Journal of Advanced Prosthodontics*, *4*, 93–96. https://doi.org/10.4047/jap.2012.4.2.93

12. Cekic-Nagas, I., Egilmez, F., Ergun, G., & Kaya, B. M. (2013). Light transmittance of zirconia as a function of thickness and microhardness of resin cements under different thicknesses of zirconia. *Medicina Oral, Patologia Oral y Cirugia Bucal*, *18*(2). https://doi.org/10.4317/medoral.18181

13. Chevalier, J. (2006). What future for zirconia as a biomaterial? *Biomaterials*, *27*(4), 535–543. https://doi.org/10.1016/j.biomaterials.2005.07.034

14. Chevalier, J., Deville, S., Münch, E., Jullian, R., & Lair, F. (2004). Critical effect of cubic phase on aging in 3 mol% yttria-stabilized zirconia ceramics for hip replacement prosthesis. *Biomaterials*, *25*(24), 5539–5545. https://doi.org/10.1016/J.BIOMATERIALS.2004.01.002

15. Cho, M. and Seol, H. 2022. Optical Properties, Microstructure, and Phase Fraction of Multi-Layered Monolithic Zirconia with and without Yttria-Gradient. *Materials*. 16(1). pp. 1-13.

16. Church, T. D., Jessup, J. P., Villa, ¢, Guillory, L., & Vandewalle, K. S. (2017). Translucency and strength of high-translucency monolithic zirconium oxide materials. *Academy of General Dentistry*, 48–52. www.agd.org/generaldentistry

17. Coskun, M. E., & Sari, F. (2019). Effects of speed sintering on multilayered monolithic zirconia. *Cumhuriyet Dental Journal*, *22*(1), 31–36. https://doi.org/10.7126/cumudj.510393

18. Curtis, A. R., Wright, A. J., & Fleming, G. J. P. (2006). The influence of surface modification techniques on the performance of a Y-TZP dental ceramic. *Journal of Dentistry*, *34*(3), 195–206. https://doi.org/10.1016/j.jdent.2005.06.006

19. Denry, I., & Kelly, J. R. (2008). State of the art of zirconia for dental applications. *Dental Materials*, *24*(3), 299–307. https://doi.org/10.1016/j.dental.2007.05.007

20. Denry, I. L., & Holloway, J. A. (2006). Microstructural and crystallographic surface changes after grinding zirconia-based dental ceramics. *Journal of Biomedical Materials Research - Part B Applied Biomaterials*, *76*(2), 440–448. https://doi.org/10.1002/jbm.b.30382

21. Dentsply Sirona. 2019. Cercon xt ML. [Online]. [Accessed November 30th, 2020]. Available from: https://assets.dentsplysirona.com/dentsply/pim/manufacturer/Prosthetics/CAD_CAM_materials/Materials/Zirconia/Cercon_xt_disc/Lab-brochure-Cercon-multi-layer-EN.pdf

22. Ebeid, K., Wille, S., Hamdy, A., Salah, T., El-Etreby, A., & Kern, M. (2014). Effect of changes in sintering parameters on monolithic translucent zirconia. *Dental Materials*, *30*(12), e419–e424. https://doi.org/10.1016/j.dental.2014.09.003

23. Elsaka, S. E. (2019). Optical and Mechanical Properties of Newly Developed Monolithic Multilayer Zirconia. *Journal of Prosthodontics*, *28*(1), e279–e284. https://doi.org/10.1111/jopr.12730

24. Fathi, A., Farzin, M., Giti, R., & Kalantari, M. H. (2019). Effects of number of firings and veneer thickness on the color and translucency of 2 different zirconia-based ceramic systems. *The Journal of Prosthetic Dentistry*, *122*(6), 565.e1-565.e7. https://doi.org/https://doi.org/10.1016/j.prosdent.2019.08.020

25. Farid, S. B. H. (2019). Structure, microstructure, and properties of bioceramics. *Bioceramics: For Materials Science and Engineering*, 39–76. https://doi.org/10.1016/B978-0-08-102233-7.00002-1

26. Garvia, R. C., & Nicholson, P. S. (1972). Phase Analysis in Zirconia Systems. Journal of the American Ceramic Society, 55(6), 303–305. doi:10.1111/j.1151-2916.1972.tb11290.x

27. Ghodsi, S., & Jafarian, Z. (2018). A Review on Translucent Zirconia. *The European Journal of Prosthodontics and Restorative Dentistry*, *26*, 62–74. https://doi.org/10.1922/EJPRD_01759Ghodsi13

28. Giordano, R., & McLaren, E. A. (2014). Ceramics overview- classification by microstructure and processing methods. *International Dentistry - African Edition*, *4*(3), 18–30.

29. Gautam, C., Joyner, J., Gautam, A., Rao, J., & Vajtai, R.. 2016. Zirconia based dental ceramics: structure, mechanical properties, biocompatibility and applications. *Dalton Transactions*. 45(48), pp. 19194-19215.

30. Guazzato, M., Albakry, M., Quach, L., & Swain, M. V. (2005). Influence of surface and heat treatments on the flexural strength of a glass-infiltrated alumina/zirconia-reinforced dental ceramic. *Dental Materials*, *21*(5), 454–463. https://doi.org/10.1016/J.DENTAL.2004.07.010

31. Hallmann, L., Ulmer, P., Reusser, E., Louvel, M., & Hämmerle, C. H. F. (2012). Effect of dopants and sintering temperature on microstructure and low temperature degradation of dental Y-TZP-zirconia. *Journal of the European Ceramic Society*, *32*(16), 4091–4104. https://doi.org/10.1016/j.jeurceramsoc.2012.07.032

32. Harada, K., Raigrodski, A. J., Chung, K. H., Flinn, B. D., Dogan, S., & Mancl, L. A. (2016). A comparative evaluation of the translucency of zirconias and lithium disilicate for monolithic restorations. *Journal of Prosthetic Dentistry*, *116*(2), 257–263. https://doi.org/10.1016/j.prosdent.2015.11.019

33. Hasegawa, H., Hioki, T., & Kamigaito, O. (1985). Cubic-to-rhombohedral phase transformation in zirconia by ion implantation. *JOURNAL OF MATERIALS SCIENCE*, *4*, 1092–1094.

34. Hatanaka, G. R., Polli, G. S., Fais, L. M. G., Maurício, J., Reis, S. N., & Pinelli, L. A. P. (2017). Zirconia changes after grinding and regeneration firing. *The Journal of Prosthetic Dentistry*, *118*(1), 61–68.

35. Hayashi, H., Saitou, T., Maruyama, N., Inaba, H., Kawamura, K., & Mori, M. (2005). Thermal expansion coefficient of yttria stabilized zirconia for various yttria contents. *Solid State Ionics*, *176*(5–6), 613–619. https://doi.org/10.1016/j.ssi.2004.08.021

36. Heidari, N. et al. 2022. Fracture Resistance and Fracture Behavior of Monolithic Multi-Layered Translucent Zirconia Fixed Dental Prostheses with Different Placing Strategies of Connector: An in vitro Study. *Clinical, Cosmetic and Investigational Dentistry.* 14(1), pp. 61-69.

37. Helvey, G. (2010). A History of Dental Ceramics. *Compendium of Continuing Education in Dentistry*, *31*(4). https://www.aegisdentalnetwork.com/cced/2010/05/a-history-of-dental-ceramics

38. Inokoshi, M., Shimizu, H., Nozaki, K., Takagaki, T., Yoshihara, K., Nagaoka, N., Zhang, F., Vleugels, J., van Meerbeek, B., & Minakuchi, S. (2018). Crystallographic and morphological analysis of sandblasted highly translucent dental zirconia. *Dental Materials*, *34*(3), 508–518. https://doi.org/10.1016/j.dental.2017.12.008

39. Inokoshi, M., Shimizubata, M., Nozaki, K., Takagaki, T., Yoshihara, K., Minakuchi, S., Vleugels, J., van Meerbeek, B., & Zhang, F. (2021). Impact of sandblasting on the flexural strength of highly translucent zirconia. *Journal of the Mechanical Behavior of Biomedical Materials*, *115*. https://doi.org/10.1016/j.jmbbm.2020.104268

40. International Organization for Standardization. 2014. ISO/FDIS 6872:2014. *Dentistry – Ceramic Materials*. Geneva, Switzerland: International Organization for Standardization.

41. Ivoclar Vivadent. (2019). *ZirCAD Labside Instructions for Use*. [Online]. [Accessed November 15th, 2020]. Available from: https://caddent.de/fileadmin/user_upload/IPS_e-max_ZirCAD_Labside_ENG.pdf

42. Kaizer, M. R., Gierthmuehlen, P. C., dos Santos, M. B., Cava, S. S., & Zhang, Y. (2017). Speed sintering translucent zirconia for chairside one-visit dental restorations: Optical, mechanical, and wear characteristics. *Ceramics International*, *43*(14), 10999–11005. https://doi.org/10.1016/j.ceramint.2017.05.141

43. Kaizer, M. R., Kolakarnprasert, N., Rodrigues, C., Chai, H., & Zhang, Y. (2020). Probing the interfacial strength of novel multi-layer zirconias. *Dental Materials*, *36*(1), 60–67. https://doi.org/10.1016/j.dental.2019.10.008

44. Kanchanavasita, W., Triwatana, P., Suputtamongkol, K., Thanapitak, A., & Chatchaiganan, M. (2014). Contrast Ratio of Six Zirconia-Based Dental Ceramics. *Journal of Prosthodontics*, *23*(6), 456–461. https://doi.org/10.1111/jopr.12143

45. Kim, H. K. (2020). Optical and mechanical properties of highly translucent dental zirconia. *Materials*, *13*(15), 1–16. https://doi.org/10.3390/ma13153395

46. Kim, M. J., Ahn, J. S., Kim, J. H., Kim, H. Y., & Kim, W. C. (2013). Effects of the sintering conditions of dental zirconia ceramics on the grain size and translucency. *Journal of Advanced Prosthodontics*, *5*(2), 161–166. https://doi.org/10.4047/jap.2013.5.2.161

47. Kitano, Y., Mori, Y., & Ishitani, A. (1988). Communications of the American Ceramic Society Rhombohedral Phase in Y203-Partially-Stabilizedl Zr02. *Journal of the American Ceramic Society*, *71*(1), C-34-C–36.

48. Kolakarnprasert, N., Kaizer, M. R., Kim, D. K., & Zhang, Y. (2019). New multi-layered zirconias: Composition, microstructure and translucency. *Dental Materials*, *35*(5), 797–806. https://doi.org/10.1016/j.dental.2019.02.017

49. Kondoh, J. (2004). Origin of the hump on the left shoulder of the X-ray diffraction peaks observed in Y2O3-fully and partially stabilized ZrO2. *Journal of Alloys and Compounds*, *375*, 270–282. https://doi.org/10.1016/J.JALLCOM.2003.11.129

50. Kosmač, T., Edomir Oblak, C. ˇ, Jevnikar, P., Funduk, N., & Marion, L. (2000). Strength and Reliability of Surface Treated Y-TZP Dental Ceramics. *Journal of Biomedical Materials Research (Applied Biomaterials)*, *53*, 304–313.

51. Kosmač, T., Oblak, C., Jevnikar, P., Funduk, N., & Marion, L. (1999). The effect of surface grinding and sandblasting on flexural strength and reliability of Y-TZP zirconia ceramic. *Dental Materials*, *15*(6), 426–433. https://doi.org/10.1016/S0109-5641(99)00070-6

52. Kumchai, H., Juntavee, P., Sun, A. F., & Nathanson, D. (2018). Effect of Glazing on Flexural Strength of Full-Contour Zirconia. *International Journal of Dentistry*, *2018*. https://doi.org/10.1155/2018/8793481

53. Kuraray Noritake. (2019). KATANA Zirconia. Multi-layered Zirconia Disc Series – Technical Guide. [Online]. [Accessed November 30th, 2020]. Available from: https://www.kuraraynoritake.eu/pub/media/pdfs/21599_1_Katana_discs_Technical_Guide_LR_63.pdf

54. Kwon, S. J., Lawson, N. C., Mclaren, E. E., Nejat, A. H., & Burgess, J. O. (2018). Comparison of the mechanical properties of translucent zirconia and lithium disilicate. *The Journal of Prosthetic Dentistry*, *120*(1), 132–137.

55. Luthardt, R. G., Holzhüter, M., Sandkuhl, O., Herold, V., Schnapp, J. D., Kuhlisch, E., & Walter, M. (2002). Reliability and properties of ground Y-TZP-zirconia ceramics. *Journal of Dental Research*, *81*(7), 487–491. https://doi.org/10.1177/154405910208100711

56. Machry, R. et al. 2022. Mechanical Characterization of a Multi-Layered Zirconia: Flexural Strength, Hardness and Fracture Toughness of the Different Layers. *Journal of the Mechanical Behavior of Biomedical Materials*. 135(1). Pp. 1-8.

57. Manziuc, M.-M., Gasparik, C., Negucioiu, M., Constantiniuc, M., Burde, A., Vlas, I., & Dudea, D. (2019). Optical properties of translucent zirconia: A review of the literature. *The EuroBiotech Journal*, *3*(1), 45–51. https://doi.org/10.2478/ebtj-2019-0005

58. Matsuzaki, F., Sekine, H., Honma, S., Takanashi, T., Furuya, K., Yajima, Y., & Yoshinari, M. (2015). Translucency and flexural strength of monolithic translucent

zirconia and porcelain-layered zirconia. *Dental Materials Journal*, *34*(6), 910–917. https://doi.org/10.4012/dmj.2015-107

59. Michailova, M., Elsayed, A., Fabel, G., Edelhoff, D., Zylla, I. M., & Stawarczyk, B. (2020). Comparison between novel strength-gradient and color-gradient multilayered zirconia using conventional and high-speed sintering. *Journal of the Mechanical Behavior of Biomedical Materials*, *111*. https://doi.org/10.1016/j.jmbbm.2020.103977

60. Nam, M.-G., & Park, M.-G. (2018). Changes in the flexural strength of translucent zirconia due to glazing and low-temperature degradation. *The Journal of Prosthetic Dentistry*, *120*(6), 969.e1-969.e6. https://doi.org/10.1016/j.prosdent.2018.07.017

61. Nejatidanesh, F., Azadbakht, K., Savabi, O., Sharifi, M., & Shirani, M. (2020). Effect of repeated firing on the translucency of CAD-CAM monolithic glass-ceramics. *The Journal of Prosthetic Dentistry*, *123*(3), 530.e1-530.e6. https://doi.org/10.1016/j.prosdent.2019.10.028

62. O'brien, W. J., Kay, K.-S., Boenke, K. M., & Groh, C. L. (1991). Sources of color variation on firing porcelain. *Journal of Dental Materials*, *7*, 170–173.

63. Ozdogan, A., & Ozdemir, H. (2020). The effects of repetitive firing processes on the optical, thermal, and phase formation changes of zirconia. *Journal of Advanced Prosthodontics*, *12*(1), 9–14. https://doi.org/10.4047/jap.2020.12.1.9

64. Ozturk, O., Uludag, B., Usumez, A., Sahin, V., & Celik, G. (2008). Clinical Implications The effect of ceramic thickness and number of firings on the color of two all-ceramic systems Ozturk et al. *The Journal of Prosthetic Dentistry*, *100*(2), 99–106.

65. Prakasam, M., Valsan, S., Lu, Y., Balima, F., Lu, W., Piticescu, R., & Largeteau, A. (2018). Nanostructured Pure and Doped Zirconia: Synthesis and Sintering for SOFC and Optical Applications. In *Sintering Technology - Method and Application*. InTech. https://doi.org/10.5772/intechopen.81323

66. Ruiz, L., & Readey, M. J. (1996). Effect of Heat Treatment on Grain Size, Phase Assemblage, and Mechanical Properties of 3 mol% Y-TZ. *Journal of American Ceramic Society*, *79*(9), 2331–2340. https://doi.org/10.1111/j.1151-2916.1996.tb08980.x.

67. Sakai, T., Sato, T., Hisanaga, R., Shinya, A., Takemoto, S., & Yoshinari, M. (2019). Optical properties and flexural strength of translucent zirconia layered with high-translucent zirconia. *Dental Materials Journal*, *38*(3), 368–377. https://doi.org/10.4012/dmj.2018-157

68. Schatz, C., Strickstrock, M., Roos, M., Edelhoff, D., Eichberger, M., Zylla, I. M., & Stawarczyk, B. (2016). Influence of specimen preparation and test methods on the flexural strength results of monolithic zirconia materials. *Materials*, *9*(3). https://doi.org/10.3390/ma9030180

69. Shackelford, J. F. (1999). *Bioceramics: applications of ceramic and glass materials in medicine*. Trans Tech Publications.

70. Shah, K., Holloway, J. A., & Denry, I. L. (2008). Effect of Coloring with Various Metal Oxides on the Microstructure, Color, and Flexural Strength of 3Y-TZP. *Journal of Biomedical Materials Research - Part B Applied Biomaterials*, *87*(2), 329–337. https://doi.org/10.1002/jbm.b.31107

71. Song, J. Y., Park, S. W., Lee, K., Yun, K. D., & Lim, H. P. (2013). Fracture strength and microstructure of Y-TZP zirconia after different surface treatments. *The Journal of Prosthetic Dentistry*, *110*(4), 274–280. https://doi.org/10.1016/S0022-3913(13)60376-5

72. Stawarczyk, B., Emslander, A., Roos, M., Sener, B., Noack, F., & Keul, C. (2014). Zirconia ceramics, their contrast ratio and grain size depending on sintering parameters. *Dental Materials Journal*, *33*(5), 591–598. https://doi.org/10.4012/dmj.2014-056

73. Stawarczyk, B., Özcan, M., Hallmann, L., Ender, A., Mehl, A., & Hämmerlet, C. H. F. (2013). The effect of zirconia sintering temperature on flexural strength, grain size, and contrast ratio. *Clinical Oral Investigations*, *17*(1), 269–274. https://doi.org/10.1007/s00784-012-0692-6

74. Tabatabaian, F., Motamedi, E., Sahabi, M., Torabzadeh, H., & Namdari, M. (2018). Effect of thickness of monolithic zirconia ceramic on final color. *The Journal of Prosthetic Dentistry*, *120*(2), 257–262.

75. Tang, X., Nakamura, T., Usami, H., Wakabayashi, K., & Yatani, H. (2012). Effects of multiple firings on the mechanical properties and microstructure of veneering ceramics for zirconia frameworks. *Journal of Dentistry*, *40*(5), 372–380. https://doi.org/10.1016/j.jdent.2012.01.014

76. Toby, B. H., & Von Dreele, R. B. (2013). “GSAS-II: the genesis of a modern open-source all purpose crystallography software package”. *Journal of Applied Crystallography*, **46**(2), 544-549. doi:10.1107/S0021889813003531

77. Ueda, K., Güth, J. F., Erdelt, K., Stimmelmayr, M., Kappert, H., & Beuer, F. (2015). Light transmittance by a multi-coloured zirconia material. *Dental Materials Journal*, *34*(3), 310–314. https://doi.org/10.4012/dmj.2014-238

78. Vichi, A., Carrabba, M., Paravina, R., & Ferrari, M. (2014). Translucency of ceramic materials for CEREC CAD/CAM system. *Journal of Esthetic and Restorative Dentistry*, *26*(4), 224–231. https://doi.org/10.1111/jerd.12105

79. Vichi, A., Sedda, M., Fabian Fonzar, R., Carrabba, M., & Ferrari, M. (2016). Comparison of contrast ratio, translucency parameter, and flexural strength of traditional and “augmented translucency” zirconia for CEREC CAD/CAM system. *Journal of Esthetic and Restorative Dentistry*, *28*, S32–S39. https://doi.org/10.1111/jerd.12172

80. Xie, H., Gu, Y., Li, Q., Qian, M., Zhang, F., Tay, F. R., & Chen, C. (2016). Effects of multiple firings on the low-temperature degradation of dental yttria-stabilized tetragonal zirconia. *The Journal of Prosthetic Dentistry*, *115*(4), 495–500.

81. Xu, Y., Han, J., Lin, H., & An, L. (2015). Comparative study of flexural strength test methods on CAD/CAM Y-TZP dental ceramics. *Regenerative Biomaterials*, *2*(4), 239–244. https://doi.org/10.1093/rb/rbv020

82. Zhang, H., Li, Z., Kim, B. N., Morita, K., Yoshida, H., Hiraga, K., & Sakka, Y. (2012). Effect of alumina dopant on transparency of tetragonal zirconia. *Journal of Nanomaterials*, *2012*. https://doi.org/10.1155/2012/269064

83. Zhang, Y. (2014). Making yttria-stabilized tetragonal zirconia translucent. *Dental Materials*, *30*(10), 1195–1203. https://doi.org/10.1016/j.dental.2014.08.375

84. Zhang, Y., & Lawn, B. R. (2018). Novel Zirconia Materials in Dentistry. *Journal of Dental Research*, *97*(2), 140–147. https://doi.org/10.1177/0022034517737483

85. Žmak, I., Ćorić, D., Mandić, V., & Ćurković, L. (2020). Hardness and indentation fracture toughness of slip cast alumina and alumina-zirconia ceramics. *Materials*, *13*(1). https://doi.org/10.3390/ma13010122

86. VITA Zahnfabrik. (2011). *VITA VM9 Working Instructions*. [Online]. [Accessed November 11, 2020]. Available from https://www.vitanorthamerica.com/datei.php?src=download/Support/Instructions-For-Use/Porcelains-and-Pressables/VITA-VM9-Working-Instructions_1190EN_0911.pdf

87. Winter, A., Schurig, A., Odenthal, A.-L., Schmitter, M., 2022. Impact of different layers within a blank on mechanical properties of multi-layered zirconia ceramics before and after thermal aging. Dent. Mater. 1–8. https://doi.org/10.1016/j.dental.2022.03.009.

CURRICULUM VITAE

[redacted]

[redacted]

[redacted]

[redacted]

[redacted]

[redacted]

[redacted]